



Chem Soc Rev

### Skin bioelectronics towards long-term, continuous health monitoring

Journal:	<i>Chemical Society Reviews</i>
Manuscript ID	CS-REV-03-2022-000207
Article Type:	Review Article
Date Submitted by the Author:	15-Mar-2022
Complete List of Authors:	<p>Wang, Yan; The University of Tokyo,  Haick, Hossam; Technion - Israel Institute of Technology, Chemical Engineering  Guo, Shuyang; University of Tokyo Graduate School of Engineering  Department of Electrical Engineering and Information Systems  Wang, Chunya; University of Tokyo Graduate School of Engineering  Department of Electrical Engineering and Information Systems  Lee, Sunghoon; University of Tokyo Graduate School of Engineering  Department of Electrical Engineering and Information Systems  Yokota, Tomoyuki; The University of Tokyo,  Someya, Takao; University of Tokyo Graduate School of Engineering  Department of Electrical Engineering and Information Systems, ; RIKEN,  Thin-Film Device Laboratory &amp; Center for Emergent Matter Science</p>

SCHOLARONE™  
Manuscripts



# Chemical Society Review

## ARTICLE

### Skin bioelectronics towards long-term, continuous health monitoring

Yan Wang<sup>abcd</sup>, Hossam Haick<sup>e</sup>, Shuyang Guo<sup>e</sup>, Chunya Wang<sup>e</sup>, Sunghoon Lee<sup>e</sup>, Tomoyuki Yokota<sup>e</sup>, Takao Someya<sup>c\*</sup>

Received 00th January 20xx,  
Accepted 00th January 20xx

DOI: 10.1039/x0xx00000x

[www.rsc.org/](http://www.rsc.org/)

Skin bioelectronics is considered as an ideal platform for personalised health care because of their unique characteristics, such as thinness, light weight, good biocompatibility, excellent mechanical robustness, and great skin conformability. Recent advances in skin-interfaced bioelectronics have promoted various applications in health care and precision medicine. Particularly, skin bioelectronics for long-term, continuous health monitoring offers powerful analysis of a broad spectrum of health status, opening a route for early disease diagnosis and treatment. In this review, we discuss 1) representative health care sensing devices, 2) material and structure selection, device properties, and wireless technologies of skin bioelectronics towards long-term, continuous health monitoring, 3) health care applications: acquisition and analysis of electrophysiological, biophysical, biochemical signals, and comprehensive monitoring, and 4) rational guidelines for the design of future skin bioelectronics for long-term, continuous health monitoring. Long-term, continuous health monitoring of advanced skin bioelectronics will open unprecedented opportunities for timely disease prevention, screening, diagnosis, and treatment, demonstrating great promise to revolutionising traditional medical practices.

## 1. Introduction

By leveraging the progressive advancement of microfabrication technologies, wireless communication, and miniaturised microelectronics, current commercialized wearables can continuously monitor individuals' physiological signals under normal life conditions.<sup>1</sup> These collected bio-signals play crucial roles in analysing health status of the wearers', especially the elderly individuals, subjects with chronic conditions, and the performance of athletes. One limitation of the commercialised wearables, such as smart watches, bands, and apparel-based gadgets, is that they cannot form conformable contact with the human skin, resulting in poor signals and wear comfort. Furthermore, these wearables are usually constrained to several specific body locations, thus limiting the mobility of the wearers.<sup>2</sup>

An emerging class of bioelectronics—skin bioelectronics—can mitigate this problem by having excellent skin conformability even under large, repetitive deformations.<sup>3,4</sup> The robust, dynamic device–skin interface makes the bioelectronics capable of monitoring real-time, continuous physiology, bioelectrical, and biochemical signals in

an imperceptible way.<sup>5,6</sup> It is touted as an ideal platform for personalised health care owing to unique characteristics, such as thinness, lightweight, good biocompatibility, excellent mechanical robustness, and exceptional skin conformability.<sup>7</sup> The rapid advancement of skin-interfaced electronics has enabled the implementation of emerging applications such as soft robotics, human-machine interfaces, and the Internet of Things,<sup>8</sup> as well as numerous biomedical applications in health monitoring, fitness/wellness, disease diagnosis, therapy and drug delivery, and smart prostheses.<sup>9–11</sup> In particular, skin bioelectronics for long-term, continuous health monitoring can collect timely, high-fidelity vital bio-signals, such as human activity, body temperature, cardiac mapping, electrophysiological signals, as well as molecular analysis of body fluid and exhalations of the subject in daily living.<sup>12–14</sup> The collected biometric information offers powerful analysis of a broad spectrum of health status, opening a route for predictive disease prevention, screening, diagnoses, and treatment in a convenient and non-invasive way.<sup>15–17</sup> Representative skin bioelectronics are shown in Fig. 1.<sup>18–29</sup> The development of skin bioelectronics has shown their capabilities of high precision health monitoring and biodiagnosis.<sup>17,30</sup> There are many reviews focused on skin or wearable electronics for health monitoring: Some summarize advanced materials or devices,<sup>7,11,31</sup> some emphases on continuous monitoring of one particular target, such as molecular, activity, or wound.<sup>13,32,33</sup> However, none of them focuses on skin bioelectronics for long-term health care. Skin bioelectronics for long-term, continuous health monitoring present tremendous capabilities for timely disease diagnosis and treatment, promising to revolutionise traditional medical practices. Therefore, there lacks a review to provide a bird's eye-view of skin bioelectronics

<sup>a</sup> Department of Chemical Engineering, Guangdong Technion-Israel Institute of Technology (GTIIT), Shantou, Guangdong 515063, China;

<sup>b</sup> Technion-Israel Institute of Technology (IIT), Haifa 32000, Israel;

<sup>c</sup> Department of Electrical Engineering and Information Systems, The University of Tokyo, Tokyo 113-8656, Japan;

<sup>d</sup> Guangdong Provincial Key Laboratory of Materials and Technologies for Energy Conversion, Guangdong Technion – Israel Institute of Technology, Shantou, Guangdong 515063, China;

<sup>e</sup> Department of Chemical Engineering and Russell Berrie Nanotechnology Institute, Technion-Israel Institute of Technology, Haifa 3200003, Israel.

\* Corresponding email: someya@ee.t.u-tokyo.ac.jp

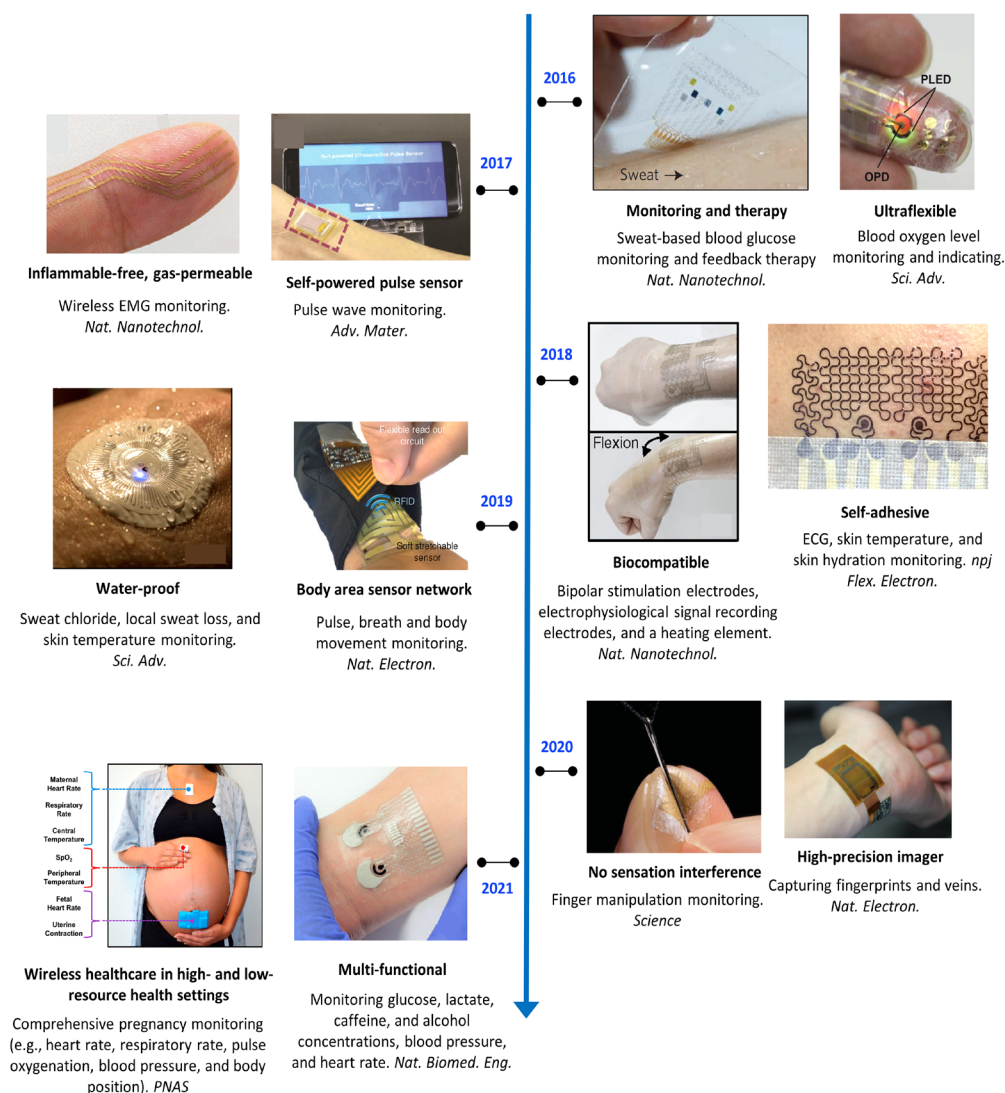


**Fig. 1** Representative examples of advanced skin bioelectronics for human health monitoring (2016–2021). Reproduced with permission from ref. 18–29. Copyright 2016, 2017, 2018, 2019, 2020, 2021 Nature Publishing Group, 2016, 2019 American Association for the Advancement of Science; 2017 Wiley-VCH; 2021 National Academy of Sciences.

with a focus on long-term, continuous health monitoring. The proposed topic is extremely timing. The knowledge and insights provided in this review will benefit the wider scientific community in three aspects: 1) stimulate development of advanced wearable technologies for high-performance skin bioelectronics; 2) encourage continued progress of skin bioelectronics towards long-term, continuous monitoring of a broad spectrum of health conditions of the subject; 3) expedite the realization of the full potential of future skin-interfaced bioelectronics that can provide point-of-care health care in the home and community settings. Moreover, a review on such topic will attract considerable scientific interests from researchers in soft electronic and biomedicine field, and significant commercial attention from users, health-care funders, tech-giants, and health-care providers.

This review begins with a highlight on representative skin-interfaced sensing devices for health care with a focus on materials, device structure, and mechanism, and then elaborates materials and structure selection, device properties, and wireless technologies of skin bioelectronics towards long-term, continuous health monitoring. The review will also highlight promising real-life applications of skin bioelectronics with long-term operation capabilities (see overview of the report in Fig. 2).<sup>34–41</sup> We then conclude with a summary of the remaining challenges, opportunities, and future directions in the field of skin bioelectronics for long-term, continuous health monitoring.

## 2. Representative health care sensing

Substantial progress has been made in recent years in the field of skin bioelectronics due to the advancement in materials science, engineering technologies, nanofabrication, and system integration.<sup>42</sup> By constructing rigid, inorganic functional materials into a soft

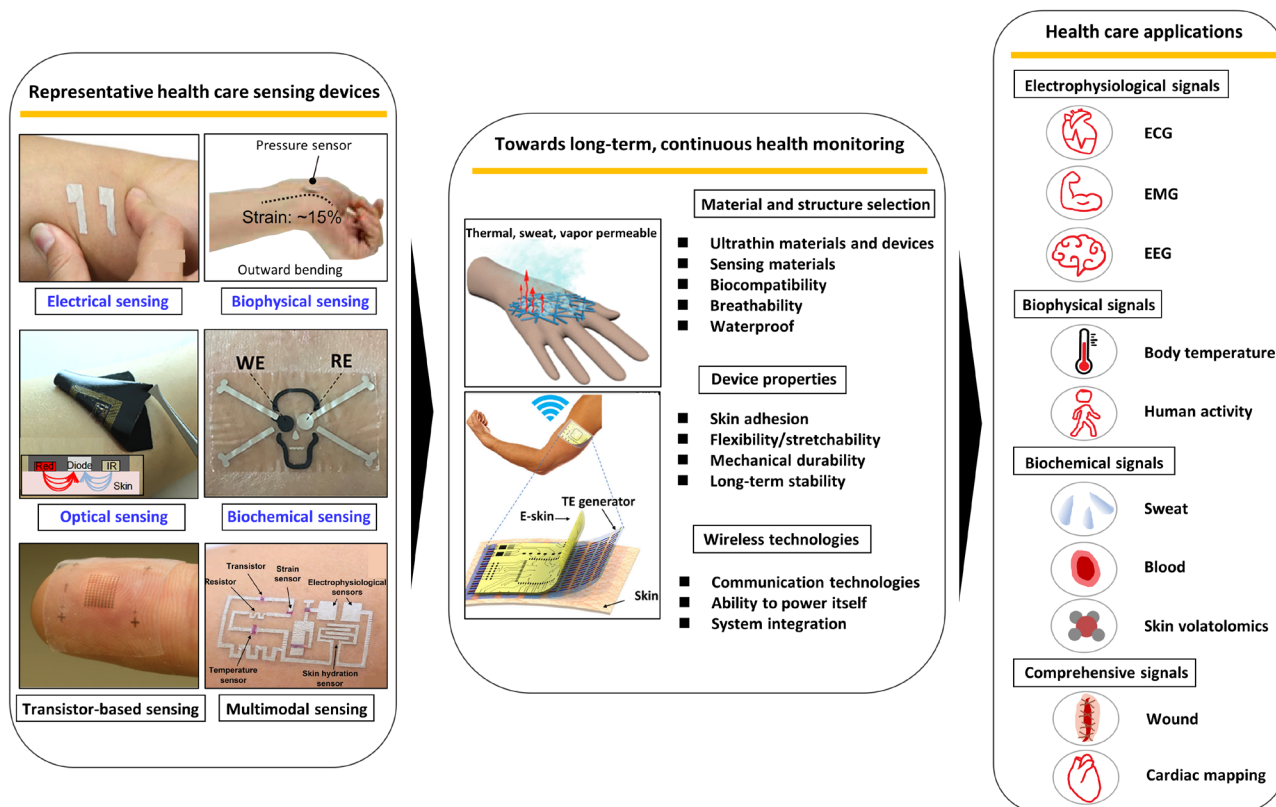


**Fig. 2** Overview of this report (section 2–4). Section 2 reviews and discusses representative skin-interfaced sensing devices for human health care. Reproduced with permission from ref. 34–39. Copyright 2019 Wiley-VCH; 2021 National Academy of Sciences; 2016 American Association for the Advancement of Science; 2018 Elsevier; 2018, 2020 Nature Publishing Group. Section 3 discusses material and structure selection, device properties, and wireless monitoring of skin bioelectronics towards long-term, continuous health monitoring. Reproduced with permission from ref. 40, 41. Copyright 2021 American Chemical Society; 2015 Elsevier. Section 4 reviews health care applications of skin bioelectronics for long-term, continuous health monitoring.

compliant format with elastomeric materials, soft bioelectronic systems can laminate conformably on arbitrary parts of the human body and maintain device functionalities under continuous, repetitive skin deformations. To realise the full potentials of skin bioelectronics in health monitoring, all skin-interfaced electronic components should have state-of-the-art operational characteristics throughout long-term, continuous wearing, during which the sensing devices extract bioinformatics from the human body, energy devices provide power source, integrated circuits process and transport data, and displays conveys results and feedback to the wearers.<sup>7</sup> Initially, we will focus on skin-integrated soft sensing devices in human health care.

In fact, our body is constantly radiating highly personalised electrical, mechanical, thermal, and biochemical signals indicating our health, emotions, and actions. For example, electrophysiological signals are generated by the electrical activities of the heart, brain, and muscles. Physical activities cause physiological response from the skin. Body secretions, such as tears and sweat, can offer crucial biomedical information (*e.g.*, pH, ions, molecules, and volatile organic compounds) for disease management.<sup>43</sup> The measurement and analysis of aforementioned health indicators will be discussed in Section 4. To collect these bio-signals, corresponding skin-mountable sensing devices have been developed.<sup>44</sup> In terms of working

mechanisms, we classify skin sensing devices into four categories: electrical, biophysical, optical, and biochemical. We further discuss other emerging sensing devices, such as transistor-based and multimodal.

## 2.1. Four sensing modalities

In this section, we discuss electrical, biophysical, optical, and then biochemical sensing devices. For each sensing modality, working mechanism, materials, and device configurations will be discussed individually.

### 2.1.1. Electrical sensing

Electrical sensors can be classified into wet and dry electrodes based on different skin contacts. As prolonged or repeated attachment to the human skin is necessary for long-term applications, wet electrodes (*e.g.*, standard Ag/AgCl gel electrodes) are not suitable considering the potential drying and skin irritation issues.<sup>45</sup> In this review, we will discuss dry electrodes. Dry electrode has direct contact with the human skin and provides a non-invasive approach for long-term biopotential signal monitoring. Minute changes in skin electrical resistance are recorded via the conformal electrical contact.<sup>46</sup> Moisture on the skin, such as sweat, enhances the stabilisation of the

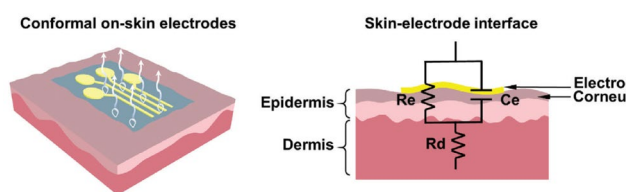


**Fig. 3** The skin-electrode interface and circuit model of on-skin electrical sensors. Reproduced with permission from ref. 47. Copyright 2021 Wiley-VCH.

dry electrodes. As shown in Fig. 3, a parallel circuit of leakage resistance and capacitance has been used to represent the electrical circuit model for a conformable electrode-skin interface.<sup>47</sup> As a result,

the signal-to-noise ratio (SNR) of the recorded biopotential signals depends on several parameters: electrode conductivity, area of skin contact, and air gap at the interface. In its simplest form, a dry electrode can be built from any conductive material that can be in contact with the human skin. To achieve skin compliance, tattoo or substrate-free dry electrodes have been developed. An ultrathin layer of conductive materials made from carbon nanomaterials, metallic nanomaterials, conductive polymers, and their hybrids has been invented for such purpose.<sup>21, 48-50</sup> Another way to achieve conformability and stretchability is to integrate aforementioned conductive materials with elastomeric materials, such as natural polymers (e.g., cellulose and silk)<sup>51</sup> silicon elastomers (e.g., Ecoflex,<sup>52</sup> polydimethylsiloxane (PDMS)),<sup>53, 54</sup> polyimide (PI),<sup>55</sup> polyethylene terephthalate (PET), polyurethane (PU),<sup>56</sup> polyethylene (PE), parylene,<sup>57</sup> acrylate,<sup>58</sup> electrospun nanofibres,<sup>27, 59</sup> and biodegradable

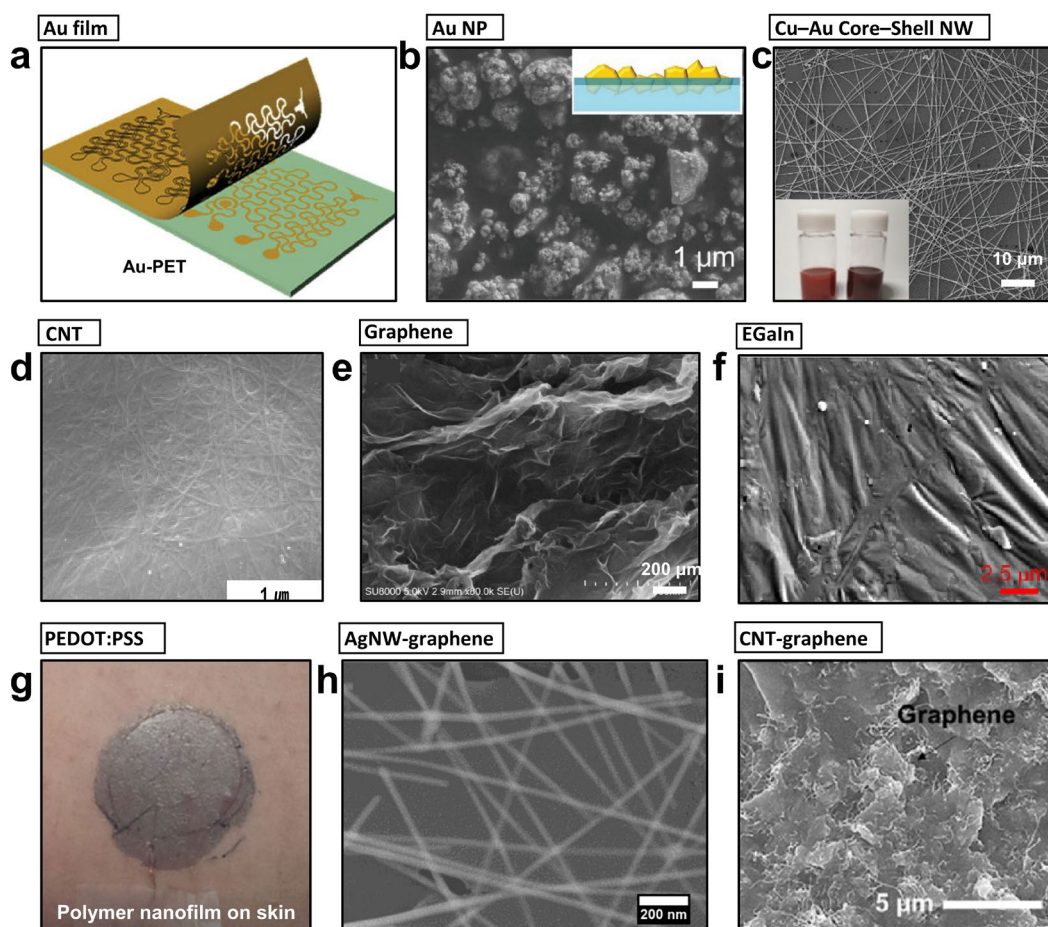


**Fig.4** Active materials for electrical sensing of skin bioelectronics. (a) Scheme of thin Au/PET film for epidermal electrical sensors. Reproduced with permission from ref. 62. Copyright 2015 Wiley-VCH. (b) Surface SEM image of AuNP. Reproduced with permission from ref.64. Copyright 2016 Wiley-VCH. (c) SEM image of oxidation-free Cu-Au core-shell NWs. Reproduced with permission from ref. 65. Copyright 2020 Wiley-VCH. (d) SEM image of CNTs. Reproduced with permission from ref. 68. Copyright 2018 IOPscience. (e) SEM image of graphene. Reproduced with permission from ref. 71. Copyright 2019 IEEE. (f) SEM image of gallium-indium alloy (EGaIn). Reproduced with permission from ref. 72. Copyright 2018 Springer Nature. (g) A photograph of PEDOT:PSS nanofilm electrode on the human skin. Reproduced with permission from ref. 74. Copyright 2015 Wiley-VCH. (h) SEM image of AgNWs-graphene hybrid materials. Reproduced with permission from ref. 76. Copyright 2019 IOPscience. (i) SEM image of CNTs-graphene hybrid materials. Reproduced with permission from ref. 77. Copyright 2016 American Chemical Society.

polymers such as poly(vinyl acetate) (PVA) and polylactic acid,<sup>60</sup> where a two-layer structure, a foam structure, or a composite film is constructed. A wide range of materials have been used as conductive

The piezoresistive effect is described as the change in electrical properties induced by mechanical deformations, *i.e.*, strain and pressure. The sensitivity of a strain gauge is characterised by a gauge

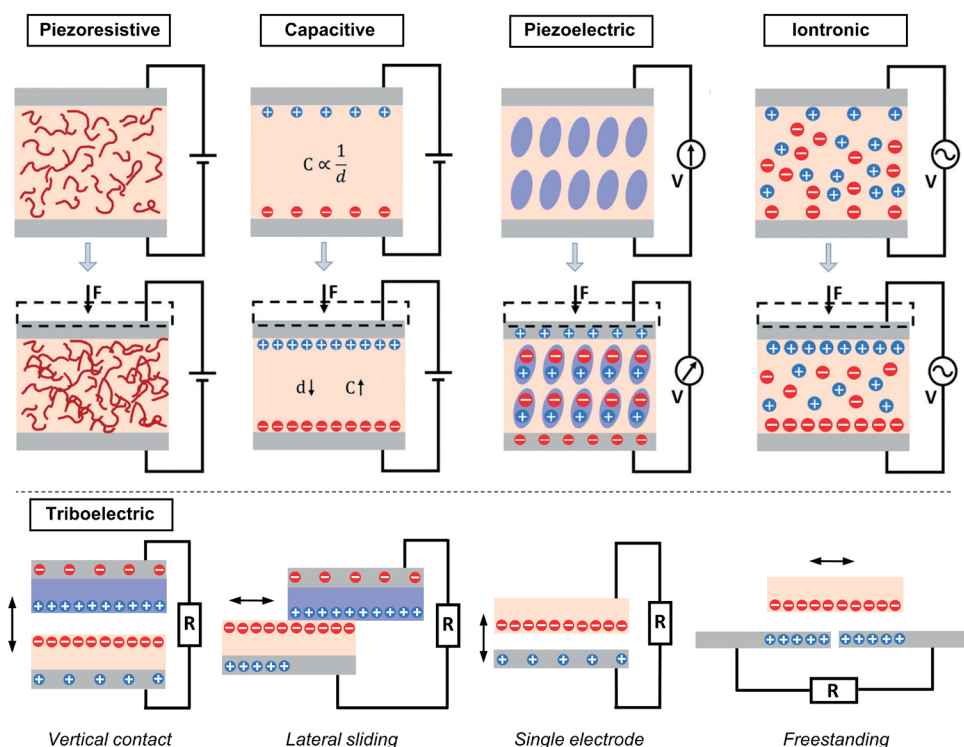


**Fig. 5** Schematics illustrating the different modalities of mechanical sensors. (a) Piezoresistivity; (b) Capacitance; (c) Piezoelectricity; (d) Iontronic; Reproduced with permission from ref. 78. Copyright 2018 Royal Society of Chemistry. (e) Four fundamental modes of triboelectricity.

building blocks to fabricate on-skin electrical sensors. Typical conductive materials are metal films,<sup>61, 62</sup> nanostructured materials<sup>63</sup> (*e.g.*, metallic nanoparticles<sup>64</sup> and nanowires,<sup>65</sup> carbon nanotubes,<sup>66-68</sup> graphene<sup>69-71</sup>), liquid metals,<sup>72, 73</sup> conducting polymers,<sup>74, 75</sup> and their hybrids (Fig. 4).<sup>76, 77</sup>

In the modern era of the Internet of Things, electrical sensors provide promising opportunities to achieve mobile health. In addition to typical biopotential recording, such as electrocardiogram (ECG), electrooculogram (EOG), electromyography (EMG), and electroencephalogram (EEG), electrical skin sensors can be used to stimulate the skin surface, or to determine the electrical properties of the skin itself, including the hydration level, electrolyte concentration, and onset of sweating.<sup>78, 79</sup>

### 2.1.2. Biophysical sensing

Skin-interfaced biophysical sensors include strain, pressure, tactile, temperature, and acoustic sensors. Their detection capability of these sensing devices ranges from identifying minor mechanical skin deformations caused by blood flow to significant skin stretching induced by bending motions of joint. In terms of working mechanisms, physical sensors can be classified into four types: piezoresistive, capacitive, piezoelectric and triboelectric, and iontronic.<sup>78</sup> The working mechanisms of each sensing modality are shown in Fig. 5.<sup>78</sup>

factor (GF):  $GF = \frac{\Delta R/R_0}{\Delta L/L_0} = \frac{\Delta R/R_0}{\epsilon}$ ,<sup>80</sup> wherein  $\Delta R$  and  $\Delta L$  are resistance and length changes, respectively;  $R_0$  and  $L_0$  are the initial resistance and device length, respectively, and  $\epsilon$  is the applied strain.<sup>81</sup> For a pressure sensor with forces applied in the normal directions, the sensitivity ( $S$ ) is denoted as:  $S = \frac{\Delta I/I_0}{\Delta P}$ . Here,  $\Delta I$  and  $\Delta P$  are current and pressure changes, respectively, and  $I_0$  is the initial current with no pressure.<sup>82, 83</sup> Among skin electronics, soft piezoresistive physical sensors have been widely investigated owing to their simple device structures. A typical piezoresistive physical sensor is constructed by depositing electrical materials onto a polymeric substrate or embedding them into polymer matrix.<sup>84, 85</sup> Commonly used polymeric substrates include PI, Parylene, poly(styrene-ethylene-butylene-styrene) SEBS, Ecoflex, PDMS, PU, and PVA.<sup>55</sup> Various kinds of electrically active materials have been utilised for the development of on-skin biophysical sensors, such as metallic materials (*e.g.*, metal films, metal liquid, metallic nanomaterials),<sup>86-88</sup> ionic liquids,<sup>80, 89</sup> carbon-based materials (*e.g.*, carbon black, graphene, carbon nanotubes),<sup>90</sup> conductive polymers,<sup>91, 92</sup> and their hybrids.<sup>93, 94</sup> For example, Ag nanowires (NWs) and AuNWs integrated percolating networks were used to fabricate on-skin transparent strain sensor for emotion monitoring, with a gauge factor of up to 236.<sup>95</sup> Resistive-type sensors developed by using these materials exhibit advantages such as high sensitivity, low detection limit, low hysteresis, and good cyclic performance. Additionally, the low working voltage and energy

consumption make resistive-type sensors an ideal candidate for ambulatory healthcare systems.<sup>96</sup>

gas).<sup>103</sup> Similar to piezoelectric sensors, triboelectric sensors are good candidates for self-powered skin sensors owing to the simple

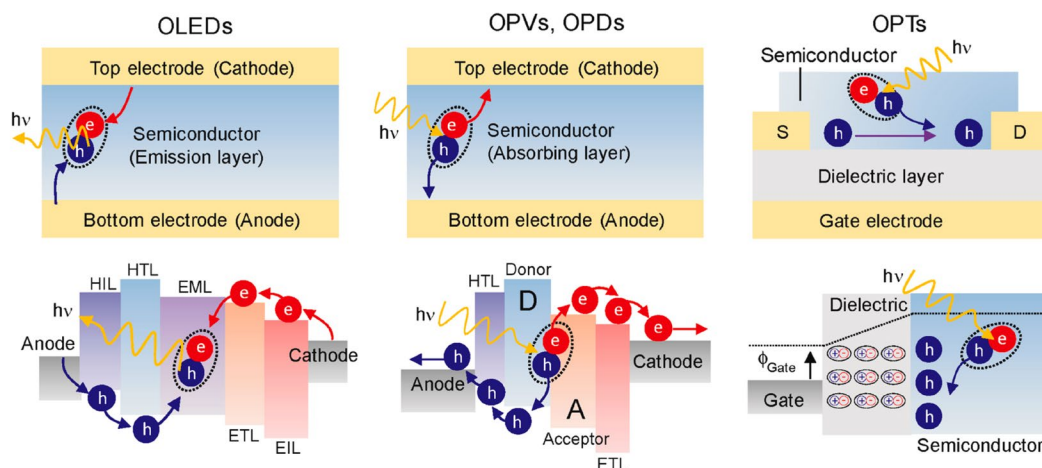


**Fig. 6** Device structure and working mechanism of organic optoelectronic devices. Reproduced with permission from ref. 116. Copyright 2015 Elsevier.

Capacitive-type sensors have a typical sandwich structure constructed by two parallel electrodes and a middle dielectric layer. The capacitance ( $C$ ) can be calculated by  $C = \epsilon_0 \frac{S}{d}$ , where  $\epsilon_0$  presents the permittivity of the dielectric layer,  $S$  and  $d$  are the electrode area and distance between electrodes, respectively.<sup>97</sup> Deformations such as strain or pressure lead to capacitance changes. Conductive materials such as metallic materials (*e.g.*, metal films, metal liquids, metallic nanomaterials) and carbon-based materials have been used to fabricate electrode plates.<sup>98</sup> Capacitive-type sensors have excellent sensing linearity, although their parasitic noises from the body and environment should be considered in real-life applications.

The piezoelectric effect is a change in electrical polarisation inside the piezoelectrical material under external force, pressure, or strain, rendering a change in surface charge (voltage) at the surface of the piezoelectric material. Piezoelectricity is generated instantaneously, hence, piezoelectric sensors have a fast response time and high sensitivity. Popular piezoelectric materials are poly(vinylidene fluoride-co-trifluoroethylene) (P(VDF-TrFE)), zinc oxide nanowires (ZnO NWs), lead zirconate titanate (PZT),<sup>99</sup> and aluminium nitride (AlN),<sup>100</sup> Recently, Sun *et al.* utilized conformable piezoelectric thin films to reliably decode facial movement, with integration of algorithms and three dimensional (3D) digital image correlation.<sup>100</sup> Piezoelectric sensors have promising features such as high sensitivity, real-time sensing, and good flexibility, and can be used as self-powered skin sensors.

The basic working mechanism of a triboelectric-type sensor is that the mechanical deformation induces relative displacement between two triboelectric parts, which leads to potential differences between the two working electrodes and drives electrons to flow across.<sup>101</sup> Zhonglin Wang *et al.* have developed numerous wearable electronics based on the triboelectric effect.<sup>102</sup> Triboelectric effect exists widely in human life, and it occurs for any material, in any state (solid, liquid,

structure, easy fabrication, various working modes, multiple options regarding materials, and high power density. Various materials can be used for triboelectric-type sensors, such as polyamide, polytetrafluoroethylene (PTFE), polyvinylidene fluoride (PVDF), and silk.<sup>104, 105</sup>

Iontronic-type sensors can substantially overcome parasitic noise by enhanced stress/pressure-induced capacitive change at the nanoscopic electric double layer (EDL) interface. They are made from ionic materials, such as ionic liquids, ionic gels, or ionic nanofibres, which are distinct from the traditional parallel-plate capacitive sensors.<sup>106, 107</sup> Iontronic sensors exhibit high transparency, good stretchability, and remarkable device sensitivity. As for on-skin applications, materials choice of iontronic sensors should be carefully considered due to the biocompatibility issues. Recently, studies have shown that modulating EDL at liquid/solid interfaces can result in electricity generation while under environmental stimuli.<sup>108, 109</sup> An EDL-based self-powered triboelectric sensor was developed using a pyramid-structured hydrogel and dielectric polymer.<sup>110</sup>

### 2.1.3. Optical sensing

Nowadays, commercialised gadgets equipped with optical sensors can measure bio-signals including step count, respiratory rate, blood oxygenation, heart rate, and even sleep habits. Such optoelectronic technologies have attracted considerable attention in the field of wearable electronics. Optical sensors are immune to electromagnetic radiation and are capable of non-invasive interrogation of biological matters at relatively large penetration depths.<sup>111</sup> A large amount of biomedical information is obtained by non-invasive skin-interfaced optical devices, where the measurement is taken while the skin is exposed to a particular wavelength of light source. The light sources are chosen based on specific applications, ranging from single-wavelength laser to narrow bandwidth light emitting diodes (LEDs). To acquire the biomedical signals, such as blood pressure, heart rate,

or glucose concentration, the optical sensors measure the change of reflected, absorbed, or refracted light.<sup>111, 112</sup> Typical optical technologies include organic light emitting diodes (OLEDs), organic photo diodes (OPDs), organic phototransistors (OPTs), photoresistors, optical fibres, colorimetric, plasmonic, and fluorometric sensors.<sup>112-116</sup> Heart rate and oxygenation are widely monitored parameters for organic optoelectronic devices. Chemical biomarkers, such as pH, metabolites (*e.g.*, glucose and lactic acid) and electrolytes (*e.g.*,  $H^+$ ,  $Na^+$  and  $Cl^-$  in body fluids) can be monitored using optical chemical sensors, such as those based on colorimetric, fluorescence, and luminescence.<sup>117-119</sup>

Organic optoelectronic devices, including OLEDs, OPDs, and OPTs can be produced on flexible elastomers to achieve wearability onto the human skin.<sup>120</sup> Wearable OLED, OPD, and OPT devices have shown promising features, such as a cost-effective, large-area, low-temperature process, and the ability to tailor optical properties via molecular engineering.<sup>116</sup> These devices are termed as photonic skin sensors. Fig. 6 displays device structure and working mechanism of organic optoelectronic devices.<sup>116</sup> OLEDs consist of organic light-emitting materials sandwiched between an anode and a cathode. Between the anode and cathode, an emissive layer (EML) is in between electron transport layer (ETL) and the hole transport layer (HTL). When a voltage is applied, electrons and holes recombine in the EML, leading to light illumination. OPDs has a structure similar to OLEDs, where a photoactive layer is sandwiched between an anode and a cathode, however with an opposite working mechanism. When an incident light has sufficient energy, excitons are generated and separated into free holes and electrons, which then diffuse to the anode and cathode through the HTL and ETL. OPTs are a type of light-sensitive organic field-effect transistors (OFETs), which are composed of gate, source, and drain electrodes, a dielectric layer, and a light-responsive semiconducting channel layer. Under illumination, the channel layer absorbs light, then a photocurrent is generated by the OPT. A photoresistor has relatively simple structure with a straightforward working mechanism, where the resistance changes under light irradiation. Compared to other optical sensors, photoresistors have longer response time, but with a large dynamic range.<sup>121</sup>

Transparent, conducting electrodes are crucial components of photonic skin sensing devices. Metallic NWs/nanofibres,<sup>122-124</sup> carbon nanomaterials (graphene and carbon nanotubes),<sup>125</sup> liquid metal,<sup>126</sup> and conducting polymers<sup>127</sup> such as poly(3,4-ethylenedioxythiophene):poly(styrenesulfonate) (PEDOT: PSS) have been utilised as electrode materials with adjustable transparency and conductivity. For active semiconducting materials, composites made of emissive polymers, ionic conductors, and salts have been used for OLEDs, whereas solution-processed bulk heterojunctions (BHJs) materials are among the popular choices for OPDs.<sup>128</sup> For photoresistors, active materials such as cadmium sulfide (CdS), molybdenum disulphide ( $MoS_2$ ), and perovskite have been reported recently.<sup>121</sup> The performance of photonic skin devices can be enhanced by tuning device interface, device structure, and components in the active layers.

#### 2.1.4. Biochemical sensing

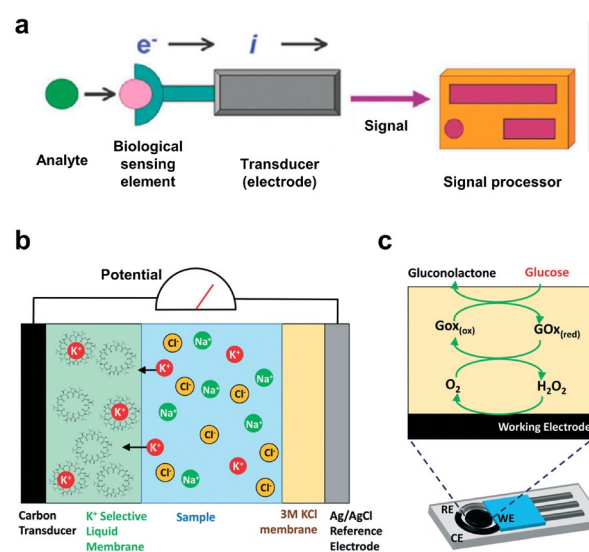


**Fig. 7** Working mechanism of electrochemical sensors. (a) Working principle of a typical electrochemical biosensor. Reproduced with permission from ref. 130. Copyright 2020 American Chemical Society. (b) Potentiometric and (c) amperometric modalities. RE is the reference electrode, CE is the counter electrode, and WE are the working electrode. Reproduced with permission from ref. 78 Copyright 2018 Royal Society of Chemistry.

Direct chemical detection is used extensively in gold-standard blood and urine tests, which usually accompanied with hospitalized bulky and expensive analytical instruments. As attractive alternatives to these bulky instruments, on-skin biochemical sensors enable dynamic assessment of human health at the molecular level. Particularly in the past 5 years, innovative materials and flexible designs have led to the development of myriad biochemical sensors that can identify and quantify representative electrolytes, metabolites, heavy metals, and toxic gases directly in body fluids, such as saliva, tears, sweat, wound, and interstitial fluid, as well as exhaled breath.<sup>13, 129</sup> As mentioned in the optical sensing subsection, a number of biochemical signals can be detected with optical sensors via chemical-to-optical transduction. In the following, we will discuss biochemical sensors using chemical-to-electrical transduction. Fig. 7a presents working principle of a typical electrochemical biosensor.<sup>130</sup> An analyte can be sampled and analysed using various electrochemical approaches, such as two major approaches of amperometric and potentiometric techniques, and others including voltametric techniques, affinity-based immunosensors and DNA sensors, which exhibit electrical changes, *i.e.*, current or potential, at functionalized electrode and transduce the correlated analyte concentrations to readable signals.<sup>130</sup> A typical soft electrochemical sensor comprises three elements: a flexible substrate, an active layer, and electrodes.<sup>131</sup> The electrodes generally comprise a working electrode (WE) or sensing electrode, a counter electrode (CE), and an additional reference electrode (RE) that help stabilise the system by maintaining a certain potential to compensate the imbalance caused by the continuous chemical reactions at the WE.<sup>132</sup> An electrolyte layer is present between the electrodes to separate

them.<sup>130</sup> Potentiometric chemical sensors measure potential change under the selective recognition of a target analyte. An ion-selective electrode is used to allow only one particular ion analyte that will determine the voltage response (Fig. 7b). In terms of amperometric chemical sensors, a potential is applied between WE and RE, leading a current change by electron-transfer reaction of in the presence of the target analyte (Fig. 7c).<sup>78</sup>

Commonly used substrate materials include the polymerics described in the section of electrical sensing, these polymers enable bio-compatible physical properties and interfaces for skin-laminated biochemical sensors. Metallic nanomaterials including transition metal-based nanomaterials, carbon-based materials, conducting polymers, and their hybrids have been commonly used for electrode preparation because of their high conductivity and easy fabrication.<sup>130, 133</sup> Among them, gold nanomaterials popularize because of their excellent biocompatibility and superior resistance to oxidation. Currently, two major approaches, such as enzymes and antibody/aptamer have been utilised to modify WEs to improve the sensitivity and selectivity of the sensor. In contrast to electrical materials that remain constant in electrodes, active materials in WEs need to have high enough sensitivity to the analyte of interest. The most common types of nanomaterials used in recent chemical sensors include transition metal-, carbon-, and polymer-based materials.<sup>131</sup> These materials are used both in solely pristine form and in combination as a form of nanocomposites, such as polymer/metal,<sup>134</sup> carbon/metal,<sup>135</sup> and polymer/carbon.<sup>136</sup>

## 2.2. Other sensing devices

With the above four well-developed sensing modalities, emerging sensor platforms have been further developed, leading to transistor-based and multimodal sensing devices. In the following part, we will focus on transistor-based and multimodal sensing devices.

### 2.2.1. Transistor-based sensing

Organic transistors have excellent biocompatibility, readout integration, large-area coverage, power efficiency, and can be easily integrated into portable electronic devices. They have been spotlighted as a tool of choice for skin bioelectronics correlated mainly to chemical and biophysical (*e.g.*, strain, pressure and temperature) sensors.<sup>137-139</sup> An obvious advantage of organic transistor-based sensors is their higher sensitivity than two-terminal-based sensors, because of their signal amplification and controllability that is obtained by modulating the gate voltage.<sup>96, 116, 140</sup> A wide range of conjugated small molecules, polymers, and room-temperature liquid crystals have been applied as active channel semiconductors in soft organic transistor devices.<sup>137</sup> The material choice depends on the applications and requirements of the specific sensors.

For chemical sensing, there are two types of transistor-based sensors: OFETs and organic electrochemical transistors (OECTs). Typically, OFETs comprise three electrodes, a semiconducting layer, and a gate dielectric layer. The semiconducting layer is usually exposed to the analyte of interest, acting as both an electronic transport material and a chemical sensing layer. For OECTs, an electrolyte is adopted instead of a dielectric layer, which is sandwiched between the gate electrode and the active semiconducting layer. Under the exposure to an analyte, potential changes occur

across the gate/electrolyte or electrolyte/channel interfaces.<sup>140, 141</sup> Although the working mechanisms are different, these transistors can interact with target analytes via similar device engineering to enable diverse biosensors.<sup>137, 142</sup> In the physical sensing area, organic transistors have been used to address the matrix reading of the pressure mappings.<sup>143</sup> Innovative printing methods, such as ink-jet, reverse offset, roll-to-roll gravure offset, screen printing, and dispersing printing, ultimately led to fabrication of organic transistor-based sensor arrays for a wide range of biomedical applications.<sup>144-147</sup> Transistor-based biophysical sensors exhibit higher sensitivity than resistive and capacitive-type devices due to their capacities to vary the conductance of channel materials by controlling the gate voltage. These features make transistor-based sensors attractive candidates for advanced skin bioelectronics.

### 2.2.2. Multimodal sensing

A single sensor monitoring system is neither practical nor ergonomically sound for long-term and continuous health monitoring. To achieve higher productivity in health monitoring, more sensing functionalities are necessary. Multimodal sensors are expected to be integrated into one skin device, such that one device can detect and quantify multiple external stimuli and provide a comprehensive analysis of the multiple bio-signals to make an accurate assessment on an individual's health condition.<sup>148, 149</sup> For example, the utilization of photoplethysmogram (PPG) sensors in combination with ECG sensors provides more reliable disease diagnosis and health-monitoring capability than a single device.<sup>150</sup> multimodal sensors can be realised by assembling sensors with various functions, which can simplify the integration of sensors and miniaturise their volume.<sup>29, 151</sup> There has been a plethora of reported multi-sensor systems that can detect multiple vital signs in a single device.<sup>23, 27, 152</sup> Concurrent detection of two or more different bio-signals,<sup>153</sup> such as temperature and pressure,<sup>154</sup> pressure and biochemical,<sup>155</sup> and biochemical, electrophysiological and skin temperature.<sup>156</sup> have been reported by a large number of researchers in the soft electronic area.

Additionally, the rapid advancements in novel sensing materials, fabrication strategies, and innovative electronic constitution not only support the progressive development of versatile integration of multimodal sensors, but also allow the realisation of sensor platforms with promising functionalities such as self-healing, visualization, diagnose and therapy, and self-powering.<sup>92, 153, 157-162</sup>

## 3. Towards long-term, continuous health monitoring

To allow long-term, continuous health monitoring, generally, skin bioelectronics should be mechanically and biologically compatible with the human body when collecting bioinformatics.<sup>163</sup> To achieve personalised medical care through long-term, continuous health monitoring, other issues, such as power sources and communication technologies, should also be considered. In this section, we will discuss material and structure selection, mechanical robustness, and wireless monitoring of skin bioelectronics for long-term, continuous health monitoring. Representative examples are presented, with a focus on discussion and comparison of the performances of various materials and designs.

### 3.1. Material and structure selection

From a material and structure perspective, recent efforts in four areas, are reviewed and discussed in this section: ultrathin materials and devices, biocompatibility, breathability, and waterproofness,

### 3.1.1. Ultrathin materials and devices

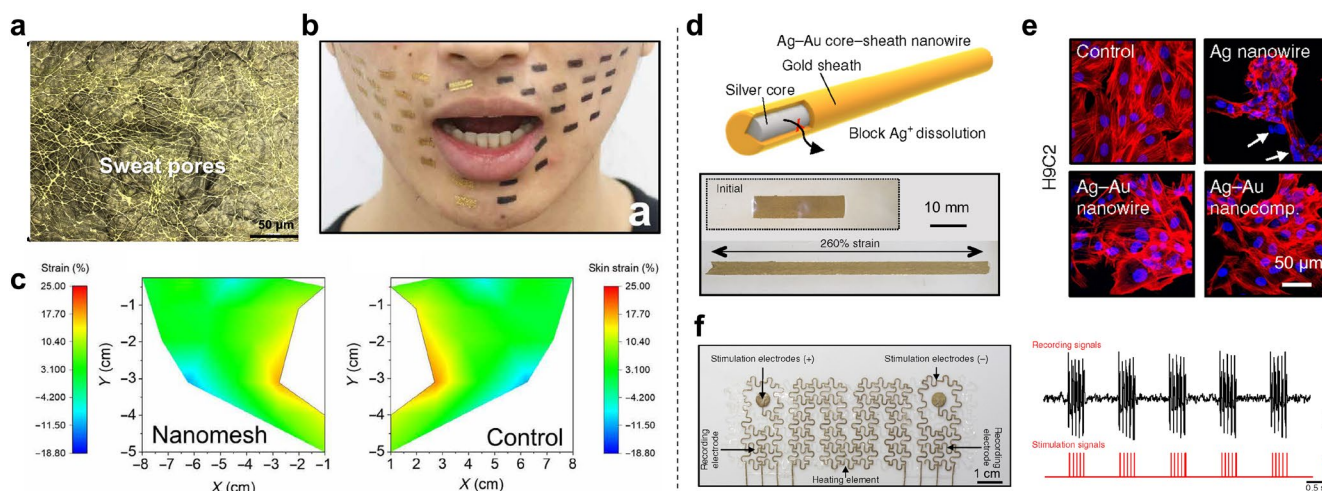


**Fig. 8** Ultrathin materials and devices, and biocompatibility of skin bioelectronic devices. (a) Microscopical images of the nanomesh strain gauge on fingertip replica, demonstrating distinct sweat pore features. (b) Photograph of a face during speech of “a.” (c) Strain mapping of the face during speech of “a.” Reproduced with permission from ref. 179. Copyright 2020 American Association for the Advancement of Science. (d) Schema of Au coated AgNW and a photograph of the Ag–Au nanocomposite before and under strain. (e) Biocompatibility test: confocal microscope image of H9C2 cells after exposure to control and Ag–Au nanocomposite samples for 24 h. (f) Multifunctional skin patch and collected EMG signals under electrical stimulation. Reproduced with permission from ref. 23. Copyright 2018 Nature Publishing Group.

To satisfy mechanical compliance, skin bioelectronics are usually made into ultrathin formats.<sup>164, 165</sup> Flexural rigidity is highly correlated with the conformability of a film to a rough surface, which is defined as  $D = \frac{Et^3}{12(1-\nu^2)}$ . Here,  $E$ ,  $t$ , and  $\nu$  denote Young’s modulus, thickness, and Poisson’s ratio of the thin film, respectively. Therefore, reducing the thickness is the most effective approach to decreasing flexural rigidity due to the cubic dependence on thickness.<sup>166, 167</sup> Ultrathin materials are the primary choice for skin bioelectronics. For example, thin PI substrates have been widely used to construct epidermal electronics.<sup>168–170</sup> Popular ultrathin materials are thin polymeric films<sup>167</sup> such as Parylene,<sup>57</sup> electrospun nanofibres,<sup>39</sup> and ultrathin conducting films from polymers<sup>171</sup> and metallic<sup>172</sup> or carbon-based<sup>173</sup> nanomaterials. With such materials, we have seen the development of various ultrathin conformable skin bioelectronics in the last six years, such as tattoo-like sensors,<sup>174, 175</sup> energy devices,<sup>176</sup> photonic skins,<sup>19</sup> and integrated circuits.<sup>177</sup> In addition to thin film formats, ultrathin porous devices have also been developed, usually accompanied with the additional advantage of gas permeability. These thin, porous devices can obtain excellent skin conformability for high-quality health monitoring. Zhou *et al.* developed a porous thermoplastic polyurethane (TPU) film using the breath-figure method. Then a highly conductive AgNW/TPU composite was fabricated by dip-coating and heat-pressing, with a total thickness of 4.6  $\mu\text{m}$ . No allergic reactions and sweat accumulation occurred after 7 days of wearing on the human skin.<sup>178</sup> The AgNW/TPU electrode

demonstrated comparable SNR of the ECG signals to that of Ag/AgCl gel electrodes. Another example is a conformable strain gauge sensor made from PU–PDMS nanomesh coated with a gold layer (Fig. 8a).<sup>179</sup> The total thickness of the nanomesh sensor was approximately  $430 \pm 18$  nm. The authors demonstrated that the nanomesh strain gauge did

not affect the natural skin motions, the face with nanomesh-attached exhibited similar strain mapping with that of the face without sensors (Fig. 8b,c). Additionally, long-term wearing of 3.5 h did not influence the sensor performance because of its ultrasoft nanomesh structure and thinness geometry.

### 3.1.2. Sensing materials

A wide of materials have been used as sensing materials to construct skin bioelectronics. Representative examples can be seen in Fig. 4, including zero dimension (0D) (*e.g.*, fullerenes, quantum dots, metallic NPs), one dimension (1D), two dimension (2D) nanomaterials, liquid materials, and polymers. Among them, 1D, *i.e.*, CNT and NWs (*e.g.*, Cu,<sup>180</sup> Ag,<sup>181</sup> Au,<sup>86</sup> and ZnO<sup>182</sup>) are one of the most promising sensing materials, due to their high electrical conductivity, intrinsic flexibility, and transparency. They are sensitive to a wide spectrum of stimuli, such as tactile, temperature, and molecules.<sup>183, 184</sup> Besides sensors, CNTs have also been applied as active channel materials for soft transistors.<sup>185</sup> To reduce contact resistance between 1D nanomaterials, many approaches have been used, such as sintering,<sup>186</sup> pressing,<sup>34</sup> increasing loading materials,<sup>187</sup> templating,<sup>188</sup> and mixing with softer fillers.<sup>189</sup> Furthermore, surface modifications have also been used to enhance contacts of 1D nanomaterial networks, leading to better electrical properties.

2D nanomaterials have a shape of sheet or membrane. They include graphene, MoS<sub>2</sub>, MXene, and black phosphorus.<sup>190</sup> As a typical 2D material, graphene can be obtained by micromechanical

exfoliation and chemical vapor deposition (CVD) method. Graphene is a film of  $sp^2$ -hybridized carbons, and exhibits excellent transparency ( $\sim 97.7\%$ ), high electrical/thermal conductivities ( $200000\text{ cm}^2/(\text{V s})$  and  $5000\text{ W/mK}$ ), and biocompatibility.<sup>50</sup> It has been extensively used as active materials for flexible/stretchable sensors to detect biophysical, electrophysiological, and biochemical signals.<sup>191</sup>  $\text{MoS}_2$  is a semiconductor, exhibiting thinness, superior photoabsorption, and piezoresistivity. It is excellent material for strain sensor,<sup>192</sup> humidity sensor,<sup>193</sup> nonvolatile memory.<sup>194</sup>  $\text{MoS}_2$  and graphene can form high-quality contact because of strong van der Waals adhesion force. Therefore, they can be integrated as promising building blocks for soft electronics and optoelectronics.<sup>50</sup>

Conductive polymers are promising sensing materials due to its advantageous electrical and mechanical properties. There are highly  $\pi$ -conjugated polymer chains in conductive polymers. By doping, conductive polymers can be conductive or semiconductive, depending on the dopant and doping level.<sup>195</sup> There are dozens of conductive polymer now, such as poly(3-hexylthiophene) (P3HT), polyaniline (PANI), PEDOT:PSS, polypyrrole (PPy), polyacetylene (PA), and polythiophene (PTh). P3HT, PANI, PEDOT:PSS, and PPy have also been employed as active channel materials in FETs. Among the available conductive polymers, PEDOT:PSS is the most studied one because of easy fabrication, high conductivity, and biocompatibility. Towards long-term health monitoring, novel materials and fabrication techniques are required while using conductive polymers. Very recently, Chen *et al.* reported a substrate-free PEDOT:PSS film as ultra-conformable E-tattoo.<sup>196</sup> The skin adhesion can be regulated during the transformation of gel to dry PEDOT:PSS. This E-tattoo could achieve higher signal quality than that of commercial Ag/AgCl electrodes. The PEDOT:PSS electrode could adhere to the human skin for more than 10 h without falling.

### 3.1.3. Biocompatibility

Skin bioelectronic devices have direct contact with the human skin, where biocompatibility is a critical parameter to be considered, especially for long-term applications.<sup>197</sup> Considerable efforts have been put into the development of biocompatible active materials and biocompatible encapsulating layers.<sup>198-200</sup> As a result, numerous biocompatible skin bioelectronics have been reported ranging from sensors,<sup>201, 202</sup> to energy devices,<sup>203, 204</sup> to integrated circuits.<sup>205</sup> For example, a biocomposite electrode was developed by using biocompatible silk fibroin (SF) and PPy.<sup>206</sup> The two materials form interlocking structures by interfacial polymerisation, thereby achieving highly adhesive and stretchable biocomposite electrodes. The electrodes could be attached to the human skin and reliable ECG signals were collected continuously during running for 2 h. This work provides impressive material solutions for future skin bioelectronics for long-term health monitoring.

To overcome the silver ion leaching and oxidation issue, a thick gold sheath was deposited on the surface of AgNW surface to obtain a biocompatible and highly conductive material (maximum conductivity of  $72,600\text{ S cm}^{-1}$ ) (Fig. 8d,e).<sup>23</sup> The conductivity of the Ag–Au nanocomposite showed negligible changes during 3 weeks of storage in phosphate-buffered saline solution. They fabricated multifunctional skin devices with the biocompatible nanocomposite by patterning on a PDMS substrate, their devices successfully

measured real-time electrophysiological signals and delivered electrical and thermal stimulation (Fig. 8f). Furthermore, Bandodkar *et al.* developed a biocompatible battery that was powered by sweat, then the battery was applied to power skin integrated circuits for continuous health monitoring.<sup>205</sup> The battery comprised skin-safe electrode and separator materials, and sweat as electrolyte. It consisted of hybrid silicone and paper-based microfluidic systems to enable rapid sweat capture and storage. The electrical isolation circuits enabled high-quality heart rate measurements from ECG signals, with performance aligned with standardised values from the American National Standards Institute/Association. A general way to quantitatively evaluate biocompatibility is cell viability assay,<sup>207, 208</sup> which is *in vitro*, *i.e.*, a cellular-level biocompatibility. A *in vivo* approach is to attach samples onto animal tissues or human skin and investigate the presence of inflammation,<sup>209</sup> fibrotic reaction,<sup>23</sup> or irritations.<sup>21</sup>

### 3.1.4. Breathability

Although many current skin bioelectronics are based on a low-permeability film-type form factor, a health microenvironment allows the human skin to 'breathe', that is, there is sufficient permeability to air, water vapour, and liquid.<sup>210, 211</sup> To realise full potential of long-term health monitoring, breathability is one of the key features to target on for skin bioelectronics.<sup>59, 212</sup> Breathable electronic devices also improve the biocompatibility of skin electronic devices because they do not cause inflammation and are gas-permeable.<sup>211</sup> Electrospun nanofibres are one of the most used materials for breathable electronics because of their porous structure, diverse configurations, and excellent mechanical properties.<sup>59, 213, 214</sup> A typical example is to use substrate-free nanomesh devices.<sup>21</sup> Simply evaporate a gold layer on a dissolvable PVA electrospun nanofibre mat; the thin gold layer would bond to the human skin after water mist treatment. No negative feedback was reported after a 7-day attachment of the nanomesh skin patch, opening possibilities for continuous, long-term health monitoring. Later, the team utilised the nanomesh system and developed several breathable skin devices, including electrical sensors,<sup>34</sup> strain gauges,<sup>179</sup> hydration sensors,<sup>79</sup> and mechanoacoustic sensors.<sup>215</sup> With all-nanofibre-based device design, mechanoacoustic heart signals were continuously monitored for 10 h.<sup>215</sup> Recently, Ma *et al.* developed highly stretchable permeable monolithic skin bioelectronics from a liquid-metal fibre mat.<sup>27</sup> The mat showed excellent biocompatibility both *in vivo* and *in vitro* tests and exhibited stretchability of over 1800% strain. One-week wearing did not cause any discomfort. The authors successfully demonstrated the reliable operation of the ECG and sweat sensors and skin heater (Fig. 9a–d).

Breathability can also be achieved by ultrathin film electronics.<sup>216</sup> For instance, a bubble-blow method was employed to fabricate a 90 nm-thick thermoplastic elastomer, then a breathable electrode was obtained by integrating the nanomembrane with AuNWs. The total thickness of the dry electrode was 160 nm. The dry electrodes could survive 5 h wearing without causing any discomfort to the subject.<sup>217</sup> Another 95-nm thick PDMS nanofilm was constructed using an effective dip-coating approach. With a gold layer deposited on the top of the nanofilm, a gas-permeable dry electrode was obtained and self-adhered to the human skin for one week high-fidelity ECG

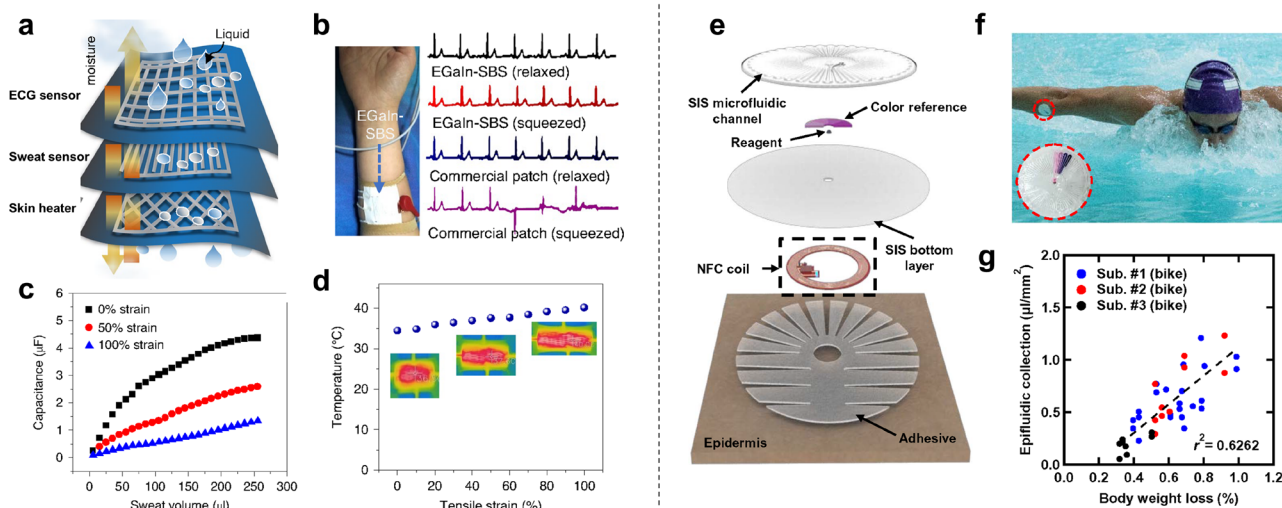


**Fig. 9** Breathable and waterproof skin bioelectronic devices. (a) Permeable monolithic skin electronics made from superelastic liquid-metal fibre mat. (b–d) The device could monitor ECG signals, sweat volume, and heating performance simultaneously. Reproduced with permission from ref. 27. Copyright 2021 Nature Publishing Group. (e) Device design of a waterproof, microfluidic skin devices for body hydration management. (f) Device used during vigorous physical activities in aquatic environment. (g) Sweat measurement. Reproduced with permission from ref. 226. Copyright 2019 American Association for the Advancement of Science.

monitoring.<sup>166</sup> Compared to film-type, well-encapsulated skin devices, breathable electronics may suffer from inferior SNR and/or weak stability due to difficult encapsulation, particularly for foam-based breathable electronics.<sup>218, 219</sup> Novel materials and fabrication technologies should be developed to solve these issues. To quantitatively evaluate breathability, water vapor transmission rate has been widely used.<sup>34, 178</sup> In this experiment, glass bottles (with a certain amount of water) are sealed with the tested samples and put in a thermostatic chamber undisturbed for a period. The weight of the bottle will be measured periodically. Some researchers also utilize commercial tools to evaluate air/water permeability rate.<sup>27, 220</sup>

### 3.1.5. Waterproofness

During long-term usage, particularly for health and fitness monitoring in athletics where there is a lot of sweat or in aquatic environment, the skin bioelectronic devices may experience deterioration or even device failure. Possible reasons could be device delamination from the skin or analyte contamination. Therefore, it is highly desired to develop waterproof or washable skin bioelectronics in varied hydrated conditions, such as sweating, raining, swimming, and showering.<sup>221</sup> Novel materials and structure engineering have been utilised to develop skin bioelectronics that are capable of sustaining high adhesion and water resistance in hydrated environments. With electrospun porous materials, researchers have achieved breathable and water-resistant skin bioelectronics by introducing hydrophobic materials.<sup>222</sup> Additionally, specialised design of fibre mats can guide the direction of sweat transport, thus maintaining the electrical performance of the skin-attached devices.<sup>223, 224</sup>

In addition to porous materials, film-type electronics have also been investigated.<sup>225</sup> Reeder *et al.* developed a waterproof, epidermal, microfluidic and electronic systems that adhere to the human skin for

sweat collection, biomarker analysis, and thermography, even in aquatic settings. They chose polymer materials with ultralow rates of water/chemical penetration, and particularly designed inlets and outlets of microfluidic channels to prevent contamination in aquatic surroundings without impeding in-flow sweat. The developed system could bond to the human skin and perform key hydration mapping via underwater sweat collection and skin thermography during vigorous physical activity in controlled, indoor conditions and in open ocean swimming, to realise personalised hydration strategies for athletics and fitness areas (Fig. 9e–g).<sup>226</sup> Because the performance of some energy generators such as biofuel cells (BFCs), triboelectric nanogenerators (TENGs), and piezoelectric nanogenerators (PENGs) suffer from humidity caused by sweat, additional encapsulations may solve the problem but result in increased thickness of the devices. Zhou *et al.* developed a waterproof magnetoelastic generators using biomechanical energy source. The magnetoelastic generator was fully water resistant without encapsulation because the magnetic field can go through water with negligible intensity loss. The integrated system could continuously measure cardiovascular health under the condition of heavy perspiration.<sup>227</sup>

## 3.2. Device property

Human skin is in time-dynamic motions, which require that skin bioelectronics can survive repetitive bending, stretching, compressing, twisting, etc. In other words, skin bioelectronics should be thin, lightweight, and have robust skin adhesion, good flexibility and stretchability and mechanical durability to ensure stable functionalities during long-term, continuous health monitoring. In the following part, we will discuss aspects of skin adhesion, flexibility/stretchability, and mechanical durability in detail.

### 3.2.1. Skin adhesion

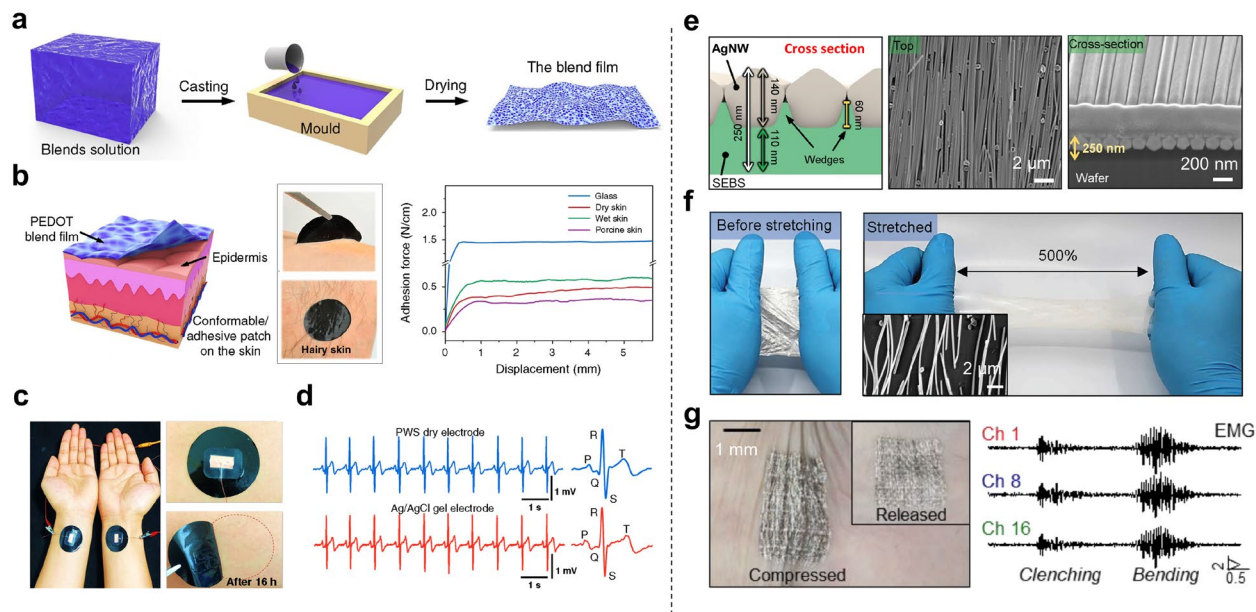


**Fig. 10** Skin adhesion and flexibility/stretchability of skin bioelectronic devices. (a) Fabrication process of the adhesive composite. (b) Adhesion performance of the PEDOT:PSS composite electrodes. (c) Photographs showing the robust adherence of dry electrodes on the human skin. No irritation was found after 16-h use at the attachment sites. (d) ECG monitoring results of the dry electrodes and Ag/AgCl commercial electrodes. Reproduced with permission from ref. 171. Copyright 2020 Nature Publishing Group. (e) Structure of AgNW/SEBS nanomembrane. (f) Photographs demonstrating nanomembranes before and under strain of 500%. Inset scanning electron microscope (SEM) image shows the surface morphology under 500% strain. (g) A photograph of an on-skin multifunctional sensor array made from the nanomembranes and the measured EMG results from three channels. Reproduced with permission from ref. 152. Copyright 2021 American Association for the Advancement of Science.

It is worth mentioning that the skin bioelectronics discussed in the subsection of ultrathin materials and devices adhere to the human skin by pure van der Waals forces, owing to their sufficient thinness and ultraflexibility.<sup>166</sup> One obvious advantage of gel-free self-adhesiveness is that the bio-devices can bond to the human skin without further external forces or adhesive materials, which are burdensome and limit individual's mobility.<sup>48, 217</sup> As a representative example, Nawrocki *et al.* reported a sub-300 nm dry thin-film electrical sensor that could self-adhere to the human skin without any additional adhesives. The dry electrode could attach to the human skin and monitored ECG and EMG signals for as long as 10 h, with a signal quality comparable to that of adhesive Ag/AgCl gel electrodes.<sup>228</sup> Generally, soft electronic devices are vulnerable to rigorous mechanical disruptions if the device thickness is ultralow.

For long-term health monitoring, good mechanical durability of the device is highly important, considering the consistent and dynamic skin motions. Therefore, advanced materials and innovative structure designs should be used to overcome the trade-off between mechanical durability and geometric thinness. With nanofibre reinforcement, Wang *et al.* developed a robust, self-adhesive dry electrodes with a thickness of 165 nm.<sup>166</sup> The reinforced PDMS nanofilm exhibited an impressively high area adhesion energy of 159  $\mu\text{J}/\text{cm}^2$ . The as-fabricated Au-PDMS-reinforced nanofilm electrode could self-adhere to the human skin for one week for high-quality ECG monitoring. It is worth to mention that direct drawn-on skin electronics can also achieve ultra-conformability with the human skin for long-term health

monitoring.<sup>38</sup> In addition to self-adhesion of ultrathin devices, for devices with a thickness approximately or over tens of micrometres, there are several strategies to obtain long-term dry skin adhesion.<sup>171</sup> One is to design adhesive structures (*e.g.*, microneedles, micropores, mushroom-shaped, and 3D suction cups) on biocompatible elastomers, such as Ecoflex<sup>229</sup> and PDMS.<sup>230</sup> Another strategy is to modify biocompatible polymers, such as PDMS and silk, to achieve dry skin adhesiveness.<sup>171, 199</sup> For instance, a sticky ECG sensor was enabled by modifying PDMS with ethoxylated polyethylenimine (PEIE).<sup>231</sup> By adding 10 wt% conductive CNT into the PDMS with 3 wt% PEIE, the authors could achieve a ECG sensor sticky to the human skin very well. The device maintained its functionality after 100 cyclic adhesion and attaching cycles to the human skin. Furthermore, it was shown 30 h of skin attachment did not cause any discomfort to the subject. These results indicate that this material has great potential for long-term health monitoring. Zhang *et al.* developed a self-adhesive dry electrode by adding D-sorbitol into the blends of PEDOT:PSS, waterborne polyurethane (WPU) (Fig. 10a,b).<sup>171</sup> This dry electrode (thickness: > 20  $\mu\text{m}$ ) achieved skin adhesive force up to 0.41 N/cm, which resulted in continuous high-performance ECG signal monitoring for 16 h, and long-term monitoring for 1 month (Fig. 10c).

### 3.2.2. Flexibility/stretchability

Mechanical flexibility/stretchability, which are the key factors in determining the comfort level of users and the portability of devices, have attracted tremendous attention worldwide for developing skin bioelectronics with such features.<sup>232</sup> Good mechanical

flexibility/stretchability enables the conformal contact with curvilinear, dynamic human skin and makes the acute health measurement possible. The ability to stretch should be over 10% strain on flat skins, and nearly 60% strain for full-range body motions, depending on the device placement and target applications. In the last six years, the progressive development of novel materials, structure engineering, and fabrication techniques has led to great advances in the mechanical flexibility/stretchability in skin bioelectronics.<sup>233, 234</sup>

There are two well-known and widely used strategies to obtain the desired mechanical flexibility/stretchability for the target applications in health monitoring: intrinsically stretchable materials and structure designs.<sup>10, 154</sup> In addition to flexible/stretchable elastomer substrates, popular intrinsically stretchable active materials include metallic/carbon-based materials, conductive polymers, organic semiconducting polymers, and nanocomposites. Intrinsically stretchable skin bioelectronics can be developed with these materials. A typical example is an intrinsically stretchable polymer transistor array with a high device density of 347 transistors per square centimetre.<sup>37</sup> The transistor was made from CNT-based electrodes, crosslinked SEBS as the dielectric, and a semiconducting ‘conjugated polymer/elastomer phase separation induced elasticity’ (CONPHINE) film. The array could be stretched both parallelly and perpendicularly up to 100% strain in the direction of charge transport, without cracks, delamination, or wrinkles. To achieve stretchability with rigid materials, appropriate geometry design can be utilised to obtain stretchable structures, such as net-shaped, island-bridge, kirigami, serpentine, and in-/out- of plane buckles.<sup>235, 236</sup> Also, many researchers have developed high-performance mechanical flexibility/stretchability with combined strategies.<sup>88</sup> For example, Wang *et al.* developed highly stretchable transparent electrode combining soft vertically aligned AuNWs and porous stretchable nanomesh structures.<sup>54</sup> The electrode had sheet resistance as low as  $1.7 \pm 0.8 \Omega$  per square, and could be stretched of over 100% strain. Apart from mechanical flexibility and stretchability, simultaneous realisation of geometry thinness is highly intriguing as for skin bioelectronics.<sup>166</sup> By manipulating AgNWs alignment with a surface nanocomposite design, Jung *et al.* reported a highly elastic nanomembrane for multifunctional skin electronics (Fig. 10e). The densely aligned AgNWs conferred high conductivity and stretchability of 540% strain, which is nearly the limit of that of the bare elastomer (570%) (Fig. 10f).<sup>152</sup> A multimodal sensor array was fabricated using photopatterned nanomembranes, where the sensors were connected by vertical interconnect access. The developed arrays could measure temperature, strain, humidity, and electrophysiological signals simultaneously (Fig. 10g).

### 3.2.3. Mechanical durability

Mechanical durability plays a pivotal role in the lifespan of skin bioelectronics for long-term, continuous health monitoring. To enable long-term applications, the skin-interfaced devices should sustain their electrical functionalities under repetitive skin deformations. This requires the mechanical robustness of two ‘soft–rigid’ interfaces: 1) rigid functional materials and soft elastomer substrates in skin bioelectronics, and 2) rigid bioelectronic devices and soft biological skin. Strategies such as an additional intermediate layer,<sup>228</sup> surface treatment,<sup>179</sup> heat pressing,<sup>34</sup> cold welding,<sup>152</sup> reinforcement,

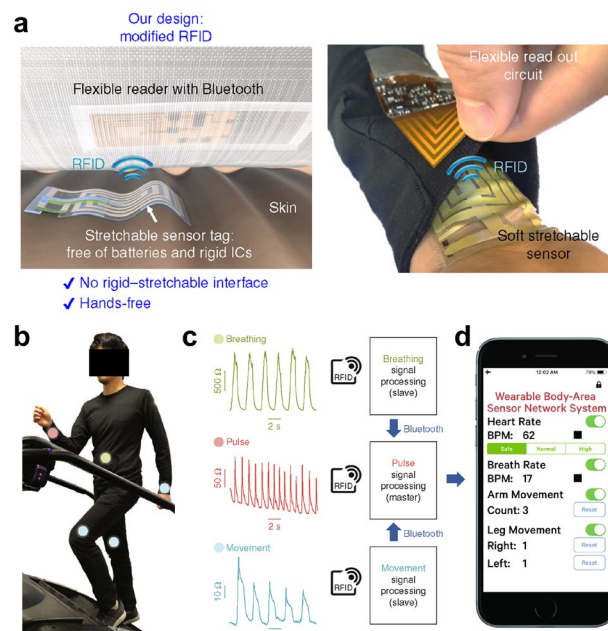


**Fig. 11** Wireless communication of skin bioelectronics. (a) Schematic design and optical photo of bodyNET, demonstrating the wireless connection between skin sensor and rigid components. (b) A photograph of bodyNET. (c) Output signals of breath, pulse, and arm movement. (d) Output signals on a smart phone. Reproduced with permission from ref. 24. Copyright 2019 Nature Publishing Group.

<sup>237</sup>infiltrating,<sup>238</sup> mixing,<sup>23</sup> and encapsulation<sup>239, 240</sup> have been employed to improve the adhesion of the rigid–soft interface during device fabrication, thus enhancing device durability. Generally, through these fabrication techniques, a functional surface composite or homogeneous composite can be obtained. A direct way to evaluate the mechanical durability of skin bioelectronics is by fatigue test via cyclic pressure loading and unloading, stretching and releasing, attaching and detaching.<sup>241–244</sup> A highly durable physical sensor was fabricated by embedding reduced graphene oxide (rGO)/deionised water (DI) liquid sensing elements into Ecoflex rubber.<sup>245</sup> Under strain or pressure, the contact change of the nanofoams in the liquid led to resistance change. The sensor exhibited stable electrical responses during 15,000 loading and unloading cycles under 25 kPa, and 10,000 stretching and releasing cycles under 40% strain.

In addition to the fatigue evaluation of mechanical durability on the skin device itself, *in vivo* evaluations have also been used for long-term health monitoring. This can be done by measuring on-skin device performance or observing the device morphology under repetitive skin deformations intentionally. For example, to evaluate the mechanical durability of nanomesh devices, the authors attached the device on the finger and measured the electrical resistance under 10,000 clenching cycles.<sup>21</sup> The sensor also survived being rubbed 20 times with a plastic pen with a pressing force of 150 kPa because of the good mechanical durability of nanomesh. As another example, a nanomesh-based strain gauge was laminated on the human wrist and monitored during 10,000 cycles of hand bending and relaxing

motions.<sup>179</sup> After 3.5 h of attachment on the human skin, the devices maintained their functionality.

### 3.2.4. Long-term stability

For continuous health monitoring, the long-term stability of skin electronics is very important. Long-term stability requires multiple aspects of characteristics including skin conformability,<sup>246-248</sup> air/water permeability,<sup>249, 250</sup> environmental stability,<sup>251-253</sup> electrical-mechanical stability,<sup>254, 255</sup> *etc.* Efforts are underway to develop stable materials and manufacturing methods to accommodate on-demand, continuous health monitoring and diagnostics.

The high conformability and adhesion in a sweaty environment over a long time is important for long-term monitoring. And the function of device should not deteriorate rapidly over time and do not generate noise. One strategy to achieve long-term stable measurements is by creating long-term stable electrodes, this allows the free connection of measurement circuits. Yang *et al.* reported a SF-based biocomposite conformal and adhesive polymer electrode by combining PPy and SF gels, which enabled long-term monitoring of mobile electrophysiological signals. The reported electrode exhibited excellent stability and sensitivity during 2 h of continuous ECG signal monitoring.<sup>256</sup> Jeong *et al.* reported a highly conformable and reusable capacitive epidermal electronic system for electrophysiological.<sup>257</sup> This is also a strategy for making long-term stable of electrodes. Another strategy to achieve long-term stability is to directly manufacture electronic skins with conformability and stability. Patel *et al.* reported a fully biocompatible and highly conductive composite ink based on a drawn-on-skin (DoS) sensor platform.<sup>38</sup> This ink can be deposited directly on human skin using a modified ballpoint pen. Sensing circuits drawn with this ink can be used to capture critical electrophysiological signals, such as EEG, EMG, ECG, *etc.*, with high signal quality. An *in situ* fabricated sensor was produced by drawing the DoS electrophysiological sensor on the forehead for recording EEG, and high signal-to-noise EEG signals were obtained on each of 3 days of testing. The sensor was not dislodged or malfunctioning during the 3 days, demonstrating the robustness of this sensor for long-term monitoring.<sup>209</sup>

Separating device from skin by packaging it in a silicone shell (*e.g.*, Ecoflex) is another strategy to achieve long-term stability.<sup>31, 258-261</sup> Stable continuous monitoring can be achieved as long as the liquid does not leak or evaporate out of the packaging over time, or its performance decreases over time. Wang *et al.* reported a stretchable strain sensor like a rubber band by filling and sealing the Ecoflex with an ionic liquid, which had excellent stability and durability. Because of the waterproof nature of Ecoflex, this sensor was stable in sweat. The electrical properties of the sensor remained virtually unchanged after 6 months of room storage.<sup>52</sup>

Skin bioelectronics with self-healing capabilities is another means of achieving long-term stability.<sup>262-264</sup> Jin *et al.* reported an intrinsically stretchable and self-healing semiconductor film, which can be used in pressure and strain monitoring.<sup>265</sup> The brittle semiconductor film was durable and self-healing because the dynamic metal-ligand coordination bonds in the film can rebuild themselves after fracture. The scarring of the cut film disappears completely within 24 h at room temperature. In addition, the electrical properties

of this semiconductor film are unaffected during 15 h of operation, even when immersed in sweat.

### 3.3. Wireless technologies

Towards long-term, continuous health monitoring, skin bioelectronic systems require urgent need for wireless communications to transmit data to the wearer and a distant server and even for a sustainable power supply. Because wired connections constrain the users' mobility and may experience frequent failed connections, they are not preferred for long-term health monitoring. Therefore, wireless technology can be adopted as the most viable and reliable alternative for data communication.<sup>44</sup>

#### 3.3.1. Communication technologies for skin bioelectronic systems

Immense efforts have been dedicated to integrating wireless technology with skin bioelectronics.<sup>266-269</sup> Popular commercial wireless technologies include Bluetooth, Bluetooth low energy (BLE), ZigBee, infrared data association (IrDA), ultra-wide band (UWB), radio frequency identification (RFID), near field communication (NFC), and wireless fidelity (Wi-Fi). Each wireless technology has different modulation, data rate, power consumption, distance range, and security.<sup>44</sup> The chosen wireless module depends on the specific requirements of the target applications. Among them, NFC and BLE are popular candidates for short-range communication in long-term monitoring systems for skin bioelectronics, owing to the advantages of low-power consumption.<sup>8</sup> Generally, there are two ways to connect the wireless system with skin sensors: one is to design a compact skin circuits with miniaturised IC chips, and the other one is to use wires to connect skin devices with IC chips fixed on clothing. The first approach should consider local mechanical constraints on the skin, whereas the second approach requires human involvement. To remove all direct contacts between rigid components and the human body, Niu *et al.* developed a specially designed RFID system, where a body area sensor network (bodyNET) composed of chip-free and battery-free stretchable skin sensor tags were wirelessly linked to flexible silicon readout circuits on textiles.<sup>24</sup> The bodyNET system had multiple sensor nodes, located in multiple places on the human body to collect various bio-signals. One node was composed of a stretchable skin sensor (target) and an on-textile flexible readout circuit (initiator), which were connected wirelessly via RFID (Fig. 11a). The skin sensor consisted of a stretchable inductor, a stretchable capacitor, and a resistive strain sensor, and the initiator was composed of an antenna signal readout circuits and flexible batteries. The developed system eliminated on-skin rigid electronic parts, resulting in improved wear comfort and mechanical robustness. The authors successfully demonstrated continuous and hands-free monitoring of respiration, pulse rate, and body movement, and long-term sleep monitoring for 1 h (Fig. 11b-d). Another work which utilised wireless powering and communication was enabled by a loop antenna on a flexible printed circuit board (PCB), which was bonded to the backside of the skin sensor.<sup>270</sup>

In the long-range communication stage, data are transmitted to a distant server and can be accessed by caregivers for the purpose of personalised health care management. In this case, safeguarding of personal medical information must be seriously taken into consideration. Methods such as encryption and authentication techniques can be utilised to secure a relatively safe transmission

channel.<sup>44</sup> This issue can also be solved using the soft form factor. Tian *et al.* confined wireless communication to within 10 cm to the human body using conductive fabrics.<sup>271</sup> This metatextile can support surface-plasmon-like modes at radio communication frequencies, enabling the propagation of wireless signals around the body without

A self-powered piezoelectric PZT pressure sensor was demonstrated to enable *in vivo* measurement of radial/carotid pulse signals in near-surface arteries. The output voltage obtained by arterial pressure successfully operated the LED and speaker module of a signal processing circuit composed of amplifiers, band-pass filters,

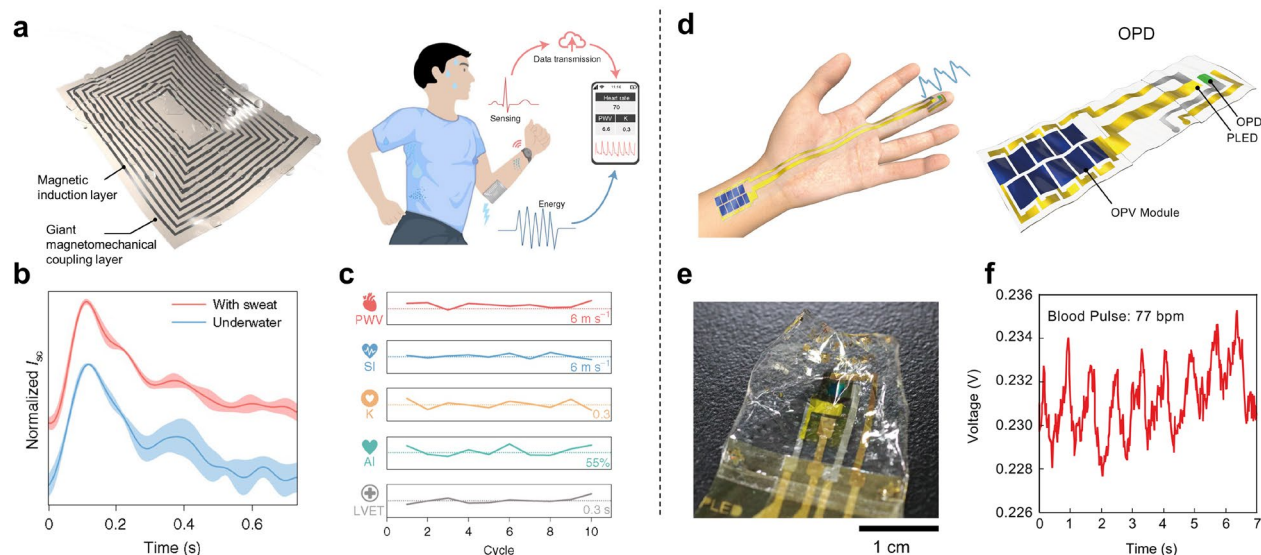


**Fig. 12** Self-powered skin bioelectronic devices. (a) Combined with a magnetic induction layer, the soft magnetoelastic composite worked as a water-resistant magnetoelastic generator adhering conformably to the human skin. (b) Arterial pulse wave recorded underwater and with sweat. (c) Extracted key arterial parameters. Reproduced with permission from ref. 227. Copyright 2021 Nature Publishing Group. (d) An ultraflexible, self-powered PPG sensor on human hands, where OPV generates electrical power from sunlight and drives polymer LED and OPD. (e) A photograph of the device. (f) Output voltage signals from PPG measurement. Reproduced with permission from ref. 279. Copyright 2021 Nature Publishing Group.

disturbance under motions. This work paves the way of soft platforms for wireless sensing, signal processing and energy transfer.

### 3.3.2. Ability to power itself

Maintaining stable operation of multiple sensors and wireless transceivers in a skin bioelectronic system requires several micro-/milliwatts of power. However, the mainstream power supply of current wearables are batteries, which are rigid, have explosive issues, and require regular charging or replacement.<sup>148, 272</sup> Therefore, it is highly desirable to develop soft, compliant, and sustainable power systems. Furthermore, the ability to power itself simplifies circuit design and enables portable sensing. There are many self-powered skin sensors and devices that harvest energy from biological, mechanical, light, or thermal sources from the human body and/or the ambient environment.<sup>234</sup> To name a few, the emerging soft skin-like energy devices include energy generation devices, such as solar cells, biofuel cells (BFCs), triboelectric nanogenerators (TENGs), and piezoelectric nanogenerators (PENGs), and energy storage devices such as supercapacitors and batteries.<sup>101, 103, 273-276</sup> The generated power can be stored in supercapacitors or batteries to drive other electronic devices.<sup>277</sup> Flexible rectifying diodes have been developed to rectify the alternating current (AC) form power from piezo/triboelectric nanogenerators to the direct current (DC) form for energy storage and further usage.<sup>278</sup>

and comparators to identify the arterial pulse.<sup>176</sup> This work evidenced that the self-powered pulse sensor could be utilised for a continuous real-time health/wellness monitoring system. Another example of harvesting mechanical forces is the use of giant magnetoelastic effect in micromagnet/silicone composites. Combined with a magnetic induction layer made from liquid-metal coils patterned on PDMS, the soft magnetoelastic composite worked as a water-resistant magnetoelastic generator adhering conformably to human skin (Fig. 12a–c).<sup>227</sup> The output electric current and voltage of the soft magnetoelastic generator survived for up to one week while submerged in artificial perspiration. Recently, an ultraflexible integrated system has been developed using an organic photovoltaic (OPV) powering polymer LEDs and OPDs. A self-powered PPG sensor was demonstrated the first time with such system, paving the way for future ambulatory health care platform (Fig. 12d–f).<sup>279</sup> Meanwhile, researchers have been investigating hybrid energy devices through the synergy of different energy devices, such as solar cells, electromagnetic generators, and electrochemical cells, in serial or parallel mode.<sup>104, 280</sup> These endeavours will greatly improve energy harvesting efficiencies and address the power issues in skin bioelectronics for long-term health care applications.<sup>281</sup>

### 3.3.3. System integration

Wireless integrated skin bioelectronics make long-term, continuous health monitoring viable, and offer opportunities for the development

of versatile skin devices as a diagnostic tool in personalised health care.<sup>282</sup> A completed integrated system is composed of skin bioelectronics, power management, and signals acquisition, processing, and transmission.<sup>268</sup> Usually, miniaturised integrated

temperature at the skin-prosthesis interface simultaneously, even during sitting, walking, and standing conditions.

Combined with advanced data processing techniques such as machine learning, integrated skin bioelectronics can be used for disease management.<sup>233, 284</sup> Recently, Zavanelli *et al.* reported a single, user-friendly skin patch for at-home wireless monitoring of sleep apnoea and sleep stages (Fig. 13a,b).<sup>285</sup> This work provided health caregivers with all clinically relevant metrics outlined by THE American Academy of Sleep Medicine (AASM) via a non-invasive approach. The skin patch consisted of a soft PPG sensor, an ECG sensor, advanced signal processing techniques, and time-series machine learning (Fig. 13c). It also realised simultaneous measurements of specific mechanical, electrical, and optical responses in a single location during obstructive sleep apnoea (OSA). These signals were analysed with a feedforward neural network (FFNN) to classify sleep into the wake, rapid eye movement (REM), and non-REM (NREM) sleep stages (Fig. 13d). Nine patients were involved in this study, four of whom exhibited apnoea symptoms after repetitive assessment. Furthermore, after integration with LED elements, an integrated on-skin platform can enable visualization of real-time health signals on the human skin.<sup>161, 177</sup>

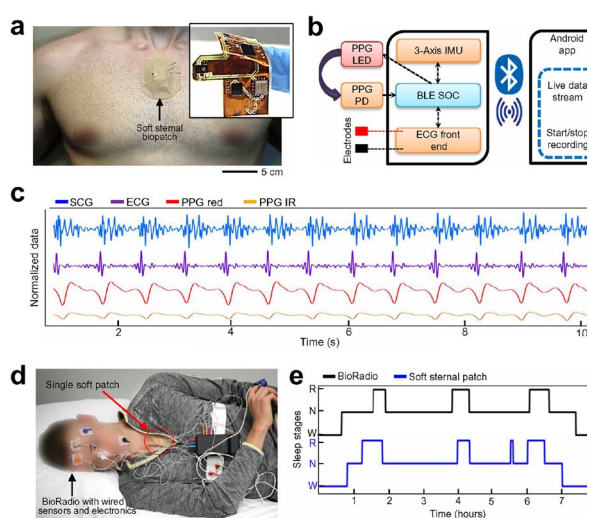


**Fig. 13** Integrated circuits of skin bioelectronics. (a) A photograph of a soft integrated skin patch attached on the human sternum. (b) Diagram of the components in the portable device. (c) Simultaneous measurements of seismocardiography (SCG), ECG, and PPG signals. (d) A photograph of a subject wearing skin patch and a commercial device. (e) Hypnogram comparison of the determined sleep stages between the soft patch and commercial device. Reproduced with permission from ref. 285. Copyright 2021 American Association for the Advancement of Science.

circuit (IC) chips are utilised for power and data management.<sup>8</sup> They are placed either on the skin by direct integrating with skin devices, or on textiles or other human belongings using wireless connections with skin devices. If IC chips are placed on the skin, the integrated platform should be soft enough to achieve skin compliance.<sup>283</sup> For instance, a wireless soft skin electronic patch was invented to measure temperature and thermal transport properties in healthy and diseased skin.<sup>267</sup> The wireless platform is a compact, miniaturised skin patch (quarter size), composed of flexible thermal actuator/sensor module and wireless platform to provide BLE communication capabilities. Additionally, computational methods have enabled the assessment of the hydration levels using bilayer models for the skin, with clinical-grade levels of accuracy. To continuously monitor pressure and temperature changes at the skin-prosthesis interface, a fully integrated platform was developed using a soft, thin, wireless, and battery-free on-skin sensors and a paired wireless module on the surface of the prosthesis socket.<sup>270</sup> The module on the socket was able to wirelessly power and communicate with the sensor, as well as a mobile gadget that could receive data and display results wirelessly. A 3D designed pressure sensor was fabricated using a compressive buckling technique, where a deformation would induce resistance changes in the strain gauges. This platform could wirelessly monitor pressure and

## 4. Health care applications

Human health can be characterised by a variety of highly personalised electrical, mechanical, thermal, and biochemical signals that are constantly radiated from the human body. Nowadays, skin bioelectronics can be designed to target specific biological signals mentioned above.<sup>267, 286</sup> Hence, long-term, continuous use of non-invasive skin bioelectronics can be of immense help in the evaluation of individuals' health and the early prediction of malfunctions of the body organs such as the heart and lungs, leading to timely and effective treatment.

### 4.1. Electrophysiological signals

As one of the vital signs, electrophysiological signals of long-term, continuous monitoring can provide critical clinical cues on an individual's health condition. In this section, we discuss typical electrophysiological signals, such as ECG, EMG, and EEG using skin bioelectronics.

#### 4.1.1. ECG

An ECG is a diagnostic tool that captures electrical signals and reveals the heart's beating process. Long-term, continuous ECG monitoring can facilitate the early diagnosis of cardiovascular disease and ensure prompt disease management. As a result, many on-skin ECG sensors have been developed for continuous cardiac health monitoring.<sup>22, 72, 287-289</sup> Compared to gel electrodes, dry electrodes have been considered as more appropriate candidates for long-term applications. Thinner devices can achieve better conformability, lower contact impedance, and consequently a larger SNR. A  $\sim 3$   $\mu\text{m}$ -thick ECG sensor was made using self-similar serpentine-structured Au/poly(methyl methacrylate) (PMMA)/PI.<sup>290</sup> The sensor could bear large, repetitive skin deformations. A continuous 48 h ECG recording was demonstrated while the electrode was laminated onto the left chest. Ameri *et al.* developed a graphene tattoo sensor that is only  $\sim 460$  nm thick. The electrical tattoo had a transparency of  $\sim 85\%$  and

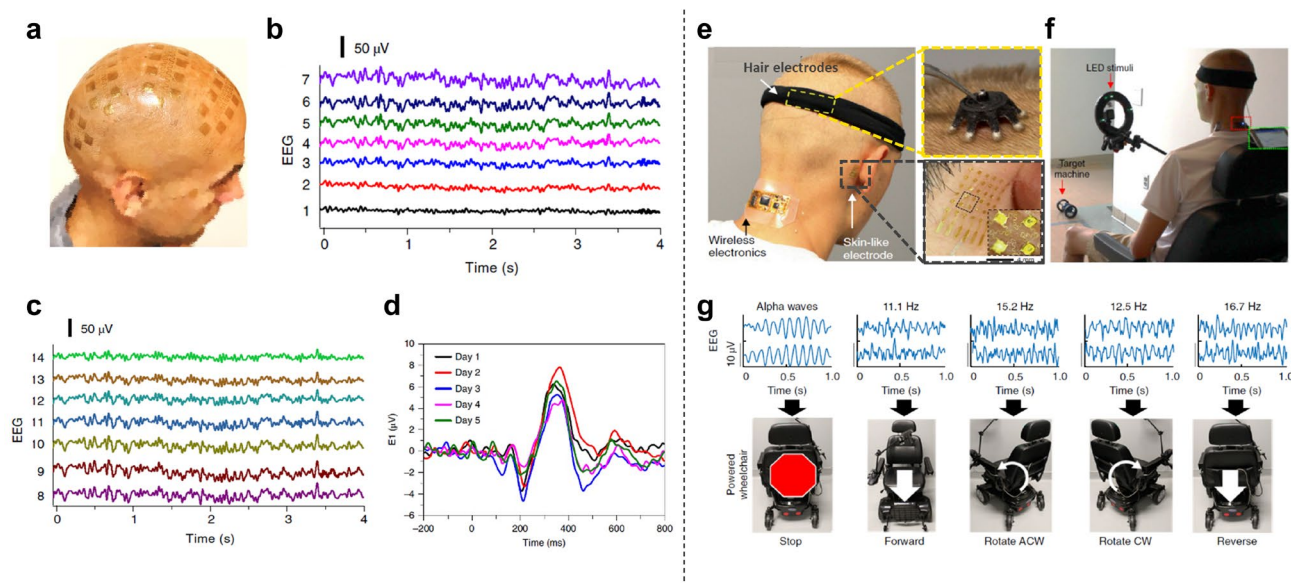


**Fig. 14** Skin bioelectronics for EEG recording. (a) Large-area epidermal electrodes covering the scalp for multi-channel EEG recording. (b,c) EEG signals collected by the epidermal multi-electrodes. (e) Event-related potentials captured by the epidermal electrode during five days of continuous wear. Reproduced with permission from ref. 229. Copyright 2019 Nature Publishing Group. (e) Flexible wireless scalp electronics composed of dry hair electrodes, skin-like membrane electrodes, and a miniaturised wireless electronic system. (f) In vivo demonstration of the wireless scalp electronics for SSVEP-based BMI. (c) EEG signals recorded by the scalp electronics, namely, alpha rhythms and SSVEPs with different frequencies, and the control of a wireless electric wheelchair via SSVEP signals. Reproduced with permission from ref. 308. Copyright 2019 Nature Publishing Group.

could be stretched to over 40% strain.<sup>48</sup> Because of the ultra-thinness, the graphene tattoo could adhere to the human skin for several hours by van der Waals forces alone. The open-mesh structure also made the sensor breathable and ultraflexible. The recorded ECG signals of the graphene tattoos had SNRs comparable to those of gold standard commercial gel electrodes. A 165 nm-thick nanofilm electrode was demonstrated to sustain one week skin attachment for long-term ECG monitoring.<sup>166</sup> The nanofilm substrate was made from reinforced PDMS by PU nanofibres, resulting with greatly improved mechanical durability. A 70 nm-thick Au layer was evaporated onto the PDMS film to obtain self-adhesive dry electrodes. The thinness geometry led to sufficient gas permeability. The nanofilm electrode achieved a high SNR (34 dB) for one week ECG monitoring. Octopus-inspired microsucker electrodes have been developed to achieve both dry and wet skin adhesion, demonstrating its promising application for long-term health monitoring.<sup>291</sup>

In a comprehensive health evaluation, ECG signals are one of the key bio-signals to be measured.<sup>168, 266</sup> For instance, in a pregnancy monitoring, Ryu *et al.* developed a time-synchronized wireless platform that could be applied to the entire continuum of antepartum and postpartum care. The system was able to continuously monitor a series of bio-signals, such as ECG, respiratory rate, pulse oxygenation, and blood pressure.<sup>28</sup>

#### 4.1.2. EMG

EMG is the recorded electrical signals induced by skeletal muscles, which can be used to evaluate neuromuscular functions, especially for

patients with stroke or Parkinson's disease. Moreover, EMG signals can be utilised to analyse ergonomics, sports science, physiotherapy treatment of motion disorders or in rehabilitation settings, or as electrical stimulators.<sup>46, 163</sup> For skin bioelectronics, surface EMG is measured non-invasively through the epidermis, which heavily depends on the skin surface over the target muscles. In this case, proper device placement is critically important to avoid motion artifacts caused by unrelated biopotential signals. Normally, electrical sensors are attached onto muscles on the face, arm, and leg, to obtain related myoelectrical signals.<sup>21, 34</sup>

Shahandashti *et al.* reported patterned Au/Cu/PI/PDMS EMG electrodes with ability for long-term health monitoring.<sup>292</sup> The contact impedance of the electrodes was comparable to that of wet Ag/AgCl electrodes, EMG signals from the forearm had an SNR of 55 dB. A wireless EMG sensing system was prepared using a printed graphene/PI/Ecoflex electrode and circuit. The subjects wore the device on the upper leg and measured the EMG signals with muscle flexion. The soft electrodes survived multiple uses (> ten times) with consistent adhesion performance and EMG signals.<sup>293</sup> After integrating with deep learning algorithm, the device could differentiate six muscle activities with an accuracy of > 97%. A SEBS nanofilm was integrated with AgNWs to obtain a breathable epidermal EMG electrode<sup>217</sup>. The thickness of the nanofilm was 90 nm, enabling an ultrathin nanofilm electrode of with a thickness of 160 nm. The resulting dry electrodes adhered to the human skin for 5 h without causing skin allergies or damage. A conformable ultrathin electrode (~ 100 nm-thick) was made by graphene/PEDOT:PSS. Five pairs of electrodes were attached to the human face muscles, the

measured EMG signals had SNR values of 20 dB. These EMG signals were then used to precisely control a robotic hand.<sup>294</sup>

#### 4.1.3. EEG

Brain-related diseases such as epileptic seizures, stroke, and neuromuscular diseases can be diagnosed by EEG monitoring, because the EEG is the recording of brain activity-related electrical potential and can provide vital information of neuronal activities.<sup>47</sup> Considering its non-invasive monitoring of brain electrical activity with high temporal resolution, portability and relatively low cost, electroencephalography has been instrumental in clinical settings and in the research field of brain-machine interfaces.<sup>295, 296</sup> Compared to other electrical biosignals such as ECG and EMG, EEG signals are relatively weak with typical microvolt-scale amplitudes and with a main frequency range of 0.3 to above 30 Hz, which makes it more challenging to achieve highly effective recording of EEG.<sup>297</sup> Conformal contact between the electrodes and the skin surface is of great importance for the continuous and stable monitoring of electrophysiological signals with a high SNR value, because it can provide intimate electrode-skin interface. Based on the electrode-skin interface state, electrodes for EEG recording can be generally categorised into three different types: wet electrodes,<sup>298</sup> semi-dry electrodes,<sup>299, 300</sup> and dry electrodes.<sup>301</sup>

In comparison with the wet and semi-dry electrodes, dry electrodes that do not require conductive gels or electrolyte fluid, show some advantageous merits such as improved user-friendliness and time-saving pre-preparation setup for portable EEG recording.<sup>302</sup> Dry electrodes with various morphologies such as skin-conformal electrodes,<sup>294, 303-305</sup> ultrathin electronic tattoos,<sup>48, 306</sup> flexible sponge electrodes,<sup>307</sup> elastomeric hair electrodes,<sup>308</sup> micro-pillar-structured electrodes,<sup>171</sup> and microneedle electrodes,<sup>309</sup> have been designed and developed for user-friendly and potential long-term EEG detecting. As for the skin-conformal and ultrathin tattoo electrodes, they are only suitable for non-hairy skin surfaces, such as the outer ear location, frontal region, and shaved scalp.<sup>303</sup> It is notable that a thin layer of spray-on bandage needs to be applied once or twice a day to facilitate strong adhesion of the ultrathin electrode platform to the skin and to provide environmental protection for long-term usage. To collect the scalp EEG signals, the hair needs to be shaved for the conformal mounting of epidermal electrodes on the scalp.<sup>229</sup> Fig. 14a shows the application of breathable large-area epidermal electrodes for the full-scalp and long-term EEG recording. Because of their thinness and softness, the large-area epidermal metal mesh electrodes incorporated with an additional thin layer of conductive polyacrylate gel to further reduce the interfacial impedance, could be conformably mounted on the scalp without hairs to record EEG signals with full-scalp coverage (Fig. 14b,c). These epidermal electrodes have the potential for long-term EEG recording, as demonstrated by the highly effective capture of P3 event-related potential components during an auditory oddball task over a five-day period of continuous wear of the electrodes (Fig. 14d).

To capture EEG signals from a hairy scalp, it is necessary to design dry electrodes with particular structures that could make the electrodes bypass hair to make good contact with the scalp, such as an elastomer leg structure,<sup>308</sup> elastic sponge structure,<sup>307</sup> micro-pillar

structure,<sup>171</sup> and microneedle structure.<sup>309</sup> For this type of dry electrodes, external mechanical fixtures and force are required to ensure the contact of electrodes with a hairy scalp. As shown in Fig. 14e, a dry hair electrode with conductive elastomer legs combined with a stretchable skin-like electrode, and a flexible miniaturised wireless electronic circuit, was developed and utilised as fully portable and wireless scalp electronics for EEG recording.<sup>308</sup> Because of the elasticity of the conductive legs of the hair electrode, slight pressure applied on the hair electrode allowed the conductive legs to separate the hairs and form good contact with the scalp, and thus a fabric headband was utilised to fix the hair electrode and apply pressure on it (Fig. 14f). This wireless scalp electronic system was demonstrated to be feasible for steady-state visually evoked potential (SSVEP) based brain-machine interfaces (BMIs) (Fig. 14f). In detail, the scalp electronics were used to record SSVEP data when the subjects gazed at different light-emitting diode stimuli and EEG alpha rhythms when the subjects closed their eyes, and then these data were utilised to wirelessly control target machines such as a wireless electric wheelchair (Fig. 14g). Despite their improved user-friendliness and long-term EEG recording potential, dry electrodes still have some limitations such as relatively high electrode-scalp impedance, inferior signal quality, and susceptibility to motion artifacts. Developing reliable and user-friendly EEG electrodes with low electrode-scalp contact impedance and long-term stable interfaces remains highly desirable and challenging for practical EEG applications in various scenarios.

## 4.2. Biophysical signals

Skin bioelectronics can measure diverse biophysical signals, such as temperature, strain, pressure, tactile, and sound. These signals provide effective cues concerning an individual's health status as well as disease prevention, diagnosis and treatment, physical therapy, and rehabilitation if measured in a long-term, continuous manner. In the following part, we introduce the measurement of typical biophysical signals, such as body temperature, human activity, and cardiac mapping.

### 4.2.1. Body temperature

Physiological temperature is a vital bio-signal that varies temporally and spatially. Deviation of a few degrees from core body temperature may cause impairment and fatality in the human body. For example, temperature changes have significant correlations with insomnia, sleep quality, stroke, skin disease, and cognitive functions.<sup>44, 267, 310</sup> Continuous measurement of localised body temperature despite large deformation is critical to understand the thermal principle of homeostasis, and to evaluate sophisticated health conditions.<sup>310, 311</sup> To this end, various skin devices have been reported for continuous temperature sensing.<sup>312, 313</sup>

Typical on-skin temperature sensors are thermo-sensitive conductive composites and conductors, while others include thermocouples, semiconductors, and field effect transistors. A negative temperature coefficient (NTC) thermistor-based artificial skin was constructed using a laser-induced reductive sintering scheme.<sup>314</sup> The temperature sensor was made from a nickel electrode and a nickel oxide sensing channel. The device exhibited a fast response time of less than 50 ms due to the thin PET substrate. The

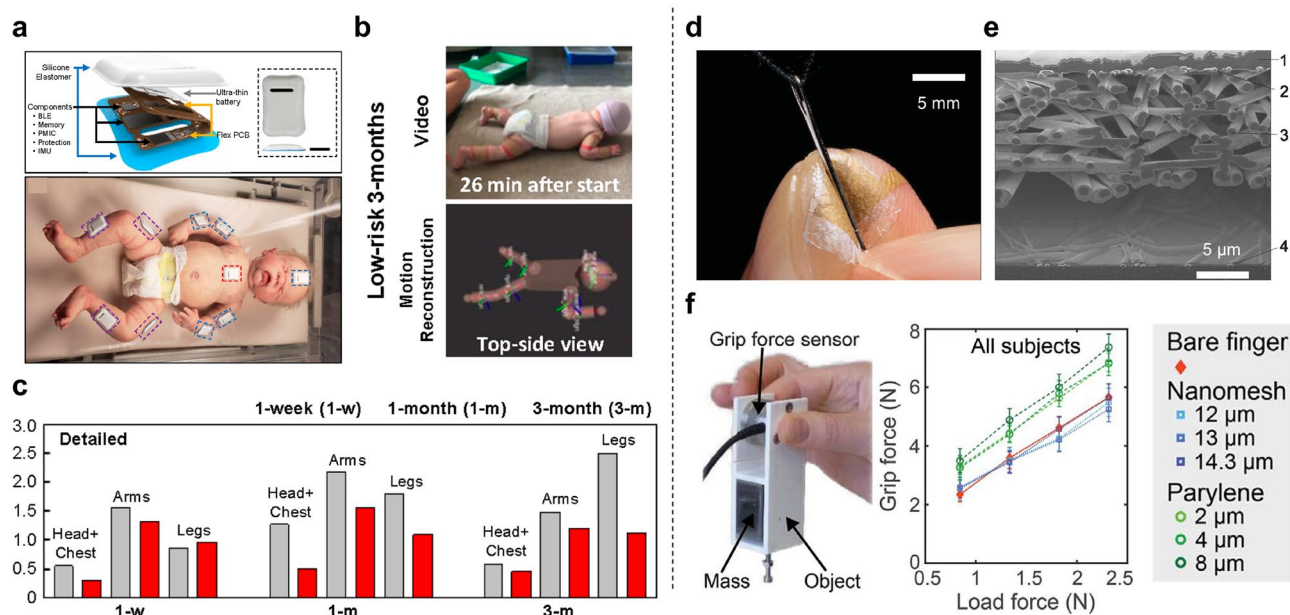


**Fig. 15** Skin bioelectronics for human activity monitoring. (a) Schematic illustration of the device and measurement setup for the monitoring of full-body motions. (b) Prone posture captured by video and results of reconstructed 3D motion. (c) Follow-up movement measurement when the subjects were 1 wk, 1 mo, and 3 mo old. Reproduced with permission from ref. 327. Copyright 2021 National Academy of Sciences. (d) A photograph showing sensor-applied fingers. (e) Cross sectional SEM image demonstrating sensor layouts. (f) Experiment setup of the evaluation of sensation effect. Results show nanomesh pressure sensors has minimal interference on natural human feelings. Reproduced with permission from ref. 25. Copyright 2020 American Association for the Advancement of Science.

value of the materials constant of thermistor was calculated to be as high as 8162 K near room temperature. The sensor was sensitive enough to capture small temperature changes caused by inhalation and exhalation. It is requisite to maintain a stable sensing performance of on-skin temperature sensors during long-term applications. A strain-insensitive temperature sensor was developed by structure designing serpentine-structured free-standing stretchable fibres of a reduced graphene oxide/PU composite. The temperature changes were negligible within the strain range of 0–50%. The device further survived 10,000 cycles of stretching and releasing at 50% strain. After integrating onto a bandage, the temperature sensor had a maximum sensing resolution of 0.1 °C. Stable on-body temperature sensing was demonstrated after attaching the bandage onto human skin, even during various body movements.<sup>315</sup> To minimise humidity disturbance, Wang *et al.* introduced a crosslinker of (3-glycidyoxypropyl)trimethoxysilane (GOPS) to PEDOT:PSS. The fully printed temperature sensor showed great stability under environmental humidity range of 30–80% RH, with a temperature sensitivity of  $-0.77\% \text{ } ^\circ\text{C}^{-1}$  between 25–50 °C. The authors finally demonstrated wireless, real-time, continuous temperature sensing after integrating with a printed flexible hybrid circuit.<sup>316</sup> For body temperature monitoring, it is necessary to require a high temperature coefficient of resistance (TCR) ranging from 34 to 42 °C.<sup>96</sup>

#### 4.2.2. Human activity

Human motion and locomotion monitoring can be useful for rehabilitation, sports, disease prevention and diagnosis, prognostic

monitoring of patients, and elderly care.<sup>44, 317</sup> Any irregular or even habitual movement can offer critical information related to human health. For example, periodic analysis of body movements can detect abnormal gait patterns and sudden hand tremors, which are the precursors of fatal diseases including Parkinson's disease, Alzheimer's disease, and diabetes, and contribute to the early management of these diseases.<sup>6, 318</sup> To monitor human activity, physical skin sensors conform to, for example, the human face, neck, hand, joints, and foot, and provide long-term, continuous signal recording induced by human motions.<sup>319, 320</sup> Thus far, numerous skin devices have been developed to detect activities ranging from subtle skin deformations induced by wrist pulses to large strains by joint bending.<sup>321-324</sup>

Movements on the human face are highly correlated to facial expressions.<sup>100</sup> Wang *et al.* reported a smart facial mask from vertically aligned AuNWs.<sup>325</sup> The skin patch was fabricated by directly growing AuNWs on an Ecolflex substrate. Due to the Jannus structure of the AuNWs and their good adhesion to the substrate, the gold film could be stretched to 800% strain. The placement of each sensor on the face was determined by the designated muscle groups related to facial expressions. Using the Facial Action Coding System (FACS) library, five different facial expressions could be readily read out from a mobile screen in real time in a wireless manner. Facilitated with algorithms and a three-dimensional digital image correlation system, Sun *et al.* reported that their developed piezoelectric thin films could differentiate facial movements from healthy individuals and patients with amyotrophic lateral sclerosis.<sup>100</sup>

As the most dynamic parts of the human body, the movements of hands and limbs have been extensively studied.<sup>326</sup> Together with machine learning techniques, Jeong *et al.* developed a skin-integrated sensor network for early identification of atypical infant movement behaviours.<sup>327</sup> Several sensors were strategically placed on different parts of the infant for full-body motion measurements, and operated in a wide-bandwidth and time-synchronized manner (Fig. 15a). The collected data were then used to reconstruct three-dimensional motions in avatar form that could be accessed by caregivers (Fig. 15b). The authors successfully demonstrated long-term and follow-up monitoring for as long as 3 months after childbirth (Fig. 15c). The reported strategy exhibits great potentiality to diagnose neurological dysfunctions at the earliest time in infancy and initiate clinical interventions.

To monitor subtle skin deformations, high sensitivity is not enough. The devices should also be designed to be soft and thin to minimise any disturbance caused by the device itself. To avoid sensation or motion disturbance on the natural skins, our group developed ultrasoft nanomesh-based strain gauges<sup>179</sup> and pressure sensors.<sup>25</sup> The pressure sensors were fabricated by laminating four layers of different nanomeshes (two electrodes, an intermediate layer, and an encapsulation layer) to the human skin (Fig. 15d,e). The overall thickness of the device was approximately 13  $\mu\text{m}$ . To quantitatively evaluate the effect of the sensor on the human sensation, the grip force was measured and compared while manipulating objects. The results show that the sensor-attached finger has comparable grip forces to those of the base fingers (Fig. 15f). A polymeric film (2  $\mu\text{m}$ -thick)-attached finger led to a 14% increase in the grip force.

### 4.3. Biochemical signals

Molecular data from the human body is an important and direct indicator of human health. Traditional clinical practices always involve invasive blood retrieval with pain and infection risk, such as finger pricking in glucose monitoring for diabetics. Soft, on-skin bioelectronic devices have gained tremendous attention because they provide a non-invasive, continuous method for label-free measurements of disease-related chemical biomarkers from body fluids, such as sweat and blood, and skin volatolomics.<sup>13</sup>

#### 4.3.1. Sweat

Sweat can be easily accessed and is widely distributed all over the human body. It contains abundant chemical components, such as metabolites (*e.g.*, glucose, lactate, and uric acid), electrolytes (*e.g.*, sodium, potassium, calcium, and chloride), exogenous agents (*e.g.*, drugs and ethanol), proteins, and hormones, which make sweat one of the ideal body fluids for biomedical sensing.<sup>328, 329</sup> Abnormal health status and disease can result in concentration changes of existing constituents or generation of new chemicals in sweat.<sup>13</sup> In recent years, many skin interfaced colorimetric, electrochemical, and microfluidic devices have been developed for continuous sweat monitoring for health management and clinical diagnostics.<sup>330, 331</sup> To collect eccrine sweat, simple and direct stimulations include intense physical activity, heat exposure, wicking, and localised chemical inducement. Among all the chemical components present in sweat, most research studies have focused on the analytics of chloride, lactate, and glucose.

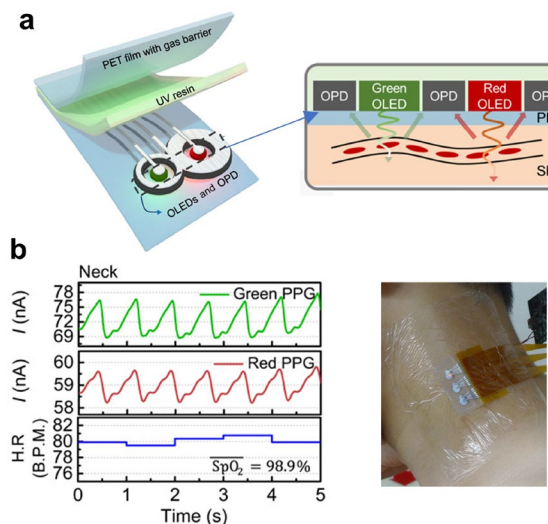


**Fig. 16** Skin bioelectronics for blood monitoring. (a) Schematic diagram of the proposed OPO sensor. Right figure shows an enlarged cross section representing the structure of the device and the light reception process in the skin medium. (b) The left figure is the PPG, heart rate, and SpO<sub>2</sub> signals obtained from the neck using red and green OLEds. H.R., heart rate; B.P.M., beats per minute. The right photograph showing the human neck applied with the skin device. Reproduced with permission from ref. 353. Copyright 2018 American Association for the Advancement of Science.

Abnormally high chloride concentration in sweat has been adopted as the gold standard for cystic fibrosis diagnosis.<sup>330, 332</sup> A newborn- safe adhesive microfluidic device was developed to non-invasively monitor sweat chloride concentrations of varying ages. The microfluidic sweat sticker could perform simple and rapid collection of sweat for cystic fibrosis diagnosis and management.<sup>333</sup> In this work, sweat capture was enabled by skin stimulation via pilocarpine iontophoresis. Microchannel structures were made using PDMS; sweat would enter the inlets (skin-faced side) from laser-patterned openings. Each chamber could collect a total volume of 47  $\mu\text{L}$ . Patterned adhesives were added to optimize sweat collection. The chloride array with reagent silver chloranilate produced a colour response proportional to the chloride concentration. The results could be read out using real-time image analysis. The device was able to validate cystic fibrosis patients with an accuracy comparable to current device platforms.

Establishing a reliable relationship between regional and whole-body sweat monitoring is a crucial step for providing new insights into the physiological relevance of sweat analysis. Recently, Baker *et al.* developed a microfluidic device for the measurement of sweat rate and chloride concentration.<sup>334</sup> It is worth to mention that the microfluidic platform can precisely capture, store, and measure in real-time at well-defined regions of the skin. The intricate microchannels were made with stacks of thin-film polymers created by laser and die cutting techniques. Even in the presence of heavy sweat excretion, the microfluidic device could conform well to the



skin of healthy subjects,<sup>360,361</sup> or of biopsy samples, taken by invasive surgical procedures from skin areas with melanoma.<sup>362-365</sup> In all of these studies, heavy, time-consuming and expensive spectrometry and/or electronic nose devices were used. To overcome these challenges, on-skin devices have been designed for sensing the disease VOCs and to continuously monitor the changes in the body in a non-invasive manner. In this wearable design, there is no need to take any specific action for collecting samples, because VOCs emitted in the skin headspace vaporise automatically and are continuously captured by the skin sensors (Fig. 17a). This unique VOC tracking enables the users to constantly check their health without interrupting daily activities. A prominent example of this approach includes an online exploratory pilot study using a wearable electronic device based on an array of cross-reactive chemiresistive films of molecularly modified gold nanoparticles (AuNPs) that are directly placed on the skin of the anterior part of the arm. This study included 29 healthy subjects and 18 patients with confirmed active pulmonary TB patients. Post-processing analysis resulted in 86.2% specificity, 94.4% sensitivity, and 89.4% accuracy in discriminating between active pulmonary TB patients and control samples (Fig. 17b).<sup>366</sup> These findings strengthen the potential of wearable devices for detecting diseases under field conditions in a real-time mode. The patches can also be worn continuously to monitor the disease treatment and to ensure that the treatment is effective. To enable extended usage periods, several studies have proposed to design a sensor array to be self-healing if scratched or cut in the device.<sup>367</sup> By integrating a self-healable polymer substrate with five kinds of GNP films, a sensor array gave a fast self-healing rate (< 3 h) and excellent healing efficiency in both the substrate and sensing films. The reported platform was used for sensing pressure and 11 kinds of VOCs that were emitted through skin and correlated with health conditions (Fig. 17c,d).<sup>367</sup> The skin-based sensor array exhibited satisfactory sensitivity, a low detection limit, and promising discrimination features in monitoring both VOC and pressure variation, even after full healing (Fig. 17c,d). These results present a new type of smart sensing device, with a desirable performance in the possible detection and/or clinical application for several different purposes.

#### 4.4. Comprehensive signals

To comprehensively evaluate some specific health conditions, such as wound healing and cardiac health, solely measuring electrophysiological, biophysical, or biochemical signals is not enough. It requires a fusion of at least two species of these signals. Here, we discuss the latest development of skin bioelectronics for wound and cardiac health monitoring.

##### 4.4.1. Wound healing

During the process of wound healing, quantitative assessment of wound parameters, such as temperature, pH, hydration, impedance, bacteria load, glucose, and uric acid, can monitor the status of wound recovery and determine the presence of infection.<sup>368-370</sup> In contrast, qualitative assessment by visual examination is more subjective and easily influenced by the surrounding environment and experience of the practitioner. Therefore, quantitative wound monitoring can help to reduce prolonged hospital stays, the number of doctor visits, and treatment-related long-term laboratory tests.<sup>33</sup> In this regard, with skin bioelectronics, abundant biophysical, chemical, or

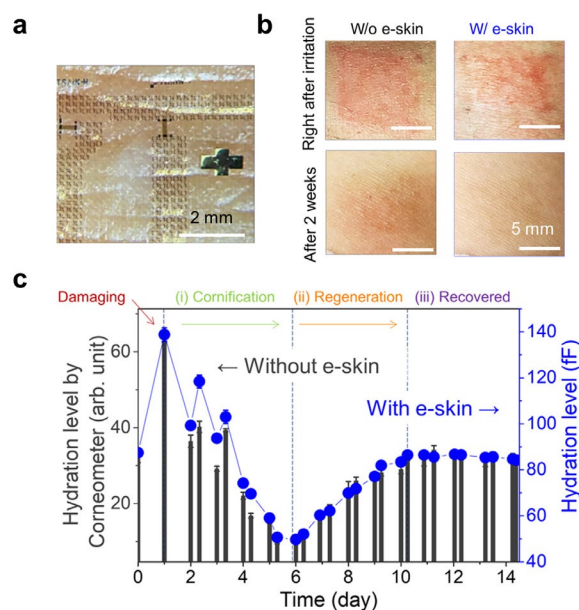


**Fig. 18** Skin bioelectronics for wound monitoring. (a) A photograph showing conformal contact of the perforated skin bioelectronic device on the human skin. (b) Long-term skin regeneration was monitored over a period of 2 weeks. (c) The graph shows the level of hydration of the inflamed skin as a function of the number of days of device lamination. A hydration sensor in the skin device was compared to a conventional hydration analyser (Corneometer CM 825). Reproduced with permission from ref. 378. Copyright 2021 American Association for the Advancement of Science.

electrophysiological markers can be used as diagnostic targets to indicate the state of wound healing.<sup>370</sup>

Suitable wound monitoring devices should protect the wound from infection and provide an environment that accelerates wound healing.<sup>371</sup> The following features are expected for a good wound monitoring devices should protect the wound from infection and provide an environment that accelerates wound healing.<sup>371</sup> The following features are expected for a good wound monitoring device: no obstruction to wound-secreted exudate, maintenance of appropriate humidity to prevent wound infection or dehydration, biocompatibility and non-toxicity, appropriate mechanical strength, permeability for gas exchange, comfort, and easy removal. Skin bioelectronics have been used to monitor human health imperceptibly and noninvasively from the skin.<sup>1, 168, 372</sup>

In recent years, there has been enormous progress in the field of on-skin devices for monitoring pH, temperature, hydration, pressure, thermal conductivity, uric acid, glucose concentrations and other parameters during the wound healing process.<sup>373-377</sup> Farooqui *et al.* constructed a wireless wound monitoring smart bandage by inkjet printing, integrating capacitive sensors and resistive sensors, the former for bleeding monitoring and pressure sensing, and the latter for pH monitoring. Tests demonstrated that bending cycles did not affect the performance of the sensor, making it promising for continuous

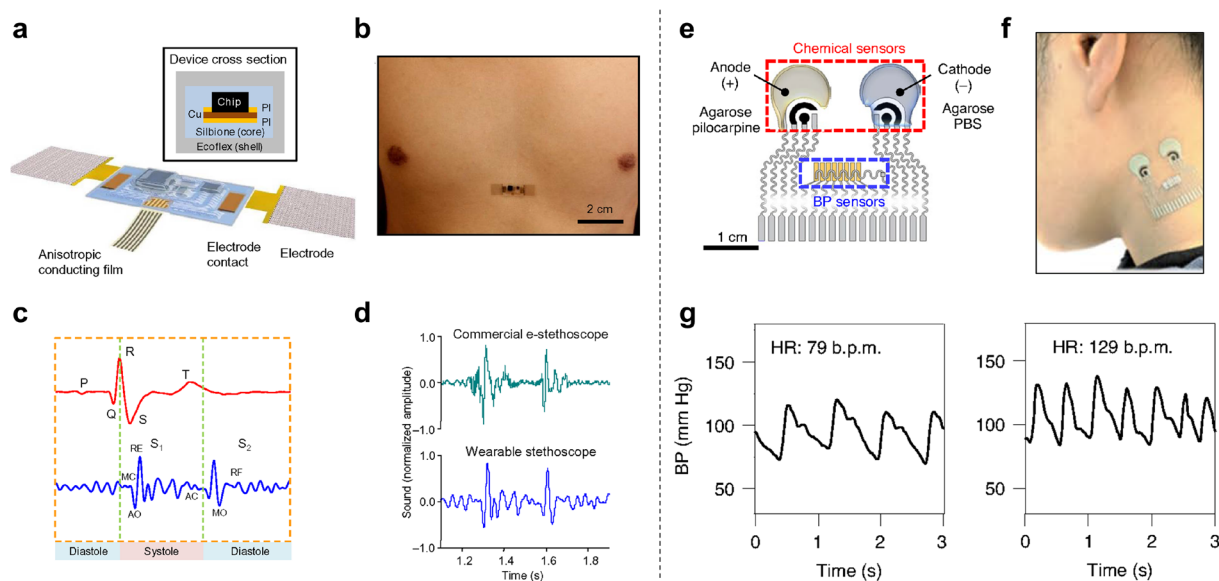


**Fig. 19** Skin bioelectronics for cardiac mapping. (a) Device structure of epidermal mechano-acoustic sensing. (b) A photograph of the epidermal skin patch on chest. (c) Measured ECG and heart sound signals. (d) Comparison of heart sound signals measured by the epidermal device and the commercial electronic stethoscope. Reproduced with permission from ref. 385. 2016 American Association for the Advancement of Science. (e) Device structure of epidermal patch for simultaneous monitoring of haemodynamic and metabolic biomarkers. (f) A photograph of the epidermal device attached onto the human neck. (g) Blood pressure measured before and after exercise. Reproduced with permission from ref. 29. Copyright 2021 Nature Publishing Group.

wound monitoring.<sup>373</sup> However, thick film-type skin devices cannot avoid the accumulation of skin by-products, such as sweat on the interface of skin and electronic devices, which hinders accurate skin sensing over a long period of attachment,<sup>378</sup> and reduces the homeostatic function of the skin (*e.g.*, skin barrier function).<sup>379</sup> The lack of permeability also leads to a disturbance in skin health information that is essential for the internal disorders (*e.g.*, allergies) and diagnosis of skin diseases (*e.g.*, erythema) monitoring. Therefore, researchers have been working on designing innovative wound monitors that can ‘breathe’. As shown in Fig. 18, a fully perforated skin device inspired by sweat pores containing inorganic sensor arrays was developed for long-term seamless skin health monitoring, and it worked well for long-term wound monitoring. The elastomer adhesives and the modulus of inorganic thin-film sensors were made to be engineered into hole patterns, which were designed precisely to avoid completely blocking the sweat pores on the human skin. To ensure the permeability, circular holes were designed, leading gas and sweat to escape through the sweat pores. Multiple sensors were also perforated to inhibit sweat retention. Because the wound was completely interacted with the outside environment, the perforated e-skin did not prohibit the wound healing process at all. Meanwhile, the good permeability avoided sensor damage due to sweat accumulation, which enabled continuous monitoring of pulse, hydration level, temperature, and photoconductance for up to two weeks. This has been demonstrated by the recovery of injured human skin with and without e-skin over a period of two weeks as shown in Fig. 18c.<sup>378</sup>

#### 4.4.2. Cardiac mapping

Cardiovascular diseases are among the leading causes of death worldwide. Heart status should be continuously monitored, especially in those with cardiovascular diseases. Skin bioelectronics offer a convenient, non-invasive approach to continuously measure bio-signals related to heart diseases.<sup>380</sup> Directly interfaced with the chest, wrist, neck, or other parts of the human body, soft bioelectronic devices can perform biophysical, biochemical, and electrophysiological sensing induced by heart activities. Related biophysical signals include blood pressure, blood flow, heartbeat, pulse wave, heart sounds, temperature, and pulse pressure.<sup>380-384</sup> Generally, to evaluate heart conditions, multiple signals should be detected simultaneously and continuously.

Liu *et al.* demonstrated a mechano-acoustic sensing platform for cardiovascular diagnostics.<sup>385</sup> The skin patch had a mass of 213.6 mg and a thickness of 2 mm with a soft form factor (effective moduli of 31.8 kPa in the x direction and 31.1 kPa in the y direction). The skin patch was also water-permeable and exhibited reversible adhesiveness (Fig. 19a,b). The sensing part was made of a mechano-acoustic sensor, low-pass and high-pass filters, a preamplifier, and capacitive electrodes for electrophysiological sensing. For a healthy individual, the first sound ( $S_1$ ) has an acoustic frequency of 10–180 Hz, the second sound ( $S_2$ ) of 50–250 Hz. The sensor covered 0.5–550 Hz frequency bandwidth, which is sufficient for cardiovascular sounds and speech. The seismocardiography measurement results were comparable to those of the JABES Electronics Stethoscope (Fig. 19c,d). Constant intensity murmur at the tricuspid and pulmonary sites was validated in an elderly female patient with tricuspid and pulmonary regurgitation. Another example is an epidermal patch that

can be used to measure blood pressure, heart rate, and metabolic biomarkers simultaneously (Fig. 19e).<sup>29</sup> The haemodynamic signals were monitored by ultrasonic transducers, which transmitted ultrasound beams to the artery under electrical pulses. Eight transducers were employed to align with the artery to obtain the optimal blood pressure value (Fig. 19f). No blood pressure waveform changed when turning the neck to 90 degrees because of the good mechanical robustness. It was validated that excise could lead to increased blood pressure, heart rate, and lactate levels (Fig. 19g). The reported epidermal patch has great implications for self-monitoring in personalised health management. Furthermore, a high-resolution (508 p.p.i.) imager has been demonstrated to obtain images of fingerprints, veins, and mapping of pulse waves. The ultrathin imager is evidenced to be an effective tool for cardiac mapping.<sup>26</sup>

## 5. Conclusions and outlook

In this report, we first review advanced sensing devices, with a focus on materials, device structures, and working principles of electrical, biophysical, optical, and biochemical sensing modalities. Then we elaborate on the requirements on the material and structure selection, device properties, and wireless technologies for skin bioelectronics towards long-term, continuous health monitoring. Finally, potential health care applications are discussed and reviewed in electrophysiological, biophysical, biochemical signals, and comprehensive monitoring.

Innovative materials design and structure engineering have made thin, soft, and biocompatible skin electronics facile and competent for long-term, continuous health monitoring. For example, advanced, non-invasive skin bioelectronic patches have shown the ability to 1) continuously monitor a specific vital signal for disease detection and management, such as diabetes and cardiac disease;<sup>385, 386</sup> and 2) comprehensively evaluate an individual's health status wirelessly, ranging from newborns to pregnant women.<sup>28, 327</sup> Despite these significant advancements in this field, many practical challenges still remain. We outline several remaining challenges with pertinent solutions below.

**Measurement capabilities.** Currently, most biophysical, electrical, optical, and biochemical sensing modalities are kept isolated from each other in skin bioelectronic devices. It limits sensing capabilities and will result in high-price products. To achieve higher productivity in health monitoring, it is necessary to combine several sensing modalities in one platform. In this case, more selective and specific bio-signals can be measured to comprehensively evaluate health conditions. Besides multi-sensing, other performances, such as good linearity and high enough sensitivity for target applications are also important parameters to be considered. Though a variety of advanced soft materials have been developed as sensing materials for skin bioelectronics. Their electrical or electrochemical properties still need further improvements to reach the established performance of the rigid electronic materials. Further studies on materials and device structures to enhance sensing capabilities are needed.

**Robust rigid-soft interface.** Thin, soft skin bioelectronics have been demonstrated to have excellent skin compliance and the ability to survive high-cycle fatigue test under repetitive mechanical deformations. However, after laminating onto the human skin, the

device is not sufficiently robust to survive long-term, continuous, time-dynamic skin deformations, including stretching, compressing, and twisting. It requires robust adhesion at the skin-device interface and robust device configuration in a dynamic environment. One possible solution is to develop ultrathin biocompatible adhesives with good mechanical robustness. However, ultrathin bioelectronic devices usually suffer from limited stretchability and mechanical durability owing to the trade-off between geometry thinness and mechanical robustness. A good understanding and further investigation on materials and rigid-soft interface design are required to prevent interface failure in long-term use.

**Long-term stability.** Long-term stability requires skin bioelectronics to have high skin compliance, mechanical durability, and stretchability. To achieve these properties simultaneously, efforts are needed to develop advanced soft nanomaterials.<sup>50</sup> Additionally, to maintain stable functionalities, skin bioelectronics should be able to survive in moisturized conditions during long-term skin attachment. To tackle this issue, hydrophobic materials or proper encapsulation are needed. In the case of reusable devices, they should be robust enough to sustain repetitive attachment and detachment cycles. In addition to the challenges mentioned above, particularly for biomedical sensors to be adopted in continuous health monitoring, effective sampling and transport of body fluids over the sensor surface is crucial for ensuring good reproducibility and avoiding contamination.<sup>78</sup> Moreover, reconcentration techniques are required considering that the analyte concentration in excretive biofluid is not as reliable as that of blood. In most cases, a simple attach-press-sensor is inadequate. Addressing challenges in long-term, continuous biochemical sensors will further involve knowledge and techniques related to fluid handling, reconcentration, incubation, and more effective sensing modalities beyond ion-selective and enzymatic approaches.

**System integration.** A final goal in this field is to achieve a closed-loop system for health care management that can be applied in real-life situations. In this endeavour, miniaturisation, sensor sophistication, analytics, power, communication, secure data management, integration, and incorporation of machine learning should all be taken into consideration for the transformation of laboratory prototypes to fully portable, multifunctional, and intelligent skin patches with long-term, continuous sensing capabilities.<sup>387</sup> A comprehensive validation of the system is necessary for widespread adoption. Immerse populations of clinical study are required to establish operational performance equivalence to existing clinical methods. Furthermore, joint efforts from materials and device engineers, data scientists, and medical professionals are required for technical progress. Users and caregivers need to be more closely involved.<sup>372</sup>

**Commercialization.** To realise commercialisation of skin bioelectronics, cost-effective fabrication technologies for high throughput and large-scale customization are needed. Traditional manufacture methods, such as photolithography, etching process, and high-vacuum deposition, need expensive equipment and are time consuming. It will increase the price of the products. Advanced fabrication techniques, such as printing, can enable mass fabrication and decrease the manufacturing cost. Furthermore, to obtain

favourable biocompatibilities, the fabrication process should not involve any toxic materials or solvents. Innovative fabrication technologies are necessary to guarantee material compatibility with the processing parameters.

Although there are unmet challenges, we believe that skin bioelectronics will realise their full potential with the ongoing development of all the aspects mentioned. Next-generation skin bioelectronics are expected to be self-powered, multifunctional, and intelligent, and able to acquire bio-signals throughout daily life for personalised health care management. It will be possible to integrate them into the lifestyles of both healthy individuals and patients, allowing health care accessibility to those living in geographically remote or economically limited areas.

## Conflicts of interest

There are no conflicts to declare.

## Acknowledgements

This work was financially supported by the Japan Science and Technology (JST) ACCEL (grant number JPMJMI17F1). Y. Wang would like to acknowledge supports from the Technion, and the start-up fund from Guangdong Technion.

## Notes and references

1. T. Someya and M. Amagai, *Nat. Biotechnol.*, 2019, **37**, 382-388.
2. T. Ray, J. Choi, J. Reeder, S. P. Lee, A. J. Aranyosi, R. Ghaffari and J. A. Rogers, *Curr. Opin. Biomed. Eng.*, 2019, **9**, 47-56.
3. D.-H. Kim, R. Ghaffari, N. Lu and J. A. Rogers, *Annu. Rev. Biomed. Eng.*, 2012, **14**, 113-128.
4. Y. Abe and M. Nishizawa, *APL Bioeng.*, 2021, **5**, 041509.
5. H. Yuk, B. Lu and X. Zhao, *Chem. Soc. Rev.*, 2019, **48**, 1642-1667.
6. Z. Lou, L. Wang, K. Jiang, Z. Wei and G. Shen, *Mater. Sci. Eng. R Rep.*, 2020, **140**, 100523.
7. J. Y. Oh and Z. Bao, *Adv. Sci.*, 2019, **6**, 1900186.
8. J. J. Kim, Y. Wang, H. Wang, S. Lee, T. Yokota and T. Someya, *Adv. Funct. Mater.*, 2021, **31**, 2009602.
9. X. Wu and H. Peng, *Sci. Bull.*, 2019, **64**, 634-640.
10. N. Matsuhisa, X. Chen, Z. Bao and T. Someya, *Chem. Soc. Rev.*, 2019, **48**, 2946-2966.
11. H. Jin, Y. S. Abu-Raya and H. Haick, *Adv. Healthc. Mater.*, 2017, **6**, 1700024.
12. J. Tu, R. M. Torrente - Rodríguez, M. Wang and W. Gao, *Adv. Funct. Mater.*, 2020, **30**, 1906713.
13. Y. Yang and W. Gao, *Chem. Soc. Rev.*, 2019, **48**, 1465-1491.
14. J. Rogers, Z. Bao and T.-W. Lee, *Acc. Chem. Res.*, 2019, **52**, 521-522.
15. S. Mirjalali, S. Peng, Z. Fang, C. H. Wang and S. Wu, *Adv. Mater. Technol.*, 2021, 2100545.
16. Z. Chen, Z. Chen, Z. Song, W. Ye and Z. Fan, *J. Semicond.*, 2019, **40**, 111601.
17. O. Zohar, M. Khatib, R. Omar, R. Vishinkin, Y. Y. Broza and H. Haick, *View*, 2021, **2**, 20200172.
18. H. Lee, T. K. Choi, Y. B. Lee, H. R. Cho, R. Ghaffari, L. Wang, H. J. Choi, T. D. Chung, N. Lu, T. Hyeon, S. H. Choi and D.-H. Kim, *Nat. Nanotechnol.*, 2016, **11**, 566-572.
19. T. Yokota, P. Zalar, M. Kaltenbrunner, H. Jinno, N. Matsuhisa, H. Kitanosako, Y. Tachibana, W. Yukita, M. Koizumi and T. Someya, *Sci. Adv.*, 2016, **2**, e1501856.
20. H. Ouyang, J. Tian, G. Sun, Y. Zou, Z. Liu, H. Li, L. Zhao, B. Shi, Y. Fan and Y. Fan, *Advanced Materials*, 2017, **29**, 1703456.
21. A. Miyamoto, S. Lee, N. F. Cooray, S. Lee, M. Mori, N. Matsuhisa, H. Jin, L. Yoda, T. Yokota and A. Itoh, *Nat. Nanotechnol.*, 2017, **12**, 907.
22. Y. Wang, Y. Qiu, S. K. Ameri, H. Jang, Z. Dai, Y. Huang and N. Lu, *npj Flex. Electron.*, 2018, **2**, 6.
23. S. Choi, S. I. Han, D. Jung, H. J. Hwang, C. Lim, S. Bae, O. K. Park, C. M. Tschabrunn, M. Lee and S. Y. Bae, *Nat. Nanotechnol.*, 2018, **13**, 1048-1056.
24. S. Niu, N. Matsuhisa, L. Beker, J. Li, S. Wang, J. Wang, Y. Jiang, X. Yan, Y. Yun, W. Burnett, A. S. Y. Poon, J. B. H. Tok, X. Chen and Z. Bao, *Nat. Electron.*, 2019, **2**, 361-368.
25. S. Lee, S. Franklin, F. A. Hassani, T. Yokota, M. O. G. Nayeem, Y. Wang, R. Leib, G. Cheng, D. W. Franklin and T. Someya, *Science*, 2020, **370**, 966-970.
26. T. Yokota, T. Nakamura, H. Kato, M. Mochizuki, M. Tada, M. Uchida, S. Lee, M. Koizumi, W. Yukita, A. Takimoto and T. Someya, *Nat. Electron.*, 2020, **3**, 113-121.
27. Z. Ma, Q. Huang, Q. Xu, Q. Zhuang, X. Zhao, Y. Yang, H. Qiu, Z. Yang, C. Wang, Y. Chai and Z. Zijian, *Nat. Mater.*, 2021, **20**, 859-868.
28. D. Ryu, D. H. Kim, J. T. Price, J. Y. Lee, H. U. Chung, E. Allen, J. R. Walter, H. Jeong, J. Cao and E. Kulikova, *Proc. Natl. Acad. Sci. USA.*, 2021, **118**, e2100466118.
29. J. R. Sempionatto, M. Lin, L. Yin, K. Pei, T. Sona-ard, A. N. de Loyola Silva, A. A. Khorshed, F. Zhang, N. Tostado and S. Xu, *Nat. Biomed. Eng.*, 2021, 737-748.
30. L. Wang, K. Jiang and G. Shen, *Appl. Phys. Lett.*, 2021, **119**, 150501.
31. Y. Liu, M. Pharr and G. A. Salvatore, *ACS nano*, 2017, **11**, 9614-9635.
32. S. C. Mukhopadhyay, *IEEE Sens. J.*, 2014, **15**, 1321-1330.
33. M. S. Brown, B. Ashley and A. Koh, *Front bioeng. biotechnol.*, 2018, **6**, 47.
34. Z. Jiang, M. O. G. Nayeem, K. Fukuda, S. Ding, H. Jin, T. Yokota, D. Inoue, D. Hashizume and T. Someya, *Adv. Mater.*, 2019, **31**, 1903446.
35. Q. Su, Q. Zou, Y. Li, Y. Chen, S.-Y. Teng, J. T. Kelleher, R. Nith, P. Cheng, N. Li, W. Liu, S. Dai, Y. Liu, A. Mazursky, J. Xu, L. Jin, P. Lopes and S. Wang, *Sci. Adv.*, 2021, **7**, eabi4563.
36. R. K. Mishra, A. Barfidokht, A. Karajic, J. R. Sempionatto, J. Wang and J. Wang, *Sens. Actuators B Chem.*, 2018, **273**, 966-972.
37. S. Wang, J. Xu, W. Wang, G.-J. N. Wang, R. Rastak, F. Molina-Lopez, J. W. Chung, S. Niu, V. R. Feig and J. Lopez, *Nature*, 2018, **555**, 83.
38. F. Ershad, A. Thukral, J. Yue, P. Comeaux, Y. Lu, H. Shim, K. Sim, N.-I. Kim, Z. Rao and R. Guevara, *Nat. Commun.*, 2020, **11**, 3823.
39. Q. Li, G. Chen, Y. Cui, S. Ji, Z. Liu, C. Wan, Y. Liu, Y. Lu, C. Wang and N. Zhang, *ACS nano*, 2021.
40. R. Tian, Y. Liu, K. Koumoto and J. Chen, *Joule*, 2019, **3**, 1399-1403.

41. J. Kim, G. A. Salvatore, H. Araki, A. M. Chiarelli, Z. Xie, A. Banks, X. Sheng, Y. Liu, J. W. Lee, K.-I. Jang, S. Y. Heo, K. Cho, H. Luo, B. Zimmerman, J. Kim, L. Yan, X. Feng, S. Xu, M. Fabiani, G. Gratton, Y. Huang, U. Paik and J. A. Rogers, *Sci. Adv.*, 2016, **2**, e1600418.
42. W. Gao, H. Ota, D. Kiriya, K. Takei and A. Javey, *Acc. Chem. Res.*, 2019, **52**, 523-533.
43. E. K. Lee, M. K. Kim and C. H. Lee, *Annu. Rev. Biomed. Eng.*, 2019, **21**, 299-323.
44. S. Majumder, T. Mondal and M. J. Deen, *Sensors*, 2017, **17**, 130.
45. Y. M. Chi, T.-P. Jung and G. Cauwenberghs, *IEEE Rev. Biomed. Eng.*, 2010, **3**, 106-119.
46. G. Acar, O. Ozturk, A. J. Golparvar, T. A. Elboshra, K. Böhlinger and M. K. Yapici, *Electronics*, 2019, **8**, 479.
47. H. Wu, G. Yang, K. Zhu, S. Liu, W. Guo, Z. Jiang and Z. Li, *Adv. Sci.*, 2021, **8**, 2001938.
48. S. Kabiri Ameri, R. Ho, H. Jang, L. Tao, Y. Wang, L. Wang, D. M. Schnyer, D. Akinwande and N. Lu, *ACS nano*, 2017, **11**, 7634-7641.
49. L. M. Ferrari, S. Sudha, S. Tarantino, R. Esposti, F. Bolzoni, P. Cavallari, C. Cipriani, V. Mattoli and F. Greco, *Adv. Sci.*, 2018, **5**, 1700771.
50. K. W. Cho, S.-H. Sunwoo, Y. J. Hong, J. H. Koo, J. H. Kim, S. Baik, T. Hyeon and D.-H. Kim, *Chem. Rev.*, 2021.
51. C. Wang, K. Xia, Y. Zhang and D. L. Kaplan, *Acc. Chem. Res.*, 2019, **52**, 2916-2927.
52. Y. Wang, S. Gong, S. J. Wang, G. P. Simon and W. Cheng, *Mater. Horiz.*, 2016, **3**, 208-213.
53. D. Qi, K. Zhang, G. Tian, B. Jiang and Y. Huang, *Adv. Mater.*, 2021, **33**, 2003155.
54. Y. Wang, S. Gong, D. Dong, Y. Zhao, L. W. Yap, Q. Shi, T. An, Y. Ling, G. P. Simon and W. Cheng, *Nanoscale*, 2018, **10**, 15948-15955.
55. M. Hassan, G. Abbas, N. Li, A. Afzal, Z. Haider, S. Ahmed, X. Xu, C. Pan and Z. Peng, *Adv. Mater. Technol.*, 2021, 2100773.
56. S. Chen, S. Peng, W. Sun, G. Gu, Q. Zhang and X. Guo, *Adv. Mater. Technol.*, 2019, **4**, 1800681.
57. R. A. Nawrocki, N. Matsuhisa, T. Yokota and T. Someya, *Adv. Electron. Mater.*, 2016, **2**, 1500452.
58. B. Hwang and T. G. Yun, *Compos. B. Eng.*, 2019, **163**, 185-192.
59. Y. Wang, T. Yokota and T. Someya, *NPG Asia Mater.*, 2021, **13**, 22.
60. Y. Okamura, K. Kabata, M. Kinoshita, D. Saitoh and S. Takeoka, *Adv. Mater.*, 2009, **21**, 4388-4392.
61. K. He, Z. Liu, C. Wan, Y. Jiang, T. Wang, M. Wang, F. Zhang, Y. Liu, L. Pan and M. Xiao, *Adv. Mater.*, 2020, **32**, 2001130.
62. S. Yang, Y. C. Chen, L. Nicolini, P. Pasupathy, J. Sacks, B. Su, R. Yang, D. Sanchez, Y. F. Chang and P. Wang, *Adv. Mater.*, 2015, **27**, 6423-6430.
63. S. Yao and Y. Zhu, *Jom*, 2016, **68**, 1145-1155.
64. I. You, B. Kim, J. Park, K. Koh, S. Shin, S. Jung and U. Jeong, *Adv. Mater.*, 2016, **28**, 6359-6364.
65. D. Kim, J. Bang, P. Won, Y. Kim, J. Jung, J. Lee, J. Kwon, H. Lee, S. Hong and N. L. Jeon, *Adv. Mater. Technol.*, 2020, **5**, 2000661.
66. M. Chu and H. E. Naguib, *Smart Mater. Struct.*, 2021, **30**, 065003.
67. H.-C. Jung, J.-H. Moon, D.-H. Baek, J.-H. Lee, Y.-Y. Choi, J.-S. Hong and S.-H. Lee, *IEEE. Trans. Biomed. Eng.*, 2012, **59**, 1472-1479.
68. B.-C. Kang and T.-J. Ha, *Jpn. J. Appl. Phys.*, 2018, **57**, 05GD02.
69. R. Kumar, R. Singh, D. Hui, L. Feo and F. Fraternali, *Compos. B. Eng.*, 2018, **134**, 193-206.
70. C. Lou, R. Li, Z. Li, T. Liang, Z. Wei, M. Run, X. Yan and X. Liu, *Sensors*, 2016, **16**, 1833.
71. P. Suvannaphaet, S. Sasivimolkul, C. Sukkasem, D. Pukesamsombut, N. Tanadchangsaeng, S. Boonyagul and S. Pechprasarn, 2019.
72. R. Guo, X. Wang, W. Yu, J. Tang and J. Liu, *Sci. China Technol. Sci.*, 2018, **61**, 1031-1037.
73. Y. Yu, J. Zhang and J. Liu, *PloS one*, 2013, **8**, e58771.
74. A. Zucca, C. Cipriani, S. Tarantino, D. Ricci, V. Mattoli and F. Greco, *Adv. Healthc. Mater.*, 2015, **4**, 983-990.
75. Y. Wang, X. Zhong, W. Wang and D. Yu, *Cellulose*, 2021, **28**, 4913-4926.
76. X. Xu, Z. Liu, P. He and J. Yang, *J. Phys. D: Appl. Phys.*, 2019, **52**, 455401.
77. T. Kim, J. Park, J. Sohn, D. Cho and S. Jeon, *ACS nano*, 2016, **10**, 4770-4778.
78. J. Heikenfeld, A. Jajack, J. Rogers, P. Gutruf, L. Tian, T. Pan, R. Li, M. Khine, J. Kim and J. Wang, *Lab on a Chip*, 2018, **18**, 217-248.
79. R. Matsukawa, A. Miyamoto, T. Yokota and T. Someya, *Adv. Healthc. Mater.*, 2020, **9**, 2001322.
80. Z. Ma, B. Su, S. Gong, Y. Wang, L. W. Yap, G. P. Simon and W. Cheng, *ACS Sens.*, 2016, **1**, 303-311.
81. S. Gong, D. T. Lai, Y. Wang, L. W. Yap, K. J. Si, Q. Shi, N. N. Jason, T. Sridhar, H. Uddin and W. Cheng, *ACS Appl. Mater. Interfaces.*, 2015, **7**, 19700-19708.
82. L. W. Yap, Q. Shi, S. Gong, Y. Wang, Y. Chen, C. Zhu, Z. Gu, K. Suzuki, Y. Zhu and W. Cheng, *Inorg. Chem. Commun.*, 2019, **104**, 98-104.
83. B. Zhu, Y. Ling, L. W. Yap, M. Yang, F. Lin, S. Gong, Y. Wang, T. An, Y. Zhao and W. Cheng, *ACS Appl. Mater. Interfaces.*, 2019, **11**, 29014-29021.
84. Y. Ling, S. Gong, Q. Zhai, Y. Wang, Y. Zhao, M. Yang and W. Cheng, *Small*, 2019, **15**, 1804853.
85. Z. Zhang, L. W. Yap, D. Dong, Q. Shi, Y. Wang, W. Cheng and X. Han, *ChemPlusChem*, 2019, **84**, 1030.
86. B. Zhu, S. Gong and W. Cheng, *Chem. Soc. Rev.*, 2019, **48**, 1668-1711.
87. Y. G. Park, G. Y. Lee, J. Jang, S. M. Yun, E. Kim and J. U. Park, *Adv. Healthc. Mater.*, 2021, 2002280.
88. S. Gong, Y. Wang, L. W. Yap, Y. Ling, Y. Zhao, D. Dong, Q. Shi, Y. Liu, H. Uddin and W. Cheng, *Nanoscale Horiz.*, 2018, **3**, 640-647.
89. D. Y. Choi, M. H. Kim, Y. S. Oh, S.-H. Jung, J. H. Jung, H. J. Sung, H. W. Lee and H. M. Lee, *ACS Appl. Mater. Interfaces.*, 2017, **9**, 1770-1780.
90. H. Huang, S. Su, N. Wu, H. Wan, S. Wan, H. Bi and L. Sun, *Front. Chem.*, 2019, **7**, 399.
91. J. Chen, Q. Yu, X. Cui, M. Dong, J. Zhang, C. Wang, J. Fan, Y. Zhu and Z. Guo, *J. Mater. Chem. C.*, 2019, **7**, 11710-11730.
92. N. Matsuhisa, S. Niu, S. J. O'Neill, J. Kang, Y. Ochiai, T. Katsumata, H.-C. Wu, M. Ashizawa, G.-J. N. Wang and D. Zhong, *Nature*, 2021, **600**, 246-252.
93. C. Choi, M. K. Choi, T. Hyeon and D. H. Kim, *ChemNanoMat*, 2016, **2**, 1006-1017.

94. J.-B. Chossat, Y.-L. Park, R. J. Wood and V. Duchaine, *IEEE Sens. J.*, 2013, **13**, 3405-3414.
95. M. D. Ho, Y. Ling, L. W. Yap, Y. Wang, D. Dong, Y. Zhao and W. Cheng, *Adv. Funct. Mater.*, 2017, **27**, 1700845.
96. X. Wang, Z. Liu and T. Zhang, *Small*, 2017, **13**, 1602790.
97. R. Nur, N. Matsuhisa, Z. Jiang, M. O. G. Nayeem, T. Yokota and T. Someya, *Nano Lett.*, 2018, **18**, 5610-5617.
98. W. Chen and X. Yan, *J. Mater. Sci. Technol.*, 2020, **43**, 175-188.
99. A. Khan, Z. Abas, H. S. Kim and I.-K. Oh, *Smart Mater. Struct.*, 2016, **25**, 053002.
100. T. Sun, F. Tasnim, R. T. McIntosh, N. Amiri, D. Solav, M. T. Anbarani, D. Sadat, L. Zhang, Y. Gu and M. A. Karami, *Nat. Biomed. Eng.*, 2020, **4**, 954-972.
101. J. Rao, Z. Chen, D. Zhao, Y. Yin, X. Wang and F. Yi, *Sensors*, 2019, **19**, 2763.
102. W. Zhong Lin, *Mater. Today*, 2017, **20**, 74-82.
103. Z. L. Wang, *Adv. Energy Mater.*, 2020, **10**, 2000137.
104. Y. Wang, Y. Yang and Z. L. Wang, *npj Flex. Electron.*, 2017, **1**, 10.
105. A. Chen, C. Zhang, G. Zhu and Z. L. Wang, *Adv. Sci.*, 2020, **7**, 2000186.
106. Z. Zhu, R. Li and T. Pan, *Adv. Mater.*, 2018, **30**, 1705122.
107. Q. Liu, Y. Liu, J. Shi, Z. Liu, Q. Wang and C. F. Guo, *Micro Nano Lett.*, 2021, **14**, 21.
108. W. Xu, H. Zheng, Y. Liu, X. Zhou, C. Zhang, Y. Song, X. Deng, M. Leung, Z. Yang, R. X. Xu, Z. L. Wang, X. C. Zeng and Z. Wang, *Nature*, 2020, **578**, 392-396.
109. G. Xue, Y. Xu, T. Ding, J. Li, J. Yin, W. Fei, Y. Cao, J. Yu, L. Yuan, L. Gong, J. Chen, S. Deng, J. Zhou and W. Guo, *Nat. Nanotechnol.*, 2017, **12**, 317-321.
110. L. Jia, Z. H. Guo, L. Li, C. Pan, P. Zhang, F. Xu, X. Pu and Z. L. Wang, *ACS nano.*, 2021.
111. Z. S. Ballard and A. Ozcan, in *Mobile Health: Sensors, Analytic Methods, and Applications*, eds. J. M. Rehg, S. A. Murphy and S. Kumar, Springer International Publishing, Cham, 2017, pp. 313-342.
112. A. Ahmad Tarar, U. Mohammad and S. K. Srivastava, *Biosensors*, 2020, **10**, 56.
113. A. K. Bansal, S. Hou, O. Kulyk, E. M. Bowman and I. D. Samuel, *Adv. Mater.*, 2015, **27**, 7638-7644.
114. L. Zhang, J. Pan, Z. Zhang, H. Wu, N. Yao, D. Cai, Y. Xu, J. Zhang, G. Sun and L. Wang, *Opto-electron. adv.*, 2020, **3**, 190022.
115. R. Fu, T. Warnakula, Q. Shi, L. W. Yap, D. Dong, Y. Liu, M. Premaratne and W. Cheng, *Nanoscale Horiz.*, 2020, **5**, 1515-1523.
116. H. Lee, Z. Jiang, T. Yokota, K. Fukuda, S. Park and T. Someya, *Mater. Sci. Eng. R Rep.*, 2021, **146**, 100631.
117. A. Koh, D. Kang, Y. Xue, S. Lee, R. M. Pielak, J. Kim, T. Hwang, S. Min, A. Banks and P. Bastien, *Sci. Transl. Med.*, 2016, **8**, 366ra165-366ra165.
118. X. Huang, Y. Liu, K. Chen, W. J. Shin, C. J. Lu, G. W. Kong, D. Patnaik, S. H. Lee, J. F. Cortes and J. A. Rogers, *Small*, 2014, **10**, 3083-3090.
119. J. Choi, D. Kang, S. Han, S. B. Kim and J. A. Rogers, *Adv. Healthc. Mater.*, 2017, **6**, 1601355.
120. B. Wang, A. D. Scaccabarozzi, H. Wang, M. Koizumi, M. I. Nugraha, Y. Lin, Y. Firdaus, Y. Wang, S. Lee and T. Yokota, *J. Mater. Chem. C.*, 2021, **9**, 3129-3135.
121. T. Yokota, K. Fukuda and T. Someya, *Adv. Mater.*, 2021, 2004416.
122. V. B. Nam and D. Lee, *Nanomaterials*, 2016, **6**, 47.
123. H. B. Lee, W.-Y. Jin, M. M. Ovhall, N. Kumar and J.-W. Kang, *J. Mater. Chem. C.*, 2019, **7**, 1087-1110.
124. Q. Huang and Y. Zhu, *ACS Appl. Mater. Interfaces.*, 2021.
125. S. H. Chae and Y. H. Lee, *Nano Converg.*, 2014, **1**, 15.
126. J. Yan, Y. Lu, G. Chen, M. Yang and Z. Gu, *Chem. Soc. Rev.*, 2018, **47**, 2518-2533.
127. S. Meer, A. Kausar and T. Iqbal, *Polym Plast Technol Eng.*, 2016, **55**, 1416-1440.
128. K. Yu, S. Rich, S. Lee, K. Fukuda, T. Yokota and T. Someya, *Proc. IEEE*, 2019, **107**, 2137-2154.
129. L. Yu, Z. Yang and M. An, *Biosci. Trends*, 2019, **13**, 308-313.
130. A. Yang and F. Yan, *ACS Appl. Electron. Mater.*, 2020, **3**, 53-67.
131. M. A. A. Mamun and M. R. Yuce, *Adv. Funct. Mater.*, 2020, **30**, 2005703.
132. M. Dervisevic, M. Alba, B. Prieto-Simon and N. Voelcker, *Nano Today*, 2020, **30**, 100828.
133. E. Dervisevic, M. Dervisevic, Y. Wang, L. F. Malaver - Ortega, W. Cheng, K. L. Tuck, N. H. Voelcker and V. Cadarso, *Electroanalysis*, 2020, **32**, 1850-1858.
134. S. G. Kim, J. Jun, J. S. Lee and J. Jang, *J. Mater. Chem. A.*, 2019, **7**, 8451-8459.
135. Z. Gao, Z. Lou, S. Chen, L. Li, K. Jiang, Z. Fu, W. Han and G. Shen, *Nano Res.*, 2018, **11**, 511-519.
136. D. Maity and R. T. R. Kumar, *ACS Sens.*, 2018, **3**, 1822-1830.
137. S. Yuvaraja, A. Nawaz, Q. Liu, D. Dubal, S. G. Surya, K. N. Salama and P. Sonar, *Chem. Soc. Rev.*, 2020, **49**, 3423-3460.
138. H. Chen, S. Dong, M. Bai, N. Cheng, H. Wang, M. Li, H. Du, S. Hu, Y. Yang and T. Yang, *Adv. Mater.*, 2015, **27**, 2113-2120.
139. Y. Zheng, R. Omar, R. Zhang, N. Tang, M. Khatib, Q. Xu, Y. Milyutin, W. Saliba, Y. Y. Broza, W. Wu, M. Yuan and H. Haick, *Adv. Mater.*, 2021, **n/a**, 2108607.
140. M. Y. Lee, H. R. Lee, C. H. Park, S. G. Han and J. H. Oh, *Acc. Chem. Res.*, 2018, **51**, 2829-2838.
141. J. Wang, S. Lee, T. Yokota, Y. Jimbo, Y. Wang, M. O. G. Nayeem, M. Nishinaka and T. Someya, *ACS Appl. Electron. Mater.*, 2020, **2**, 3601-3609.
142. H. Lee, S. Lee, W. Lee, T. Yokota, K. Fukuda and T. Someya, *Adv. Funct. Mater.*, 2019, **29**, 1906982.
143. T. Someya, T. Sekitani, S. Iba, Y. Kato, H. Kawaguchi and T. Sakurai, *Proc. Natl. Acad. Sci. USA.*, 2004, **101**, 9966-9970.
144. T. Yokota, Y. Inoue, Y. Terakawa, J. Reeder, M. Kaltenbrunner, T. Ware, K. Yang, K. Mabuchi, T. Murakawa and M. Sekino, *Proc. Natl. Acad. Sci. USA.*, 2015, **112**, 14533-14538.
145. N. Matsuhisa, D. Inoue, P. Zalar, H. Jin, Y. Matsuba, A. Itoh, T. Yokota, D. Hashizume and T. Someya, *Nat. Mater.*, 2017, **16**, 834-840.
146. Z. Liu, Z. Yin, J. Wang and Q. Zheng, *Adv. Funct. Mater.*, 2019, **29**, 1806092.
147. M. Song, J. Seo, H. Kim and Y. Kim, *ACS omega*, 2017, **2**, 4065-4070.
148. M. Ha, S. Lim and H. Ko, *J. Mater. Chem. B.*, 2018, **6**, 4043-4064.
149. R. Gravina, P. Alinia, H. Ghasemzadeh and G. Fortino, *Inf. Fusion*, 2017, **35**, 68-80.
150. H. U. Chung, A. Y. Rwei, A. Hourlier-Fargette, S. Xu, K. Lee, E. C. Dunne, Z. Xie, C. Liu, A. Carlini and D. H. Kim, *Nat. Med.*, 2020, **26**, 418-429.

151. W. A. D. M. Jayathilaka, K. Qi, Y. Qin, A. Chinnappan, W. Serrano - García, C. Baskar, H. Wang, J. He, S. Cui and S. W. Thomas, *Adv. Mater.*, 2019, **31**, 1805921.
152. D. Jung, C. Lim, H. J. Shim, Y. Kim, C. Park, J. Jung, S. I. Han, S.-H. Sunwoo, K. W. Cho and G. D. Cha, *Science*, 2021, **373**, 1022-1026.
153. K. Xu, Y. Lu and K. Takei, *Adv. Mater. Technol.*, 2019, **4**, 1800628.
154. Z. Lou, S. Chen, L. Wang, R. Shi, L. Li, K. Jiang, D. Chen and G. Shen, *Nano Energy*, 2017, **38**, 28-35.
155. Y. Ai, Z. Lou, S. Chen, D. Chen, Z. M. Wang, K. Jiang and G. Shen, *Nano Energy*, 2017, **35**, 121-127.
156. S. Hozumi, S. Honda, T. Arie, S. Akita and K. Takei, *ACS Sens.*, 2021, **6**, 1918-1924.
157. T. An, Y. Ling, S. Gong, B. Zhu, Y. Zhao, D. Dong, L. W. Yap, Y. Wang and W. Cheng, *Adv. Mater. Technol.*, 2019, **4**, 1800473.
158. E. J. Markvicka, M. D. Bartlett, X. Huang and C. Majidi, *Nat. Mater.*, 2018, **17**, 618-624.
159. D. Son, J. Kang, O. Vardoulis, Y. Kim, N. Matsuhisa, J. Y. Oh, J. W. To, J. Mun, T. Katsumata and Y. Liu, *Nat. Nanotechnol.*, 2018, **13**, 1057-1065.
160. J. Zhu, Z. Ren and C. Lee, *ACS nano*, 2020, **15**, 894-903.
161. M. K. Choi, J. Yang, T. Hyeon and D.-H. Kim, *npj Flex. Electron.*, 2018, **2**, 10.
162. K. Yamagishi, I. Kirino, I. Takahashi, H. Amano, S. Takeoka, Y. Morimoto and T. Fujie, *Nat. Biomed. Eng.*, 2019, **3**, 27-36.
163. Y. Chen, Y. Zhang, Z. Liang, Y. Cao, Z. Han and X. Feng, *npj Flex. Electron.*, 2020, **4**, 2.
164. S. Choi, H. Lee, R. Ghaffari, T. Hyeon and D. H. Kim, *Adv. Mater.*, 2016, **28**, 4203-4218.
165. T. Someya, Z. Bao and G. G. Malliaras, *Nature*, 2016, **540**, 379-385.
166. Y. Wang, S. Lee, H. Wang, Z. Jiang, Y. Jimbo, C. Wang, B. Wang, J. J. Kim, M. Koizumi, T. Yokota and T. Someya, *Proc. Natl. Acad. Sci. USA.*, 2021, **118**.
167. K. Yamagishi, S. Takeoka and T. Fujie, *Biomater. Sci.*, 2019, **7**, 520-531.
168. D.-H. Kim, N. Lu, R. Ma, Y.-S. Kim, R.-H. Kim, S. Wang, J. Wu, S. M. Won, H. Tao, A. Islam, K. J. Yu, T.-i. Kim, R. Chowdhury, M. Ying, L. Xu, M. Li, H.-J. Chung, H. Keum, M. McCormick, P. Liu, Y.-W. Zhang, F. G. Omenetto, Y. Huang, T. Coleman and J. A. Rogers, *Science*, 2011, **333**, 838-843.
169. G. Schwartz, B. C. K. Tee, J. Mei, A. L. Appleton, D. H. Kim, H. Wang and Z. Bao, *Nat. Commun.*, 2013, **4**, 1859.
170. W. H. Yeo, Y. S. Kim, J. Lee, A. Ameen, L. Shi, M. Li, S. Wang, R. Ma, S. H. Jin and Z. Kang, *Adv. Mater.*, 2013, **25**, 2773-2778.
171. L. Zhang, K. S. Kumar, H. He, C. J. Cai, X. He, H. Gao, S. Yue, C. Li, R. C.-S. Seet and H. Ren, *Nat. Commun.*, 2020, **11**, 4683.
172. Y. J. Fan, X. Li, S. Y. Kuang, L. Zhang, Y. H. Chen, L. Liu, K. Zhang, S. W. Ma, F. Liang and T. Wu, *ACS nano*, 2018, **12**, 9326-9332.
173. S. M. Lee, H. J. Byeon, J. H. Lee, D. H. Baek, K. H. Lee, J. S. Hong and S.-H. Lee, *Sci. Rep.*, 2014, **4**, 6074.
174. J. A. Rogers, *Nat. Nanotechnol.*, 2017, **12**, 839-840.
175. S. Gong, L. W. Yap, B. Zhu, Q. Zhai, Y. Liu, Q. Lyu, K. Wang, M. Yang, Y. Ling, D. T. H. Lai, F. Marzbanrad and W. Cheng, *Adv. Mater.*, 2019, **31**, 1903789.
176. D. Y. Park, D. J. Joe, D. H. Kim, H. Park, J. H. Han, C. K. Jeong, H. Park, J. G. Park, B. Joung and K. J. Lee, *Adv. Mater.*, 2017, **29**, 1702308.
177. J. Kim, H. J. Shim, J. Yang, M. K. Choi, D. C. Kim, J. Kim, T. Hyeon and D. H. Kim, *Adv. Mater.*, 2017, **29**, 1700217.
178. W. Zhou, S. Yao, H. Wang, Q. Du, Y. Ma and Y. Zhu, *ACS nano*, 2020, **14**, 5798-5805.
179. Y. Wang, S. Lee, T. Yokota, H. Wang, Z. Jiang, J. Wang, M. Koizumi and T. Someya, *Sci. Adv.*, 2020, **6**, eabb7043.
180. Y. Feng and J. Zhu, *Sci. China Mater.*, 2019, **62**, 1679-1708.
181. J. Kwon, Y. D. Suh, J. Lee, P. Lee, S. Han, S. Hong, J. Yeo, H. Lee and S. H. Ko, *J. Mater. Chem. C.*, 2018, **6**, 7445-7461.
182. X. Xiao, L. Yuan, J. Zhong, T. Ding, Y. Liu, Z. Cai, Y. Rong, H. Han, J. Zhou and Z. L. Wang, *Adv. Mater.*, 2011, **23**, 5440-5444.
183. M. Rdest and D. Janas, *Sensors*, 2021, **21**, 5847.
184. S. Gong and W. Cheng, *Adv. Electron. Mater.*, 2017, **3**, 1600314.
185. L. Cai and C. Wang, *Nanoscale Res. Lett.*, 2015, **10**, 320.
186. D. J. Lee, Y. Oh, J.-M. Hong, Y. W. Park and B.-K. Ju, *Sci. Rep.*, 2018, **8**, 14170.
187. Y. Zhao, D. Dong, S. Gong, L. Brassart, Y. Wang, T. An and W. Cheng, *Adv. Electron. Mater.*, 2019, **5**, 1800462.
188. H. Wu, D. Kong, Z. Ruan, P.-C. Hsu, S. Wang, Z. Yu, T. J. Carney, L. Hu, S. Fan and Y. Cui, *Nat. Nanotechnol.*, 2013, **8**, 421-425.
189. P. Lee, J. Ham, J. Lee, S. Hong, S. Han, Y. D. Suh, S. E. Lee, J. Yeo, S. S. Lee and D. Lee, *Adv. Funct. Mater.*, 2014, **24**, 5671-5678.
190. C. Choi, Y. Lee, K. W. Cho, J. H. Koo and D.-H. Kim, *Acc. Chem. Res.*, 2018, **52**, 73-81.
191. Y. Qiao, X. Li, T. Hirtz, G. Deng, Y. Wei, M. Li, S. Ji, Q. Wu, J. Jian and F. Wu, *Nanoscale*, 2019, **11**, 18923-18945.
192. W. Wu, L. Wang, Y. Li, F. Zhang, L. Lin, S. Niu, D. Chenet, X. Zhang, Y. Hao and T. F. Heinz, *Nature*, 2014, **514**, 470-474.
193. J. Zhao, N. Li, H. Yu, Z. Wei, M. Liao, P. Chen, S. Wang, D. Shi, Q. Sun and G. Zhang, *Adv. Mater.*, 2017, **29**, 1702076.
194. D. Son, S. I. Chae, M. Kim, M. K. Choi, J. Yang, K. Park, V. S. Kale, J. H. Koo, C. Choi and M. Lee, *Adv. Mater.*, 2016, **28**, 9326-9332.
195. C. Wang, C. Wang, Z. Huang and S. Xu, *Adv. Mater.*, 2018, **30**, 1801368.
196. Y. Chen, G. Zhou, X. Yuan, C. Li, L. Liu and H. You, *Biosens. Bioelectron.*, 2022, 114118.
197. S. Song, K. Y. Kim, S. H. Lee, K. K. Kim, K. Lee, W. Lee, H. Jeon and S. H. Ko, *Adv. Biomed. Res.*, 2021, 2100111.
198. S. Stauss and I. Honma, *Bull. Chem. Soc. Jpn.*, 2018, **91**, 492-505.
199. D. Gao, K. Parida and P. S. Lee, *Adv. Funct. Mater.*, 2020, **30**, 1907184.
200. Y. Cao and K. Urich, *J. Bioact. Compat. Polym.*, 2019, **34**, 3-15.
201. A. M. Soomro, F. Jabbar, M. Ali, J.-W. Lee, S. W. Mun and K. H. Choi, *J. Mater. Sci. Mater.*, 2019, **30**, 9455-9465.
202. X. Liang, H. Li, J. Dou, Q. Wang, W. He, C. Wang, D. Li, J. M. Lin and Y. Zhang, *Adv. Mater.*, 2020, **32**, 2000165.
203. J. Chen, S. K. Oh, N. Nabulsi, H. Johnson, W. Wang and J.-H. Ryou, *Nano Energy*, 2019, **57**, 670-679.
204. L. Wang, W. Liu, Z. Yan, F. Wang and X. Wang, *Adv. Funct. Mater.*, 2021, **31**, 2007221.
205. A. J. Bandodkar, S. P. Lee, I. Huang, W. Li, S. Wang, C. J. Su, W. J. Jeang, T. Hang, S. Mehta, N. Nyberg, P. Gutruf, J. Choi,

- J. Koo, J. T. Reeder, R. Tseng, R. Ghaffari and J. A. Rogers, *Nat. Electron.*, 2020, **3**, 554-562.
206. H. Yang, S. Ji, I. Chaturvedi, H. Xia, T. Wang, G. Chen, L. Pan, C. Wan, D. Qi and Y.-S. Ong, *ACS Mater. Lett.*, 2020, **2**, 478-484.
207. D. Kim, J. Bang, P. Won, Y. Kim, J. Jung, J. Lee, J. Kwon, H. Lee, S. Hong and N. L. Jeon, *Advanced Materials Technologies*, 2020, **5**, 2000661.
208. L. Mou, J. Qi, L. Tang, R. Dong, Y. Xia, Y. Gao and X. Jiang, *Small*, 2020, **16**, 2005336.
209. S. Patel, F. Ershad, J. Lee, L. Chacon-Alberly, Y. Wang, M. A. Morales-Garza, A. Haces-Garcia, S. Jang, L. Gonzalez, L. Contreras, A. Agarwal, Z. Rao, G. Liu, I. R. Efimov, Y. S. Zhang, M. Zhao, R. R. Isseroff, A. Karim, A. Elgalad, W. Zhu, X. Wu and C. Yu, *Small*, 2022, DOI: <https://doi.org/10.1002/sml.202107099>, 2107099.
210. W. Yang, N. W. Li, S. Zhao, Z. Yuan, J. Wang, X. Du, B. Wang, R. Cao, X. Li and W. Xu, *Adv. Mater. Technol.*, 2018, **3**, 1700241.
211. F. Chen, Q. Huang and Z. Zheng, *Small Structures*, 2021, DOI: 10.1002/sstr.202100135, 2100135.
212. S. S. H. Abir, M. U. K. Sadaf, S. K. Saha, A. Touhami, K. Lozano and M. J. Uddin, *ACS Appl. Mater. Interfaces.*, 2021, **0**, null.
213. Y. J. Fan, P. T. Yu, F. Liang, X. Li, H. Y. Li, L. Liu, J. W. Cao, X. J. Zhao, Z. L. Wang and G. Zhu, *Nanoscale*, 2020, **12**, 16053-16062.
214. Y. Zhang, T. Zhang, Z. Huang and J. Yang, *Adv. Sci.*, 2022, DOI: <https://doi.org/10.1002/advs.202105084>, 2105084.
215. M. O. G. Nayeem, S. Lee, H. Jin, N. Matsuhisa, H. Jinno, A. Miyamoto, T. Yokota and T. Someya, *Proc. Natl. Acad. Sci. USA.*, 2020, **117**, 7063-7070.
216. Y. Fang, Y. Li, Y. Li, M. Ding, J. Xie and B. Hu, *ACS Appl. Mater. Interfaces.*, 2020, **12**, 23689-23696.
217. X. Yang, L. Li, S. Wang, Q. Lu, Y. Bai, F. Sun, T. Li, Y. Li, Z. Wang and Y. Zhao, *Adv. Electron. Mater.*, 2020, **6**, 2000306.
218. Y. Xu, B. Sun, Y. Ling, Q. Fei, Z. Chen, X. Li, P. Guo, N. Jeon, S. Goswami, Y. Liao, S. Ding, Q. Yu, J. Lin, G. Huang and Z. Yan, *Proc. Natl. Acad. Sci. USA.*, 2020, **117**, 205-213.
219. B. Sun, R. N. McCay, S. Goswami, Y. Xu, C. Zhang, Y. Ling, J. Lin and Z. Yan, *Adv. Mater.*, 2018, **30**, 1804327.
220. Q. Xu, H. Liu, X. Zhong, B. Jiang and Z. Ma, *ACS Appl. Mater. Interfaces.*, 2020, **12**, 36609-36619.
221. Y. Niu, H. Liu, R. He, Z. Li, H. Ren, B. Gao, H. Guo, G. M. Genin and F. Xu, *Mater. Today*, 2020.
222. W. Yuan, C. Zhang, B. Zhang, X. Wei, O. Yang, Y. Liu, L. He, S. Cui, J. Wang and Z. L. Wang, *Adv. Mater. Technol.*, 2021, **n/a**, 2101139.
223. H. Huang, N. Wu, H. Liu, Y. Dong, L. Han, S. Wan, G. Dou and L. Sun, *Adv. Mater. Interfaces.*, 2021, 2101602.
224. B. Dai, K. Li, L. Shi, X. Wan, X. Liu, F. Zhang, L. Jiang and S. Wang, *Adv. Mater.*, 2019, **31**, 1904113.
225. S. Ji, C. Wan, T. Wang, Q. Li, G. Chen, J. Wang, Z. Liu, H. Yang, X. Liu and X. Chen, *Adv. Mater.*, 2020, **32**, 2001496.
226. J. T. Reeder, J. Choi, Y. Xue, P. Gutruf, J. Hanson, M. Liu, T. Ray, A. J. Bandodkar, R. Avila and W. Xia, *Sci. Adv.*, 2019, **5**, eaau6356.
227. Y. Zhou, X. Zhao, J. Xu, Y. Fang, G. Chen, Y. Song, S. Li and J. Chen, *Nat. Mater.*, 2021, **20**, 1670-1676.
228. R. A. Nawrocki, H. Jin, S. Lee, T. Yokota, M. Sekino and T. Someya, *Adv. Funct. Mater.*, 2018, **28**, 1803279.
229. L. Tian, B. Zimmerman, A. Akhtar, K. J. Yu, M. Moore, J. Wu, R. J. Larsen, J. W. Lee, J. Li, Y. Liu, B. Metzger, S. Qu, X. Guo, K. E. Mathewson, J. A. Fan, J. Cornman, M. Fatina, Z. Xie, Y. Ma, J. Zhang, Y. Zhang, F. Dolcos, M. Fabiani, G. Gratton, T. Bretl, L. J. Hargrove, P. V. Braun, Y. Huang and J. A. Rogers, *Nat. Biomed. Eng.*, 2019, **3**, 194-205.
230. S. Baik, H. J. Lee, D. W. Kim, J. W. Kim, Y. Lee and C. Pang, *Adv. Mater.*, 2019, **31**, 1803309.
231. Y. Yamamoto, D. Yamamoto, M. Takada, H. Naito, T. Arie, S. Akita and K. Takei, *Adv. Healthc. Mater.*, 2017, **6**, 1700495.
232. J. A. Rogers, T. Someya and Y. Huang, *Science*, 2010, **327**, 1603-1607.
233. Y. Zheng, N. Tang, R. Omar, Z. Hu, T. Duong, J. Wang, W. Wu and H. Haick, *Adv. Funct. Mater.*, 2021, 2105482.
234. H. Kim, K. R. Pyun, M. T. Lee, H. B. Lee and S. H. J. A. F. M. Ko, *Adv. Funct. Mater.*, 2021, 2110535.
235. S. Li, G. Liu, R. Li, Q. Li, Y. Zhao, M. Huang, M. Zhang, S. Yin, Y. Zhou and H. Tang, *ACS nano.*, 2021.
236. Y. Liu, K. He, G. Chen, W. R. Leow and X. Chen, *Chem. Rev.*, 2017, **117**, 12893-12941.
237. W. Shuang, D. Xiaosheng, L. Yaofa, L. Shiyu, Z. Mi, D. Zongliang, C. Xu and W. Haibo, *Chem. Eng. J.*, 2021, **408**, 127363.
238. Y. Ling, K. Guo, B. Zhu, B. Prieto-Simon, N. H. Voelcker and W. Cheng, *Nanoscale Horiz.*, 2019, **4**, 1380-1387.
239. P. Jin, P. Wang, W. Pang, H. Wang, Y. Jiao, J. Zhang, B. Lu, B. Liu, Y. Chen, Y. Ma and X. Feng, *Adv. Mater. Technol.*, **n/a**, 2101126.
240. C. Kwon, D. Seong, J. Ha, D. Chun, J.-H. Bae, K. Yoon, M. Lee, J. Woo, C. Won, S. Lee, Y. Mei, K.-I. Jang, D. Son and T. Lee, *Adv. Funct. Mater.*, 2020, **30**, 2005447.
241. J. Pan, B. Hao, W. Song, S. Chen, D. Li, L. Luo, Z. Xia, D. Cheng, A. Xu and G. Cai, *Compos. B. Eng.*, 2020, **183**, 107683.
242. M. Li, W.-Y. Cheng, Y.-C. Li, H.-M. Wu, Y.-C. Wu, H.-W. Lu, S.-L. Cheng, L. Li, K.-C. Chang and H.-J. Liu, *Nano Energy*, 2021, **79**, 105405.
243. X. Zheng, P. Wang, X. Zhang, Q. Hu, Z. Wang, W. Nie, L. Zou, C. Li and X. Han, *Compos. Part A Appl. Sci.*, 2022, **152**, 106700.
244. J. Qiu, T. Yu, W. Zhang, Z. Zhao, Y. Zhang, G. Ye, Y. Zhao, X. Du, X. Liu and L. Yang, *ACS Mater. Lett.*, 2020, **2**, 999-1007.
245. M. Xu, J. Qi, F. Li and Y. Zhang, *Nanoscale*, 2018, **10**, 5264-5271.
246. S. H. Jeong, S. Zhang, K. Hjort, J. Hilborn and Z. Wu, *Adv. Mater.*, 2016, **28**, 5830-5836.
247. M. Liao, P. Wan, J. Wen, M. Gong, X. Wu, Y. Wang, R. Shi and L. Zhang, *Adv. Funct. Mater.*, 2017, **27**, 1703852.
248. J.-H. Kim, S.-R. Kim, H.-J. Kil, Y.-C. Kim and J.-W. Park, *Nano Lett.*, 2018, **18**, 4531-4540.
249. J. A. Rogers, *Jama*, 2015, **313**, 561-562.
250. C. Pang, C. Lee and K. Y. Suh, *J. Appl. Polym. Sci.*, 2013, **130**, 1429-1441.
251. B. K. Lee, J. H. Ryu, I. B. Baek, Y. Kim, W. I. Jang, S. H. Kim, Y. S. Yoon, S. H. Kim, S. G. Hong and S. Byun, *Adv. Healthc. Mater.*, 2017, **6**, 1700621.
252. L. M. Ferrari, U. Ismailov, J.-M. Badier, F. Greco and E. Ismailova, *npj Flex. Electron.*, 2020, **4**, 4.
253. H. Jung, J. Moon, D. Baek, J. Lee, Y. Choi, J. Hong and S. Lee, *IEEE. Trans. Biomed. Eng.*, 2012, **59**, 1472-1479.

254. J. Song, X. Feng and Y. Huang, *Natl. Sci. Rev.*, 2016, **3**, 128-143.
255. S. Cheng and Z. Wu, *Adv. Funct. Mater.*, 2011, **21**, 2282-2290.
256. H. Yang, S. Ji, I. Chaturvedi, H. Xia, T. Wang, G. Chen, L. Pan, C. Wan, D. Qi, Y.-S. Ong and X. Chen, *ACS Mater. Lett.*, 2020, **2**, 478-484.
257. J.-W. Jeong, M. K. Kim, H. Cheng, W.-H. Yeo, X. Huang, Y. Liu, Y. Zhang, Y. Huang and J. A. Rogers, *Adv. Healthc. Mater.*, 2014, **3**, 642-648.
258. Y. Ma, M. Pharr, L. Wang, J. Kim, Y. Liu, Y. Xue, R. Ning, X. Wang, H. U. Chung and X. Feng, *Small*, 2017, **13**, 1602954.
259. X. Wang, Y. Ma, Y. Xue, H. Luan, M. Pharr, X. Feng, J. A. Rogers and Y. Huang, *Int. J. Solids Struct.*, 2017, **117**, 137-142.
260. C. H. Lee, Y. Ma, K. I. Jang, A. Banks, T. Pan, X. Feng, J. S. Kim, D. Kang, M. S. Raj and B. L. McGrane, *Adv. Funct. Mater.*, 2015, **25**, 3698-3704.
261. R. Guo, X. Wang, W. Yu, J. Tang and J. Liu, *Science China Technological Sciences*, 2018, **61**, 1031-1037.
262. Y. Yang and M. W. Urban, *Chem. Soc. Rev.*, 2013, **42**, 7446-7467.
263. C. Gong, J. Liang, W. Hu, X. Niu, S. Ma, H. T. Hahn and Q. Pei, *Adv. Mater.*, 2013, **25**, 4186-4191.
264. Y. Huang, M. Zhong, Y. Huang, M. Zhu, Z. Pei, Z. Wang, Q. Xue, X. Xie and C. Zhi, *Nat. Commun.*, 2015, **6**, 10310.
265. J. Y. Oh, D. Son, T. Katsumata, Y. Lee, Y. Kim, J. Lopez, H.-C. Wu, J. Kang, J. Park, X. Gu, J. Mun, N. G.-J. Wang, Y. Yin, W. Cai, Y. Yun, J. B.-H. Tok and Z. Bao, *Sci. Adv.*, 2019, **5**, eaav3097.
266. K.-I. Jang, K. Li, H. U. Chung, S. Xu, H. N. Jung, Y. Yang, J. W. Kwak, H. H. Jung, J. Song, C. Yang, A. Wang, Z. Liu, J. Y. Lee, B. H. Kim, J.-H. Kim, J. Lee, Y. Yu, B. J. Kim, H. Jang, K. J. Yu, J. Kim, J. W. Lee, J.-W. Jeong, Y. M. Song, Y. Huang, Y. Zhang and J. A. Rogers, *Nat. Commun.*, 2017, **8**, 15894.
267. K. Kwon, H. Wang, J. Lim, K. S. Chun, H. Jang, I. Yoo, D. Wu, A. J. Chen, C. G. Gu, L. Lipschultz, J. U. Kim, J. Kim, H. Jeong, H. Luan, Y. Park, C.-J. Su, Y. Ishida, S. R. Madhupathy, A. Ikoma, J. W. Kwak, D. S. Yang, A. Banks, S. Xu, Y. Huang, J.-K. Chang and J. A. Rogers, *Proc. Natl. Acad. Sci. U. S. A.*, 2021, **118**, e2020398118.
268. Z. Huang, Y. Hao, Y. Li, H. Hu, C. Wang, A. Nomoto, T. Pan, Y. Gu, Y. Chen, T. Zhang, W. Li, Y. Lei, N. Kim, C. Wang, L. Zhang, J. W. Ward, A. Maralani, X. Li, M. F. Durstock, A. Pisano, Y. Lin and S. Xu, *Nat. Electron.*, 2018, **1**, 473-480.
269. J. Byun, Y. Lee, J. Yoon, B. Lee, E. Oh, S. Chung, T. Lee, K.-J. Cho, J. Kim and Y. Hong, *Sci. Robot.*, 2018, **3**, eaas9020.
270. J. W. Kwak, M. Han, Z. Xie, H. U. Chung, J. Y. Lee, R. Avila, J. Yohay, X. Chen, C. Liang, M. Patel, I. Jung, J. Kim, M. Namkoong, K. Kwon, X. Guo, C. Ogle, D. Grande, D. Ryu, D. H. Kim, S. Madhupathy, C. Liu, D. S. Yang, Y. Park, R. Caldwell, A. Banks, S. Xu, Y. Huang, S. Fatone and J. A. Rogers, *Sci. Adv.*, 2020, **12**, eabc4327.
271. X. Tian, P. M. Lee, Y. J. Tan, T. L. Wu, H. Yao, M. Zhang, Z. Li, K. A. Ng, B. C. Tee and J. S. Ho, *Nat. Electron.*, 2019, **2**, 243-251.
272. N. P. Shetti, A. Mishra, S. Basu, R. J. Mascarenhas, R. R. Kakarla and T. Aminabhavi, *ACS Biomater. Sci. Eng.*, 2020, **6**, 1823-1835.
273. L. Hu, C. Tianrui, G. Yansong, L. Kui, J. Yanli, L. Dengfeng, J. Xinran, W. Yang, H. Xingcan, W. Han, L. Yiming, L. Jian, B. Yiming, G. Kai, Z. Nianrong, M. Hua, H. Dongsheng, L. Zhou, Y. Xinge and C. Lingqian, *Nano Energy*, 2022, **92**, 106786.
274. Y. Hao, X. He, L. Wang, X. Qin, G. Chen and J. Yu, *Adv. Funct. Mater.*, 2021, 2109790.
275. A. J. Bandodkar, *J. Electrochem. Soc.*, 2016, **164**, H3007.
276. L. Manjakkal, L. Yin, A. Nathan, J. Wang and R. Dahiya, *Adv. Mater.*, 2021, 2100899.
277. X. Pu, M. Liu, X. Chen, J. Sun, C. Du, Y. Zhang, J. Zhai, W. Hu and Z. L. Wang, *Sci. Adv.*, 2017, **3**, e1700015.
278. Y. Zhang, Z. Mei, T. Wang, W. Huo, S. Cui, H. Liang and X. Du, *Nano Energy*, 2017, **40**, 289-299.
279. H. Jinno, T. Yokota, M. Koizumi, W. Yukita, M. Saito, I. Osaka, K. Fukuda and T. Someya, *Nat. Commun.*, 2021, **12**, 2234.
280. H. Li, W. Lian, T. Cheng, W. Zhang, B. Lu, K. Tan, C. Liu and C. Shen, *ACS Sustain. Chem. Eng.*, 2021, **0**, null.
281. J. Zhang, Y. He, C. Boyer, K. Kalantar-Zadeh, S. Peng, D. Chu and C. H. Wang, *Nanoscale Adv.*, 2021, **3**, 5465-5486.
282. W. Gao, S. Emaminejad, H. Y. Y. Nyein, S. Challa, K. Chen, A. Peck, H. M. Fahad, H. Ota, H. Shiraki, D. Kiriya, D.-H. Lien, G. A. Brooks, R. W. Davis and A. Javey, *Nature*, 2016, **529**, 509-514.
283. H. Zhang, R. He, H. Liu, Y. Niu, Z. Li, F. Han, J. Li, X. Zhang and F. Xu, *Sens. Actuator A Phys.*, 2021, **322**, 112611.
284. Q. Shi, B. Dong, T. He, Z. Sun, J. Zhu, Z. Zhang and C. Lee, *InfoMat*, 2020, **2**, 1131-1162.
285. N. Zavanelli, H. Kim, J. Kim, R. Herbert, M. Mahmood, Y.-S. Kim, S. Kwon, N. B. Bolus, F. B. Torstrick, C. S. Lee and W.-H. Yeo, *Sci. Adv.*, 2021, **7**, eabl4146.
286. S. Patel, H. Park, P. Bonato, L. Chan and M. Rodgers, *J. Neuroeng. Rehabilitation*, 2012, **9**, 21.
287. S. Ramasamy and A. Balan, *Sens. Rev.*, 2018.
288. Y. Yamamoto, D. Yamamoto, M. Takada, H. Naito, T. Arie, S. Akita and K. Takei, *Adv. Healthc. Mater.*, 2017, **6**, 1700495.
289. H. U. Chung, B. H. Kim, J. Y. Lee, J. Lee, Z. Xie, E. M. Ibler, K. Lee, A. Banks, J. Y. Jeong and J. Kim, *Science*, 2019, **363**.
290. W. Dong, X. Cheng, T. Xiong and X. Wang, *Biomed. Microdevices*, 2019, **21**, 6.
291. S. Chun, W. Son, D. W. Kim, J. Lee, H. Min, H. Jung, D. Kwon, A.-H. Kim, Y.-J. Kim and S. K. Lim, *ACS Appl. Mater. Interfaces.*, 2019, **11**, 16951-16957.
292. P. F. Shahandashti, H. Pourkheyrollah, A. Jahanshahi and H. Ghafoorifard, *Sens. Actuator A Phys.*, 2019, **295**, 678-686.
293. Y.-T. Kwon, H. Kim, M. Mahmood, Y.-S. Kim, C. Demolder and W.-H. Yeo, *ACS Appl. Mater. Interfaces.*, 2020, **12**, 49398-49406.
294. Y. Zhao, S. Zhang, T. Yu, Y. Zhang, G. Ye, H. Cui, C. He, W. Jiang, Y. Zhai and C. Lu, *Nat. Commun.*, 2021, **12**, 4880.
295. M. Seeber, L.-M. Cantonas, M. Hoevens, T. Sesia, V. Visser-Vandewalle and C. M. Michel, *Nat. Commun.*, 2019, **10**, 753.
296. U. Chaudhary, N. Birbaumer and A. Ramos-Murguialday, *Nat. Rev. Neurol.*, 2016, **12**, 513-525.
297. H. N. Oon, A. Saidatul and Z. Ibrahim, 2018.
298. G. Li, J. Wu, Y. Xia, Y. Wu, Y. Tian, J. Liu, D. Chen and Q. He, *J. Neural Eng.*, 2020, **17**, 026001.
299. J.-Y. Kim, Y. J. Yun, J. Jeong, C.-Y. Kim, K.-R. Müller and S.-W. Lee, *Sci. Adv.*, 2021, **7**, eabe7432.
300. G. Li, S. Wang and Y. Y. Duan, *Sens. Actuators B Chem.*, 2018, **277**, 250-260.
301. G. Li, J. Wu, Y. Xia, Q. He and H. Jin, *J. Neural Eng.*, 2020.

302. L. Yang, Q. Liu, Z. Zhang, L. Gan, Y. Zhang and J. Wu, *Adv. Mater. Technol.*, 2021, 2100612.
303. J. J. Norton, D. S. Lee, J. W. Lee, W. Lee, O. Kwon, P. Won, S.-Y. Jung, H. Cheng, J.-W. Jeong and A. Akce, *Proc. Natl. Acad. Sci. USA.*, 2015, **112**, 3920-3925.
304. L. Tian, B. Zimmerman, A. Akhtar, K. J. Yu, M. Moore, J. Wu, R. J. Larsen, J. W. Lee, J. Li and Y. Liu, *Nat. Biomed. Eng.*, 2019, **3**, 194-205.
305. P. Won, J. J. Park, T. Lee, I. Ha, S. Han, M. Choi, J. Lee, S. Hong, K.-J. Cho and S. H. Ko, *Nano Lett.*, 2019, **19**, 6087-6096.
306. D. Kireev, E. Okogbue, R. Jayanth, T.-J. Ko, Y. Jung and D. Akinwande, *ACS nano*, 2021, **15**, 2800-2811.
307. S. Lin, J. Liu, W. Li, D. Wang, Y. Huang, C. Jia, Z. Li, M. Murtaza, H. Wang and J. Song, *Nano Lett.*, 2019, **19**, 6853-6861.
308. M. Mahmood, D. Mzurikwao, Y.-S. Kim, Y. Lee, S. Mishra, R. Herbert, A. Duarte, C. S. Ang and W.-H. Yeo, *Nat. Mach. Intell.*, 2019, **1**, 412-422.
309. M. Mahmood, S. Kwon, Y.-S. Kim, P. Siriaraya, J. Choi, O. Boris, K. Kang, K. Jun Yu, Y. C. Jang and C. S. Ang, *Adv. Sci.*, 2021.
310. Q. Li, L. N. Zhang, X. M. Tao and X. Ding, *Adv. Healthc. Mater.*, 2017, **6**, 1601371.
311. J. Yang, D. Wei, L. Tang, X. Song, W. Luo, J. Chu, T. Gao, H. Shi and C. Du, *RSC Adv.*, 2015, **5**, 25609-25615.
312. Y. Su, C. Ma, J. Chen, H. Wu, W. Luo, Y. Peng, Z. Luo, L. Li, Y. Tan and O. M. Omisore, *Nanoscale Res. Lett.*, 2020, **15**, 200.
313. B. A. Kuzubasoglu and S. K. Bahadir, *Sens. Actuator A Phys.*, 2020, 112282.
314. J. Shin, B. Jeong, J. Kim, V. B. Nam, Y. Yoon, J. Jung, S. Hong, H. Lee, H. Eom and J. Yeo, *Adv. Mater.*, 2020, **32**, 1905527.
315. T. Q. Trung, T. M. L. Dang, S. Ramasundaram, P. T. Toi, S. Y. Park and N.-E. Lee, *ACS Appl. Mater. Interfaces.*, 2018, **11**, 2317-2327.
316. Y.-F. Wang, T. Sekine, Y. Takeda, K. Yokosawa, H. Matsui, D. Kumaki, T. Shiba, T. Nishikawa and S. Tokito, *Sci. Rep.*, 2020, **10**, 2467.
317. T. Q. Trung and N. E. Lee, *Adv. Mater.*, 2016, **28**, 4338-4372.
318. Z. Sun, S. Yang, P. Zhao, J. Zhang, Y. Yang, X. Ye, X. Zhao, N. Cui, Y. Tong and Y. Liu, *ACS Appl. Mater. Interfaces.*, 2020, **12**, 13287-13295.
319. J. Park, M. Kim, Y. Lee, H. S. Lee and H. Ko, *Sci. Adv.*, 2015, **1**, e1500661.
320. L. Dejace, N. Laubeuf, I. Furfaro and S. P. Lacour, *Adv. Intell. Syst.*, 2019, **1**, 1900079.
321. C. Tan, Z. Dong, Y. Li, H. Zhao, X. Huang, Z. Zhou, J.-W. Jiang, Y.-Z. Long, P. Jiang and T.-Y. Zhang, *Nat. Commun.*, 2020, **11**, 3530.
322. X. Wang, J. Li, H. Song, H. Huang and J. Gou, *ACS Appl. Mater. Interfaces.*, 2018, **10**, 7371-7380.
323. L. Lan, T. Yin, C. Jiang, X. Li, Y. Yao, Z. Wang, S. Qu, Z. Ye, J. Ping and Y. Ying, *Nano Energy*, 2019, **62**, 319-328.
324. Z. Song, W. Li, Y. Bao, F. Han, L. Gao, J. Xu, Y. Ma, D. Han and L. Niu, *ACS Appl. Mater. Interfaces.*, 2018, **10**, 42826-42836.
325. Y. Wang, S. Gong, S. J. Wang, X. Yang, Y. Ling, L. W. Yap, D. Dong, G. P. Simon and W. Cheng, *ACS nano*, 2018, **12**, 9742-9749.
326. S. Díaz, J. B. Stephenson and M. A. Labrador, *Appl. Sci.*, 2020, **10**, 234.
327. H. Jeong, S. S. Kwak, S. Sohn, J. Y. Lee, Y. J. Lee, M. K. O'Brien, Y. Park, R. Avila, J.-T. Kim and J.-Y. Yoo, *Proc. Natl. Acad. Sci. USA.*, 2021, **118**.
328. J. Choi, R. Ghaffari, L. B. Baker and J. A. Rogers, *Sci. Adv.*, 2018, **4**, eaar3921.
329. A. J. Bandodkar, W. J. Jeang, R. Ghaffari and J. A. Rogers, *Annu. Rev. Anal. Chem.*, 2019, **12**, 1-22.
330. R. Ghaffari, D. S. Yang, J. Kim, A. Mansour, J. A. Wright Jr, J. B. Model, D. E. Wright, J. A. Rogers and T. R. Ray, *ACS Sens.*, 2021.
331. A. Pal, V. G. Nadiger, D. Goswami and R. Martinez, *Biosens. Bioelectron.*, 2020, **160**, 112206.
332. D.-H. Choi, A. Thaxton, I. cheol Jeong, K. Kim, P. R. Sosnay, G. R. Cutting and P. C. Searson, *J. Cyst. Fibros.*, 2018, **17**, e35-e38.
333. T. R. Ray, M. Ivanovic, P. M. Curtis, D. Franklin, K. Guventurk, W. J. Jeang, J. Chafetz, H. Gaertner, G. Young, S. Rebollo, J. B. Model, S. P. Lee, J. Ciraldo, J. T. Reeder, A. Hourlier-Fargette, A. J. Bandodkar, J. Choi, A. J. Aranyosi, R. Ghaffari, S. A. McColley, S. Haymond and J. A. Rogers, *Sci. Transl. Med.*, 2021, **13**, eabd8109.
334. L. B. Baker, J. B. Model, K. A. Barnes, M. L. Anderson, S. P. Lee, K. A. Lee, S. D. Brown, A. J. Reimel, T. J. Roberts, R. P. Nuccio, J. L. Bonsignore, C. T. Ungaro, J. M. Carter, W. Li, M. S. Seib, J. T. Reeder, A. J. Aranyosi, J. A. Rogers and R. Ghaffari, *Sci. Adv.*, 2020, **6**, eabe3929.
335. R. P. Peters, M. A. van Agtmael, S. A. Danner, P. H. Savelkoul and C. M. Vandenbroucke-Grauls, *Lancet Infect. Dis.*, 2004, **4**, 751-760.
336. M. Hallek, B. D. Cheson, D. Catovsky, F. Caligaris-Cappio, G. Dighiero, H. Döhner, P. Hillmen, M. J. Keating, E. Montserrat, K. R. Rai and T. J. Kipps, *Blood*, 2008, **111**, 5446-5456.
337. A. D. Association, *Diabetes care*, 2004, **27**, s5-s10.
338. Y. Sun and N. Thakor, *IEEE. Trans. Biomed. Eng.*, 2016, **63**, 463-477.
339. H. M. Lee, D. J. Kim, H. K. Yang, K. S. Kim, J. W. Lee, E. J. Cha and K. A. Kim, 2009.
340. E. Gil, R. Bailon, J. Maria Vergara and P. Laguna, *IEEE. Trans. Biomed. Eng.*, 2010, **57**, 1079-1088.
341. M. Yelderian and W. New, *Anesthesiologists*, 1983, **59**, 349-351.
342. S. Chen, J. Qi, S. Fan, Z. Qiao, J. C. Yeo and C. T. Lim, *Adv. Healthc. Mater.*, 2021, **10**, 2100116.
343. A. Jubran, *Crit. Care*, 2015, **19**, 272.
344. Y. Mendelson, *Clin. Chem.*, 1992, **38**, 1601-1607.
345. N. D. Giardino, L. Chan and S. Borson, *Appl. Psychophysiol. Biofeedback.*, 2004, **29**, 121-133.
346. K. K. Tremper, *Chest*, 1989, **95**, 713-715.
347. M. W. Wukitsch, M. T. Petterson, D. R. Tobler and J. A. Pologe, *J. Clin. Monit.*, 1988, **4**, 290-301.
348. Y. Lee, H. Lee, J. Jang, J. Lee, M. Kim, J. Lee, H. Kim, S. Yoo and H. J. Yoo, *IEEE Trans. Emerg. Sel. Topics Circuits Syst.*, 2017, **7**, 50-59.
349. D. Han, Y. Khan, J. Ting, S. M. King, N. Yaacobi-Gross, M. J. Humphries, C. J. Newsome and A. C. Arias, *Adv. Mater.*, 2017, **29**, 1606206.
350. S. Cai, X. Xu, W. Yang, J. Chen and X. Fang, *Adv. Mater.*, 2019, **31**, 1808138.
351. Y. J. Hong, H. Jeong, K. W. Cho, N. Lu and D.-H. Kim, *Adv. Funct. Mater.*, 2019, **29**, 1808247.

352. C. M. Lochner, Y. Khan, A. Pierre and A. C. Arias, *Nat. Commun.*, 2014, **5**, 5745.
353. H. Lee, E. Kim, Y. Lee, H. Kim, J. Lee, M. Kim, H.-J. Yoo and S. Yoo, *Sci. Adv.*, 2018, **4**, eaas9530.
354. S. Abdollahi, E. J. Markvicka, C. Majidi and A. W. Feinberg, *Adv. Healthc. Mater.*, 2020, **9**, 1901735.
355. T. Tamura, Y. Maeda, M. Sekine and M. Yoshida, *Electronics*, 2014, **3**, 282-302.
356. B. de Lacy Costello, A. Amann, H. Al-Kateb, C. Flynn, W. Filipiak, T. Khalid, D. Osborne and N. M. Ratcliffe, *J. Breath Res.*, 2014, **8**, 014001.
357. Y. Y. Broza, R. Vishinkin, O. Barash, M. K. Nakhleh and H. Haick, *Chem. Soc. Rev.*, 2018, **47**, 4781-4859.
358. Y. Y. Broza, P. Mochalski, V. Ruzsanyi, A. Amann and H. Haick, *Angew. Chem. Int. Ed.*, 2015, **54**, 11036-11048.
359. H. Haick, Y. Y. Broza, P. Mochalski, V. Ruzsanyi and A. Amann, *Chem. Soc. Rev.*, 2014, **43**, 1423-1449.
360. Y. Y. Broza, L. Zuri and H. Haick, *Sci. Rep.*, 2014, **4**, 4611.
361. P. Mochalski, J. King, K. Unterkofler, H. Hinterhuber and A. Amann, *J. Chromatogr. B*, 2014, **959**, 62-70.
362. T. Abaffy, R. Duncan, D. D. Riemer, O. Tietje, G. Elgart, C. Milikowski and R. A. DeFazio, *PLoS one*, 2010, **5**, e13813.
363. T. Abaffy, M. Möller, D. Riemer, C. Milikowski and R. DeFazio, *Metabolomics*, 2013, **9**, 998-1008.
364. J. Kwak, M. Gallagher, M. H. Ozdener, C. J. Wysocki, B. R. Goldsmith, A. Isamah, A. Faranda, S. S. Fakharzadeh, M. Herlyn and A. C. Johnson, *J. Chromatogr. B*, 2013, **931**, 90-96.
365. G. Pennazza, M. Santonico, A. Bartolazzi, R. Paolesse, C. Di Natale, R. Bono, V. Tamburrelli, S. Cristina and A. D'Amico, *Procedia Chem.*, 2009, **1**, 995-998.
366. R. Vishinkin, R. Busool, E. Mansour, F. Fish, A. Esmail, P. Kumar, A. Gharaa, J. C. Cancilla, J. S. Torrecilla, G. Skenders, M. Leja, K. Dheda, S. Singh and H. Haick, *Adv. Sci.*, 2021, 2100235.
367. H. Jin, T.-P. Huynh and H. Haick, *Nano Lett.*, 2016, **16**, 4194-4202.
368. N. Tang, Y. Zheng, D. Cui and H. Haick, *Adv. Healthc. Mater.*, 2021, **10**, 2101292.
369. Y. Hattori, L. Falgout, W. Lee, S. Y. Jung, E. Poon, J. W. Lee, I. Na, A. Geisler, D. Sadhwani and Y. Zhang, *Advanced healthcare materials*, 2014, **3**, 1597-1607.
370. Q. Zeng, X. Qi, G. Shi, M. Zhang and H. Haick, *ACS nano*, 2022.
371. E. Cho, M. Mohammadifar and S. Choi, presented in part at the 2017 IEEE 30th Int. Conf. Micro Electro Mechanical Systems (MEMS), 2017.
372. S. Xu, A. Jayaraman and J. A. Rogers, *Nature*, 2019, **571**, 319-321.
373. M. F. Farooqui and A. Shamim, *Sci. Rep.*, 2016, **6**, 28949.
374. B. Melai, P. Salvo, N. Calisi, L. Moni, A. Bonini, C. Paoletti, T. Lomonaco, V. Mollica, R. Fuoco and F. Di Francesco, *Annu Int Conf IEEE Eng Med Biol Soc*, 2016, **2016**, 1898-1901.
375. X. Liu and P. B. Lillehoj, *Biosens. Bioelectron.*, 2017, **98**, 189-194.
376. D. A. Jankowska, M. B. Bannwarth, C. Schulenburg, G. Faccio, K. Maniura-Weber, R. M. Rossi, L. Scherer, M. Richter and L. F. Boesel, *Biosens. Bioelectron.*, 2017, **87**, 312-319.
377. M. Sharifuzzaman, A. Chhetry, M. A. Zahed, S. H. Yoon, C. I. Park, S. Zhang, S. Chandra Barman, S. Sharma, H. Yoon and J. Y. Park, *Biosens. Bioelectron.*, 2020, **169**, 112637.
378. H. Yeon, H. Lee, Y. Kim, D. Lee, Y. Lee, J.-S. Lee, J. Shin, C. Choi, J.-H. Kang, J. M. Suh, H. Kim, H. S. Kum, J. Lee, D. Kim, K. Ko, B. S. Ma, P. Lin, S. Han, S. Kim, S.-H. Bae, T.-S. Kim, M.-C. Park, Y.-C. Joo, E. Kim, J. Han and J. Kim, *Sci. Adv.*, 2021, **7**, eabg8459.
379. D. Y. M. Leung, A. Calatroni, L. S. Zaramela, P. K. LeBeau, N. Dyjack, K. Brar, G. David, K. Johnson, S. Leung, M. Ramirez-Gama, B. Liang, C. Rios, M. T. Montgomery, B. N. Richers, C. F. Hall, K. A. Norquest, J. Jung, I. Bronova, S. Kreimer, C. C. Talbot, D. Crumrine, R. N. Cole, P. Elias, K. Zengler, M. A. Seibold, E. Berdyshev and E. Goleva, *Sci. Transl. Med.*, 2019, **11**, eaav2685.
380. F. Ershad, K. Sim, A. Thukral, Y. S. Zhang and C. Yu, *APL Mater.*, 2019, **7**, 031301.
381. H. Xu, J. Liu, J. Zhang, G. Zhou, N. Luo and N. Zhao, *Adv. Mater.*, 2017, **29**, 1700975.
382. C. Wang, X. Li, H. Hu, L. Zhang, Z. Huang, M. Lin, Z. Zhang, Z. Yin, B. Huang, H. Gong, S. Bhaskaran, Y. Gu, M. Makihata, Y. Guo, Y. Lei, Y. Chen, C. Wang, Y. Li, T. Zhang, Z. Chen, A. P. Pisano, L. Zhang, Q. Zhou and S. Xu, *Nat. Biomed. Eng.*, 2018, **2**, 687-695.
383. D. Cheng, J. Wang, T. Yokota and T. Someya, *Biomed. Opt. Express*, 2022, **13**, 838-849.
384. K. Meng, X. Xiao, W. Wei, G. Chen, A. Nashalian, S. Shen, X. Xiao and J. Chen, *Adv. Mater.*, 2022, DOI: <https://doi.org/10.1002/adma.202109357>, 2109357.
385. Y. Liu, J. J. S. Norton, R. Qazi, Z. Zou, K. R. Ammann, H. Liu, L. Yan, P. L. Tran, K.-I. Jang, J. W. Lee, D. Zhang, K. A. Kilian, S. H. Jung, T. Bretl, J. Xiao, M. J. Slepian, Y. Huang, J.-W. Jeong and J. A. Rogers, *Sci. Adv.*, 2016, **2**, e1601185.
386. R. Guy, *Nat. Nanotechnol.*, 2016, **11**, 493-494.
387. K. San Chun, Y. J. Kang, J. Y. Lee, M. Nguyen, B. Lee, R. Lee, H. H. Jo, E. Allen, H. Chen and J. Kim, *Sci. Adv.*, 2021, **7**, eabf9405.